NASA CR-174661

SHOCK TUBE STUDY OF THE FUEL STRUCTURE EFFECTS ON THE CHEMICAL KINETIC MECHANISMS RESPONSIBLE FOR SOOT FORMATION

by

Michael Frenklach

Department of Chemical Engineering
Louisiana State University

prepared for

NATIONAL AERONAUTICS AND SPACE ADMINISTRATION

NASA Lewis Research Center

Contract NAS 3-23542

November 1983

1. Report No.	2. Government Accession No.	3. Recipient's Catalog No.
NASA CR-174661		

4. Title and Subtitle	5. Report Date
SHOCK TUBE STUDY OF THE FUEL STRUCTURE EFFECTS ON THE CHEMICAL KINETIC MECHANISMS RESPONSIBLE FOR SOOT FORMATION	APRIL 1984
	6. Performing Organization Code

7. Author(s)	8. Performing Organization Report No.
M. FRENKLACH	
	10. Work Unit No.

9. Performing Organization Name and Address	11. Contract or Grant No.
DEPARTMENT OF CHEMICAL ENGINEERING LOUISIANA STATE UNIVERSITY BATON ROUGE, LOUISIANA 70803	NAS 3-23542
	13. Type of Report and Period Covered
12. Sponsoring Agency Name and Address	CONTRACTOR REPORT
NATIONAL AERONAUTICS AND SPACE ADMINISTRATION WASHINGTON, D.C. 20546	14. Sponsoring Agency Code

15. Supplementary Notes

PROJECT MANAGER, JOHN B. HAGGARD, AEROTHERMODYNAMICS AND FUELS DIVISION, NASA LEWIS RESEARCH CENTER, CLEVELAND, OHIO 44135

16. Abstract

Soot formation in toluene-, benzene-, and acetylene-oxygen-argon mixtures was investigated to study soot formation in a combustion environment. It was observed that high concentrations of oxygen completely suppress soot formation. The addition of oxygen at relatively low concentrations uniformly suppresses soot formation at high pressures, while at relatively lower pressures it suppresses soot formation at higher temperatures while promoting soot production at lower temperatures. The observed behavior may indicate that oxidation reactions compete with ring fragmentation. The main conclusion to be drawn from the results of this work is that the soot formation mechanism is probably the same for the pyrolysis and oxidation of hydrocarbons. That is, the addition of oxygen does not alter the soot route but rather promotes or inhibits this route by means of competitive reactions. An approach to empirical modeling of soot formation during pyrolysis of aromatic hydrocarbons is also presented.

17. Key Words (Suggested by Author(s))	18. Distribution Statement
SOOT SHOCK TUBES CHEMICAL REACTIONS	UNCLASSIFIED- UNLIMITED

19. Security Classif. (of this report)	20. Security Classif. (of this page)	21. No. of pages	22. Price*
UNCLASSIFIED	UNCLASSIFIED	99	

*For sale by the National Technical Information Service, Springfield, Virginia 22161

TABLE OF CONTENTS

SUMMARY

The formation of soot always accompanies the combustion of hydrocarbon fuels. Sooting causes several undesirable effects and becomes particularly severe with synthetic fuels. Although the recent "oil crisis" seems to be over, the development and future use of synthetic fuels are inevitable. Soot formation is one of the challenging problems in the development of these new fuels.

The Combustion Laboratory at Louisiana State University has long been engaged in studies of soot formation. Both experimental and theoretical studies have been conducted. The ultimate goal of this program is the development of a detailed kinetic model for soot formation during the combustion of hydrocarbons. The objective of the experimental part of the contract is to establish quantitative relationships between the parameters of soot formation (i.e. soot yields, induction times, and rates of formation) and experimental conditions, such as temperature, pressure, composition of the mixture and molecular structure of the fuel molecules. The experiments have involved pyrolysis and oxidation of a variety of hydrocarbon fuels using state-of-the-art shock-tube, laser diagnostic and data processing techniques.

As a result of our activity in recent years, a conceptual model for soot formation during the pyrolysis of aromatic hydrocarbons was developed. Under the current contract, a conceptual model for soot formation during pyrolysis of non-aromatic hydrocarbons was completed. It was suggested that the incipient soot formation from hydrocarbons must follow the route of consecutive production of conjugated reactive structures. The difference in soot formation characteristics between various hydrocarbons is determined by the initiation process, i.e. by the reactions leading to these reactive structures.

Soot formation in toluene-, benzene-, and acetylene-oxygen-argon mixtures was investigated to study soot formation in a combustion environment. It was observed that high concentrations of oxygen completely suppress soot formation. The addition of oxygen at relatively low concentrations uniformly suppresses soot formation at high pressures, while at relatively lower pressures it suppresses soot formation at higher temperatures while promoting soot production at lower temperatures. The observed behavior may indicate that oxidation reactions compete with ring fragmentation. The main conclusion to be drawn from the results of this work is that the soot formation mechanism is probably the same for the pyrolysis and oxidation of hydrocarbons. That is, the addition of oxygen does not alter the soot route but rather promotes or inhibits this route by means of competitive reactions.

INTRODUCTION

The formation of soot always accompanies the combustion of hydrocarbon fuels. Soot production causes several undesirable effects such as air pollution, emission of carcinogenic materials and a decrease in the efficiency of practical combustion systems. Sooting is particularly severe with synthetic fuels due to their higher aromatic content.

The subject of soot formation attracted particular attention with the recent "oil crisis". Although the "crisis" seems to be over, the development and future use of synthetic fuels are inevitable. One must realize that the many scientific and technological problems associated with future fuels may require time to be resolved. Soot formation is certainly one of those challenging problems.

The Combustion Laboratory at Louisiana State University has long been engaged in studies of soot formation. Both experimental and theoretical studies have been conducted. The experiments have involved pyrolysis and oxidation of a variety of fuels using state-of-the art shock tube, laser diagnostic and data processing techniques. The ultimate goal of this program is the development of a detailed kinetic model for soot formation during the combustion of hydrocarbons.

1. Literature Survey

During the last few years a number of excellent reviews have appeared covering various aspects of soot formation [1-10]. Here we will concentrate on the subject of the ongoing research program, namely shock-tube oxidation of hydrocarbons and closely related topics.

a) Oxidation and Pyrolysis of Aromatic Hydrocarbons in Shock Tubes.

Early shock tube works were not concerned with formation of soot; rather, they concentrated on ignition delay times and the initial stages of pyrolysis and oxidation of aromatic fuels. Kogarko and Borisov [11] measured the induction periods for 3% benzene - air mixtures. Miyama extended their measurements to a range of benzene concentrations [12]. He also determined ignition delays for other aromatic hydrocarbons: toluene, o-xylene, m-xylene, p-xylene, ethylbenzene, propylbenzene and 1,3,5-trimethylbenzene [13]. The most recent measurements of ignition delay times for benzene and toluene were reported by Matula and Farmer [14], Burcat et al. [15], and Durgaprasad [16]. Table 1 summarizes the ignition delay data, where τ is the ignition delay time defined as the time from the onset of reaction to the instant of ignition. The bracketed quantities in Table I, [fuel], [oxygen], [inert] are molar concentrations (mol/cm^3).

TABLE I. IGNITION DELAY TIMES

$$\tau = 10^{A}\, e^{\theta/T}\, [\text{Fuel}]^{\alpha}\, [\text{Oxygen}]^{\beta}\, [\text{Inert}]^{\gamma}$$

Fuel (vol%)	Oxidizer (vol%)	Inert (vol%)	Temperature Range (K)	Pressure Range (atm)	A	$\theta \times 10^{-3}$ (K)	α	β	γ	Reference
Benzene 3	Air 97		1100-1500	40-80	-13.6	26.2	-	-	-	11
Benzene 0.5-2.75	Oxygen 7.25-19.5	Argon 80-90	1090-1615	5.40-7.08	-10.0	21.4	0	-1	0	12,13
Toluene 0.25-2.75	Oxygen 7.25-9.75	Argon 90	1230-1805	4.82-6.70	-10.22	23.8	0	-1	0	13
o-Xylene 0.25-2.75	Oxygen 7.25-9.75	Argon 90	1250-2035	2.77-7.03	- 9.29	20.4	0	-1	0	13
m-Xylene 0.25-2.75	Oxygen 7.25-9.75	Argon 90	1235-1985	3.35-7.70	- 9.24	20.5	0	-1	0	13
p-Xylene 0.25-2.75	Oxygen 7.25-9.75	Argon 90	1235-1985	3.93-7.03	- 8.98	19.4	0	-1	0	13
Ethylbenzene 0.25-2.25	Oxygen 7.75-9.75	Argon 90	1120-1900	4.08-6.19	- 8.33	15.7	0	-1	0	13
Propylbenzene 0.25-1.0	Oxygen 9.0-9.75	Argon 90	1190-1870	4.46-5.90	-10.52	22.2	0	-1	0	13
1,3,5-trimethyl-benzene 0.25-1.0	Oxygen 9.0-9.25	Argon 90	1235-1925	3.96-5.69	-11.72	28.1	0	-1	0	13

TABLE I. (continued)

Fuel (vol%)	Oxidizer (vol%)	Inert (vol%)	Temperature Range (K)	Pressure Range (atm)	A	$\theta \times 10^{-3}$ (K)	α	β	γ	Reference
Toluene 0.61-2.44	Oxygen 2.74-18.0	Argon 80.0-96.65	1193-1700	2.5-9.7	-17.10	29.6	-0.081	-1.71	0.64	14
Benzene 0.12-0.42	Oxygen 1.58-1.88	Argon 98	1438-2107	2.10-3.39	- 7.62	13.7	0	0	0	16
Toluene 0.10-0.37	Oxygen 1.63-1.90	Argon 98	1470-2135	2.15-3.33	-17.26	15.8	0	-1.4	0	16

The units are: τ in s, T in K, concentration in mol/cm^3.

The first shock tube studies with aromatic hydrocarbons were probably done in 1963. Bauer and Aten [17] measured absorption spectra of benzene and of hexafluorobenzene diluted in argon over the temperature range from 690 to 1900 K. They suggested a chain mechanism for the initial stages of benzene pyrolysis which can be abbreviated to

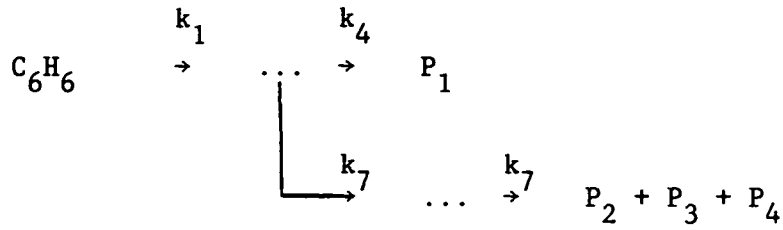

where: $P_1 = C_4H_2$

$P_2 = C_{12}H_{10}$

$P_3 = C_8H_6$

$P_4 = C_{10}H_8$.

Orr [18] investigated combustion of dilute fuel-oxygen-argon mixtures for ethylene, acetylene, isooctane, n-heptane, benzene, and H_2-CO. The rates of formation of reactants, intermediates and products were studied by observing the infrared emissions. Orr found that production of CO from benzene was considerably slower than from other fuels studied.

Asaba and Fujii [19] investigated pyrolysis of 10-20% benzene-argon mixtures at temperatures from 1400 to 1900 K. A single-pulse shock-tube technique accompanied by light absorption was employed. They found that the pyrolysis reaction was slowed considerably by the addition of hydrogen and promoted by the addition of methane. To explain the experimental results, the authors proposed a new chain mechanism for benzene pyrolysis:

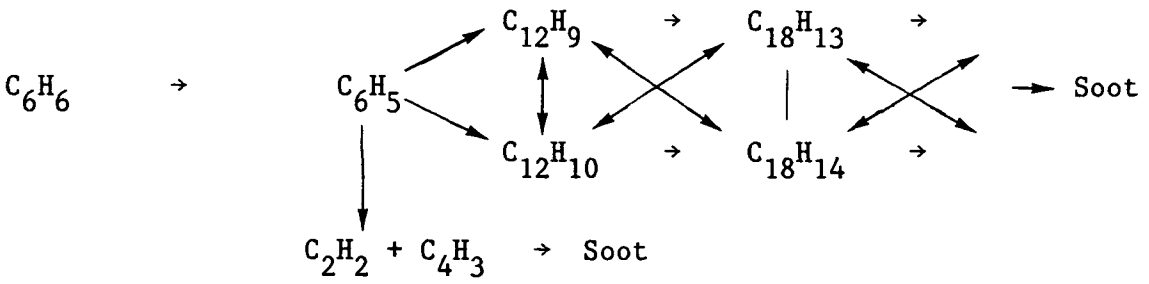

Later, Fujii and Asaba [20] and Fujii et al. [21] extended this study to include the oxidation of rich and lean mixtures of benzene and oxygen. Their reaction mechanism provided a reasonable description of the ignition characteristics measured by Miyama [13] but it failed to predict the correct concentrations for all the species. McLain et al. [22] modified the mechanism of Fujii and Asaba for benzene oxidation and suggested a reaction mechanism for toluene oxidation. The latter mechanisms predicted the ignition delays reasonably well but overestimated the concentration of CO and underestimated the concentration of CO_2.

Troe and co-workers [23] reported rate constants for the unimolecular decomposition of toluene, $C_6H_5CH_3$, and of the benzyl radical, $C_6H_5CH_2$. They clearly demonstrated that both decompositions are within the fall-off region at pressures up to 30 atm. Dzarnoski et al. [24] measured the rate constant of the reaction

$$CH_3 + C_6H_5CH_3 \rightarrow CH_4 + C_6H_5CH_2.$$

A number of rate constants for reactions of aromatic hydrocarbons were recently determined by methods other than shock tube [25-31].

Kern et al. [32] have recently investigated the product distribution in the shock tube pyrolysis of toluene and benzene. The major products detected by a time-of-flight mass spectrometer were acetylene and polyacetylenes. No products with a mass greater than 92 (for toluene) or 78 (for benzene) were detected. Their results parallel those of Smith [33,34], which were obtained in high-

temperature-low-pressure-Knudsen-cell experiments. The results of very-low-pressure pyrolyses of several aromatic species have recently appeared in the literature [35-37]. A new mechanism for high-temperature oxidation of aromatic hydrocarbons has been recently suggested by Glassman and co-workers [38].

Mar'yasin and Nabutovskii [39,40] were probably the first to include quantitative, although very approximate, measurements of soot in the single-pulse shock-tube studies of the pyrolysis of aromatic hydrocarbons. They pyrolyzed 3-5% benzene-argon mixtures behind reflected shock waves at temperatures from 1400 to 2500 K. Concentrations of hydrogen, methane, ethylene, acetylene, vinylacetylene, diacetylene and benzene were analyzed by gas-chromatograph and the amount of soot formed was determined by weighing the soot deposited on the walls and optical windows of the shock tube. Induction times for soot appearance were quantified and correlated to the initial temperature and benzene concentration.

Park and Appleton [41] employed a laser extinction technique (633 nm, He-Ne) to study soot oxidation rates in an oxygen atmosphere behind reflected shock waves at temperatures of 1700-4000 K and pressures of 0.05 - 13 atm.

In their classical work, Graham et al. [42,43] investigated soot formation in pyrolyses of benzene, toluene, ethylbenzene and other aromatic fuels highly diluted in argon behind incident shock waves. Their experimental conditions covered a temperature range of 1600-2300 K at a total carbon concentration in the shock-heated gases of (1.5-3.0) x 10^{17} atoms/cm^3. Soot was monitored by laser-light extinction measurements at three different wavelengths (488 nm of argon-ion laser and 632.8 nm and 3.39 μm of He-Ne laser) and by light scattering (488 nm of argon-ion laser). Samples of soot particles formed in the incident shock flows were examined by electron microscope. Their main conclusions were:

a) Soot yield passes through a well-pronounced maximum around 1750 K. Complete conversion of fuel carbon to soot was assumed at the maximum point.

b) "... aromatic hydrocarbons can form soot by two very different pathways, one direct and one indirect." That is:

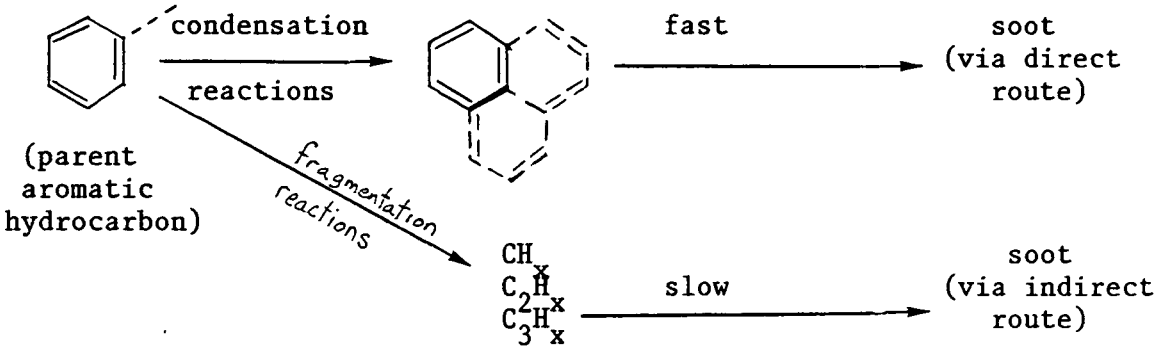

Thus, the maximum in soot yield was explained by competition between condensation and fragmentation of the aromatic ring.

c) The authors suggested a model of "free-molecule coagulation of an aerosol comprised of spherical sticky particles whose size distribution is of the self-preserving form". Interpreting the experimental results in light of this model, they estimated that the particle did not grow larger then about 40 nm. The later development of this aspect is reported in [44,45].

Wang et al. [46] conducted experiments similar to those of Graham et al. [42] but behind reflected shock waves. They confirmed the existence of a maximum for soot production as a function of temperature. The maximum conversion of carbon atoms to soot was estimated to be approximately 80%. Wang et al. [46,47] also determined:

a) hydrogen and oxygen suppress soot formation;

b) pressure does not have significant effect on soot formation;

c) the amount of soot formed increases with increasing initial concentration of aromatic hydrocarbon;

d) induction times of soot appearance were determined as a function of the temperature and initial composition of the mixture;

e) based on thermodynamic considerations, the precursor to soot was suggested to be $C_{96}H_{24}$.

Vaughn et al. [48,49] conducted a single-pulse shock-tube study of thermal decomposition of benzene diluted in argon. The reaction was studied over a temperature range of 1300-2300 K with initial benzene concentrations of (0.4-1.25) x 10^{-6} mole/cm and reaction times of 0.1 to 3.0 msec. The stable products formed were analyzed by gas chromatography and mass spectrometry. The amount of soot formed was determined by gravimetric methods. Product analysis showed that the principal products were acetylene and styrene. Smaller concentrations of diacetylene, methane, vinylacetylene, ethylene and toluene were observed. Their main conclusions were:

a) acetylene is principally formed directly from ring scission, C_4 compounds are formed primarily via acetylene recombination, and styrene is formed mainly by an "acetylenic reaction with the benzene ring";

b) soot yields increase from zero at 1300 K to a plateau value of 0.8 at about 1900 K;

c) the amount of soot formed decreases when the initial concentration of aromatic hydrocarbon is increased. (Note that this observation is opposite to that of Wang et al. [46]).

Later, Nelson et al. [50] extended these studies to include laser extinction measurements. Soot yields determined by the optical method exhibited maxima similar to those of Graham et al. [42] and Wang et al. [46]. However, the dependency on the initial concentration of benzene obtained was similar to

that of Vaughn et al. [49]. Nelson et al. [50] reported that soot yields formed in pyrolyses of toluene were larger than those obtained in pyrolyses of benzene. In their work induction times for soot appearance were determined by a laser extinction technique and soot samples were analyzed by a transmission electron microscope. The authors also suggested that "the primary impact of ring fragmentation is not on the nucleation of soot, but rather on the surface growth".

Evans and Williams [51] characterized soot particles formed behind reflected shocks by a transmission electron microscope. They found that the agglomeration of soot particles depends on experimental conditions. Williams' graduate student, Durgaprasad [16], reported that the pyrolysis of toluene resulted in larger amounts of soot than that of benzene. Farmer, Edelman, and co-workers [52,53] attempted quasi-global modeling to predict soot emissions in practical combustion environments.

Frenklach et al. [54] re-investigated soot formation in the pyrolysis of toluene behind reflected shock waves at conditions similar to those of Wang et al. [46,47] and Kern et al. [32]. Soot was monitored by attenuation of a laser beam in the visible (632.8 nm) and the infrared (3.39 μm) regions of the spectrum. The experimental data indicated that the position of measured maximum in soot yield is not universal, but rather is dependent on controllable experimental variables including observation time, total pressure and initial hydrocarbon concentration, as well as the wavelength employed in the measurements. The observed pressure effect could not be rationalized within Graham's model which was discussed earlier in the text. Frenklach et al. [54] proposed a new conceptual model for soot formation during the high temperature pyrolysis of aromatic hydrocarbons. The model is described in terms of the kinetic skeleton:

$$A \xrightarrow{k_1} X \qquad \text{(R1)}$$

$$A + X \xrightarrow{k_2} S \qquad \text{(R2)}$$

where A, X, and S denote an intact aromatic ring, intermediate species and soot, respectively. Reactions (R1) and (R2) generalize the fragmentation of the ring and the free-radical polymerization, respectively. This new model explains and unifies the various experimental facts and theoretical hypotheses. Employing a laser Doppler velocimeter, Frenklach et al. [55] measured the size of soot particles formed in the reactive flow. The particle size appeared to be of the order of a micron meaning that:

a) agglomeration of the primary soot spheres takes place prior to the onset of cooling and

b) the use of the Rayleigh limit of the Mie scattering theory for the determination of absolute soot yield is invalid and leads to an overestimation of the conversion of hydrocarbon to soot.

There are a number of current programs. Rawlins et al. [56,57] have been conducting an experimental program on the pyrolysis and oxidation of aromatic hydrocarbons behind incident shock waves. A variety of light extinction and emission measurements have been performed. Colket and Seery [58] have been conducting single-pulse shock-tube studies on the pyrolysis of toluene. Bauer and Zhang [59] have been performing single-pulse shock-tube studies on the pyrolysis of di- and tri-cyclic aromatics.

b) Oxidation and Pyrolysis of Non-Aromatic Hydrocarbons in Shock Tubes.

The chemistry of non-aromatic hydrocarbons is much better known than that of aromatics. Shock tube investigations have been recently reviewed by

Khandelwal and Skinner [60]. Since this review, a number of relevant papers have appeared. Frank and Just [61] reported decomposition of acetylene and diacetylene using atomic resonance absorption spectroscopy technique for hydrogen atoms. Bar-Nun and Dove [62] investigated acetylene pyrolysis and oxidation by water vapor. Koike and Morinaga [63] studied pyrolysis of acetylene and ethylene by UV absorption. Kern et al. [32] reported the results on pyrolysis of acetylene and 1,3-butadiene obtained behind reflected shock waves by time-of-flight mass spectrometry. Kiefer and co-workers [64-66] have studied the pyrolysis of ethylene, propane and propene by means of laser-schlieren technique. Colket [67] has been conducting experiments on the pyrolysis of 1,3-butadiene in single-pulse shock tube studies.

The pyrolysis of acetylene has received the most attention. The experimental results obtained in a variety of kinetic studies were summarized by Tanzawa and Gardiner in a kinetic model [68,69]. The model reproduces the general sequence

$$C_2H_2 \rightarrow C_4H_3 \rightarrow C_4H_2 \rightarrow C_6H_2 \rightarrow C_8H_2 \rightarrow \ldots$$

suggested by Gay et al. [70] for acetylene pyrolysis and predicts the establishment of equilibrium among the smaller acetylenes and acetylenic radicals prior to soot formation. Modeling of acetylene oxidation has been recently reported by a number of researchers [71-73]. No reactions leading to soot, however, have been suggested.

Graham et al. [43-45] were the first to monitor soot behind shock waves. The authors reported that much less soot was formed from acetylene than from aromatic hydrocarbons. Fussey and co-workers [74-76] employed a variety of optical techniques in studies of the pyrolysis of ethane, ethylene, acetylene and propylene. The authors determined that soot is formed more readily from acetylene than from ethylene and ethane. They determined the induction times

for soot appearance and postulated that these times are independent of experimental technique. Induction times for soot appearance in acetylene pyrolysis were also obtained by Tanzawa and Gardiner [69] and Yoshizawa et al. [77].

Frenklach et al. [78] have systematically investigated soot formation in pyrolysis of acetylene, allene and 1,3-butadiene. Soot was monitored by laser extinction at 632.8 nm and 3.39 μm behind reflected shock waves. The authors' major conclusions were the following:

- The induction times for soot appearance are dependent on the wavelength of extinction which invalidates the assumption of Fussey et al. [74];
- The formation of soot during acetylene pyrolysis is not only strongly dependent on the initial concentration of acetylene, the fact which has been reported by a number of researchers [42,69,74-77], but also exhibits the existence of a maximum in soot yield with temperature at higher concentrations of acetylene. The maximum occurs at significantly higher temperatures than in pyrolysis of aromatics;
- In acetylene pyrolysis, a decrease in total pressure shifts the soot bell to higher temperatures with a significant increase in the maximum soot yield;
- Soot is formed much faster and in much larger quantities from allene than from 1,3-butadiene;
- The most efficient "building blocks" for the formation of soot precursors in the pyrolysis of aliphatic hydrocarbons seem to be species with C-to-H ratios of approximately unity which have conjugated molecular configuration. Since aromatic

> form provides the ultimate delocalization of π-electron density and thus the ultimate stabilization and reactivity, the incipient soot formation from hydrocarbons should follow the route of consecutive production of the conjugated reactive structures. The difference in soot formation characteristics between various hydrocarbons is determined by the initiation process, i.e. by the reactions leading to these reactive structures.

The conceptual model developed for soot formation is pyrolysis of non-aromatic hydrocarbons is discussed in Subsection 3b of DISCUSSION.

2. Objective of the Present Work

The main objective of the present work was to investigate soot formation characteristics in oxidation of aromatic and non-aromatic hydrocarbons. Toluene and acetylene were the chosen representatives of these two classes of hydrocarbons. These are the species for which soot formation dependencies were established in the previous pyrolysis studies [54,78]. The oxidation was conducted at the conditions of the previous pyrolysis experiments, in order to compare the results of both studies.

It was recently reported by Wang et al. [46,47] and Rawlins et al. [56,57,80] that oxygen suppresses soot formation from toluene. The results obtained in the present work indicate that, depending upon experimental conditions, oxygen also promotes the production of soot. This also appeared to be true in the case of acetylene: depending on the experimental conditions, oxygen promotes or suppresses the formation of soot.

Some of the results obtained during this contract are already reported in the literature. The entire list of publications resulting from this contract is given in Appendix A. The professional personnel of LSU involved in this contract is given in Appendix B.

APPARATUS AND PROCEDURES

The experimental apparatus and procedures used in this study were similar to those described in our previous works on pyrolysis of aromatic hydrocarbons [57,78]. The experiments have been conducted behind reflected shock waves in a conventional stainless steel shock tube: 7.62 cm i.d., 3 m driver section and 7.3 m driven section. The double diaphragm burst technique was employed, using either Mylar or aluminum foils as the diaphragm material. Both mechanical (Edwards ED-500) and diffusion (Edwards Speedivac E-04) pumps were used in the shock tube gas-handling and vacuum systems. The systems could be evacuated to less than 10^{-5} torr. The driver gas was helium. The test gas mixtures were prepared manometrically in a stainless steel tank and allowed to mix for at least 24 hours prior to experimental runs. A Wallace and Tiernan Model FA-145 manometer was used for precise pressure readings. The stated purities of the gases were: argon-99.995%, helium-99.99% oxygen-99.5% and acetylene-99.6%. The toluene (Reagent, Baker) and benzene (Spectranalyzed, Fisher) were purified by repeated freezing and evacuation. The shock tube was cleaned after every run.

The state of the gas behind the reflected shock waves was calculated in a standard manner assuming full relaxation and no chemical reaction [79] and using the measured incident shock velocity extrapolated to the end wall of the shock tube. The observed shock wave attenuation was approximately 2%/m. Shock

velocities were measured using four piezoelectric pressure transducers to trigger the start and stop channels of an interval timer. All pressure transducers and optical windows were mounted flush with the surface of the shock tube to minimize flow distortion.

The soot conversion was determined by measuring the attenuation of the beam from a 15 mw cw He-Ne Spectra-Physics laser which was operated in the visible (632.8 nm) region of the spectrum. The laser beam crossed the shock tube at a point 10 mm from the end plate. High quality sapphire windows were used. The attenuated laser light was monitored by an RCA 1P28 photomultiplier, whose output signal was amplified and displayed on a Nicolet Model 2090-3 digital oscilloscope. The design of the optical system was optimized so that emission was only a negligible component (less than 0.1%) of the extinction signal. This was achieved by using the laser beam at maximum power, a narrow-band interference filter centered at 632.8 nm and a number of optical stops. Careful alignment and adjustment of the optical system at 632.8 nm resulted in an excellent signal-to-noise ratio of the absorption signal. As in our previous studies [54,78], the induction time for soot appearance was defined by the point of maximum curvature in the extinction signal and the soot yields were calculated according to Graham's model [42,43] but leaving out the quantity $E(m) = - \mathrm{Im}\ [(m^2-1)/(m^2+2)]$, where m is the complex refractive index of soot particles. This arbitrary form of reporting the results was chosen to emphasize the ambiguity in the value of m and, what seems to be even more important, in the laser-extinction model itself [54,55].

In addition to the extinction measurements, the infrared emission was also monitored by employing two side-looking In-Sb detectors operated in a photoconductive mode. The detectors were located on the opposite side walls of

the shock tube, 65 mm away from the end plate. The fields of view were determined by vertical 1 x 4 mm slits. Two narrow-band interference filters, 4.78±0.08 μm and 4.25±0.05 μm, were used in an attempt to isolate the CO and CO_2 emissions, respectively (the center of CO band is at 4.75 μm and the center of CO_2 band is at 4.35 μm).

The pressure behind reflected shock waves was monitored by a calibrated piezoelectric pressure transducer located on the upper wall of the shock tube, 10 mm away from the end wall. Output signals from the pressure transducer, the 1P28 photomultiplier and the two In-Sb detectors were amplified, displayed and recorded on Nicolet, Model 2090-3, digital oscilloscopes. The data were transferred from a Nicolet oscilloscope to an Apple II microcomputer via a GPIB/IEEE-488 interface. The data were reduced using PASCAL language programs in the Apple II before being transferred to the IBM main frame computer.

RESULTS

The initial conditions used in this experimental work are summarized in Table II. Mixtures A and C were used to test the reproducibility of the soot formation results, with data in literature. Mixtures B and D were used to study the effect of oxygen on soot formation from toluene. Mixtures E, F and G were used to complete the data on pyrolysis of toluene, which were used for empirical modeling of soot formation. Mixtures I, J, L, M and N were used to study soot formation in oxidation of acetylene. These experiments were designed so that the effects of temperature, pressure and oxygen concentration could be clearly observed. Mixtures O and P were used to study the pyrolysis and oxidation of benzene, respectively.

TABLE II. Experimental Conditions

Mixture	Composition (% vol. in argon) Fuel	O_2	Temperature (K)	Pressure (bar)	C x 10^6 (mol/cm^3)	[C] x 10^{-17} (carbon atoms/cm^3)
A	0.311, C_7H_8	-	1525-2349	1.98-3.00	14.52-15.74	1.90-2.06
B	0.311, C_7H_8	0.311	1496-2391	1.87-3.08	15.03-15.49	1.97-2.03
C	1.75, C_7H_8	-	1684-2813	0.32-0.66	2.31- 3.13	1.71-2.31
D	1.75, C_7H_8	1.75	1668-2932	0.33-0.68	2.29- 3.15	1.69-2.33
E	0.10, C_7H_8	-	1647-2051	2.07-2.70	15.23-15.73	0.64-0.67
F	0.5627, C_7H_8	-	1463-2480	0.31-0.58	2.54- 2.89	0.60-0.69
G	1.0, C_{7H8}	-	1529-2932	1.99-3.73	14.83-16.10	6.25-6.79
H	4.65 C_2H_2	-	1687-3123	1.25-2.33	8.70- 9.22	4.87-5.16
I	4.65, C_2H_2	4.65	1532-3490	1.10-3.14	7.91-11.05	4.43-6.19
J	4.65, C_2H_2	1.5	1429-2259	1.08-1.70	8.74- 9.34	4.89-5.23
K	20.00 C_2H_2	-	1748-2802	0.28-0.49	1.95- 2.25	4.69-5.41
L	20.00, C_2H_2	6.45	1379-2623	0.22-0.37	1.73- 2.48	4.16-5.96
M	20.00, C_2H_2	4.30	1431-2758	0.20-0.40	1.67- 2.42	4.01-5.83
N	20.00, C_2H_2	2.15	1578-2997	0.26-0.50	1.70- 2.36	4.09-5.68
O	0.311, C_6H_6	-	1561-2273	1.94-2.87	14.90-15.59	1.67-1.75
P	0.311, C_6H_6	0.311	1516-2243	1.98-2.83	15.16-15.68	1.70-1.76

These experiments were performed with the partial support of the Office of Fossil Energy, U.S. Department of Energy, under the auspices of Grant Number DE-FG22-80PC30247.

Figures 1 and 2 present typical experimental records and Figure 3 explains our definitions of the induction time for soot appearance, τ_{soot}, and the rate of soot production, R_{soot}. There were some instances when the induction time and/or rate of soot formation could not be measured. They were: 1) when the shape of the laser extinction trace was such that the inflection point on the trace could not be clearly defined, which was particularly true for acetylene mixtures at low pressures; 2) at very low temperatures when τ_{soot} was longer than the observation time; 3) at very high temperatures when the induction time was very small or close to zero. It might still be possible to measure the rate of soot formation under condition 3).

Comparing the corresponding infrared emissions obtained at similar conditions in pyrolysis and oxidation of toluene (Figs. 1 and 2), we noted a slight decrease in the emission when oxygen was added. Since we would expect no CO or CO_2 to be present in pyrolysis, the observed decrease in the emission signals indicates that these signals are primarily due to the "black body radiation" of soot particles and the contribution from CO and CO_2 molecules is probably negligible. Therefore, we must conclude that it is impossible to monitor CO and CO_2 under the conditions employed. Rawlins and co-workers [80] came to a similar conclusion in their work. Therefore, no further attempts to monitor CO and CO_2 were undertaken in the rest of the study.

The measured soot yields, induction times for soot appearance and rates of soot formation are reported in Figures 4 through 25. Figures 4-7 show the effect of oxygen on soot formation from toluene at high pressures. As can be seen from these figures, oxygen suppresses the formation of soot; this effect is qualitatively somewhat similar to that resulting from a reduction in the initial concentration of toluene (see Fig. 26). At lower pressures (Figs. 8-11), the

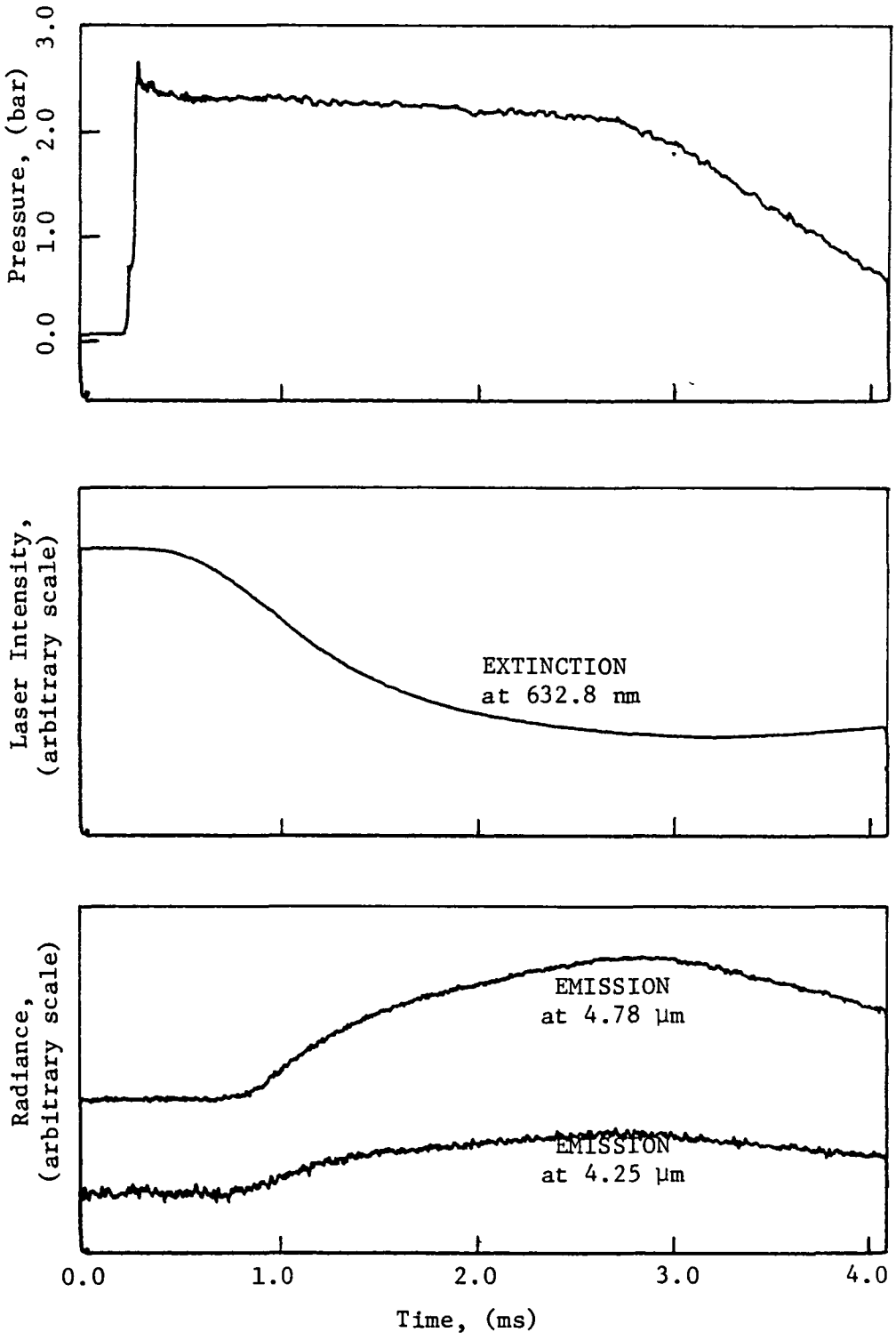

FIGURE 1. Experimental records obtained with a 0.311% toluene-argon mixture at reflected shock conditions of T_5 = 1885K, P_5 = 2.37 bar and $[C]_5 = 1.99 \times 10^{17}$ carbon-atoms/cm^3.

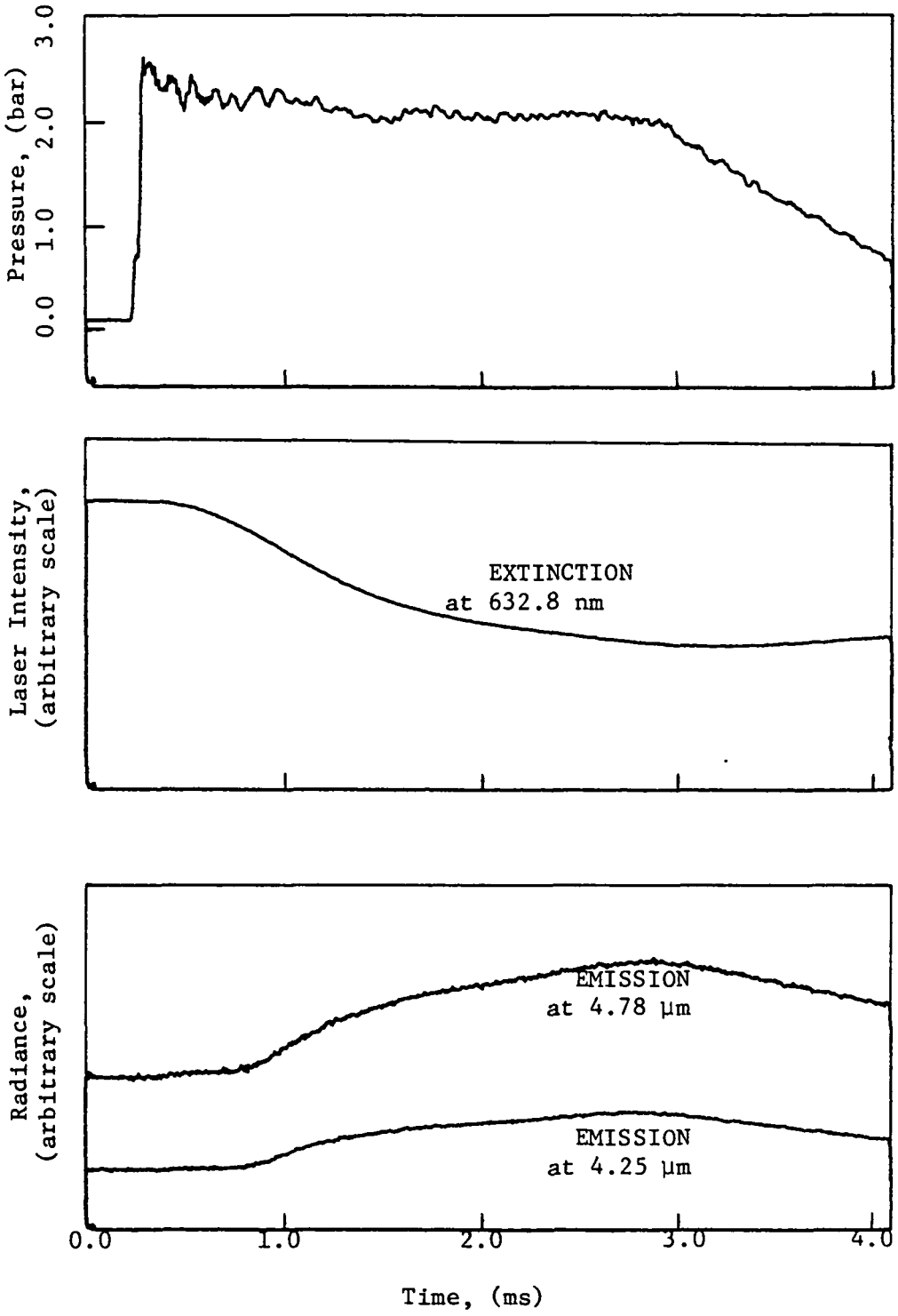

FIGURE 2. Experimental records obtained with a 0.311% toluene - 0.311% oxygen-argon mixture at reflected shock conditions of T_5 = 1898K, P_5 = 2.42 bar and $[C]_5$ = 2.01 x 10^{17} carbon-atoms/cm^3.

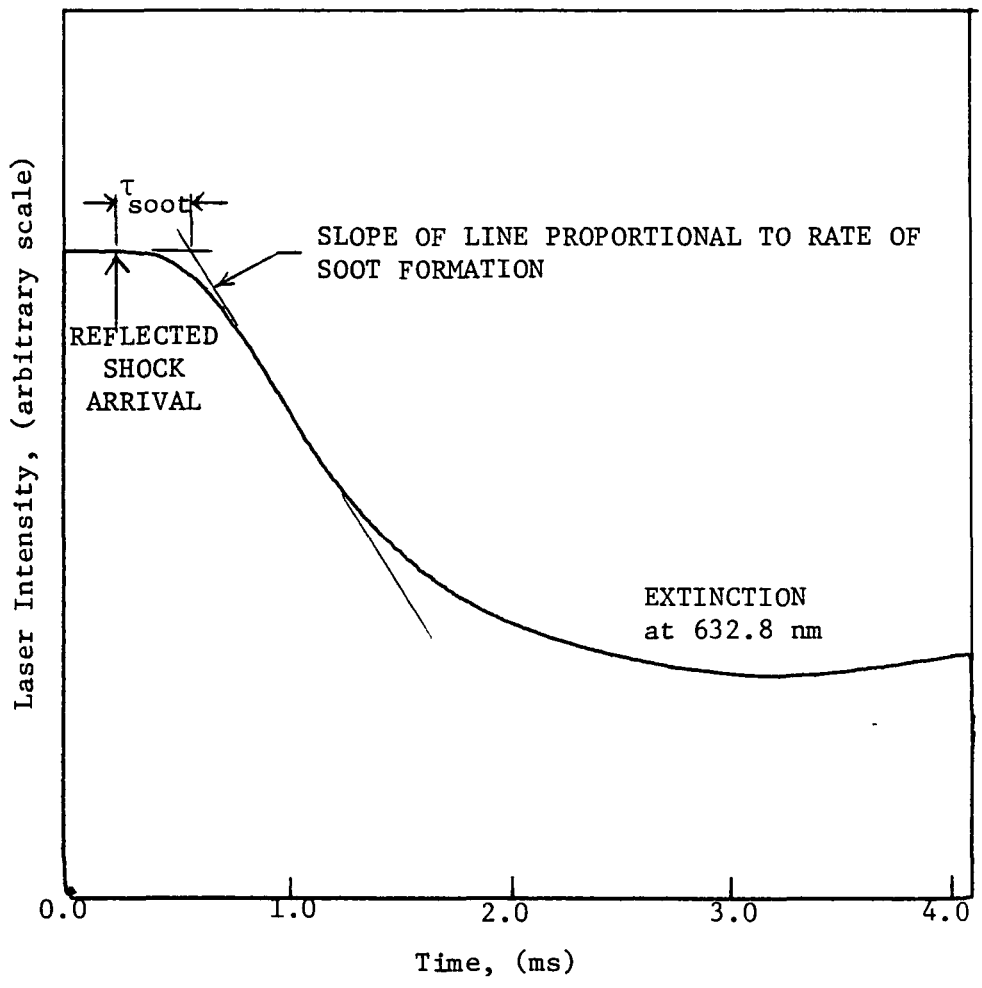

FIGURE 3. Definitions of induction time for soot appearance, τ_{soot}, and rate of soot formation, R_{soot}.

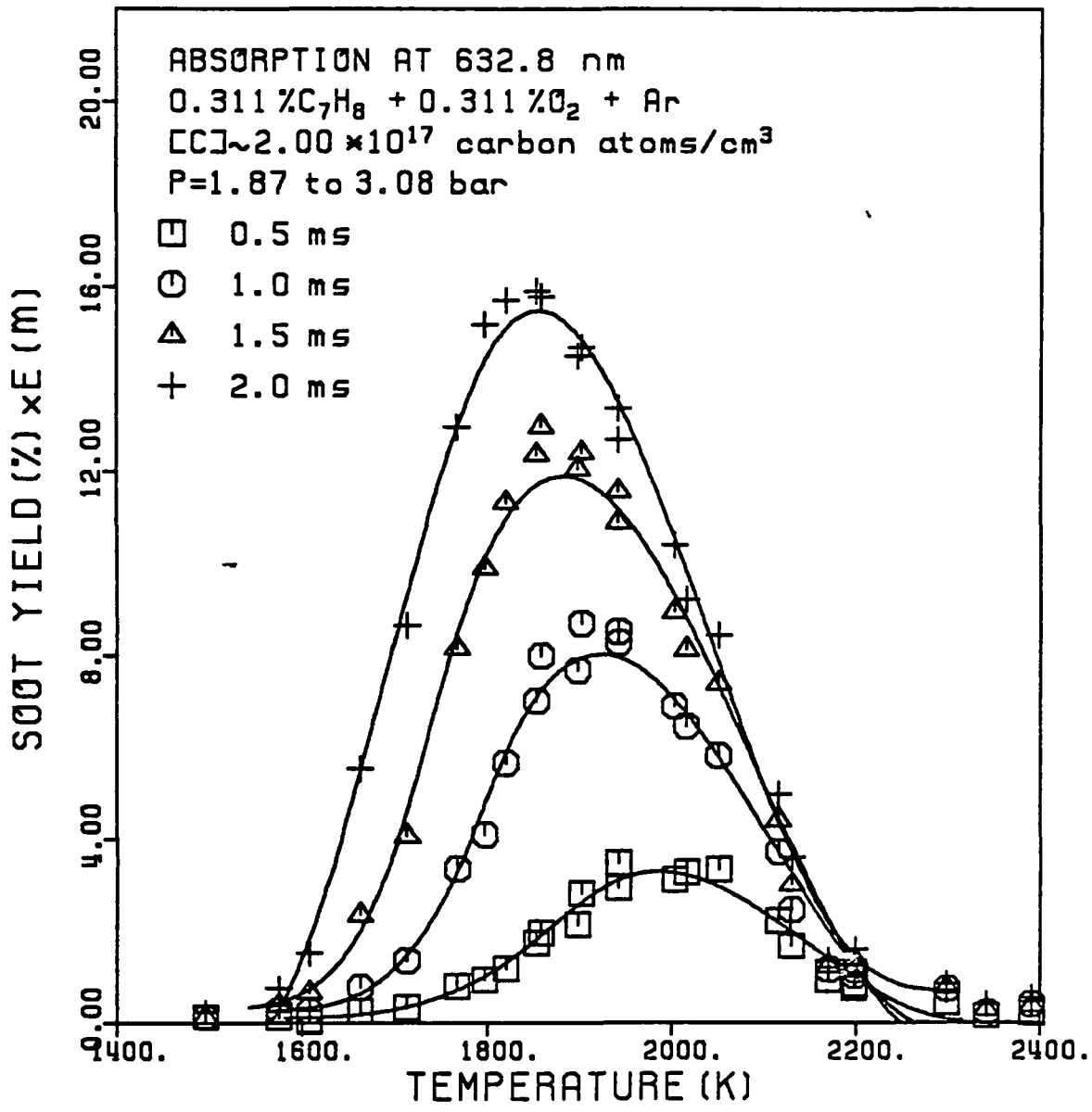

FIGURE 4. Soot yields versus temperature at different reaction times in 0.311% toluene - 0.311% oxygen-argon mixtures.

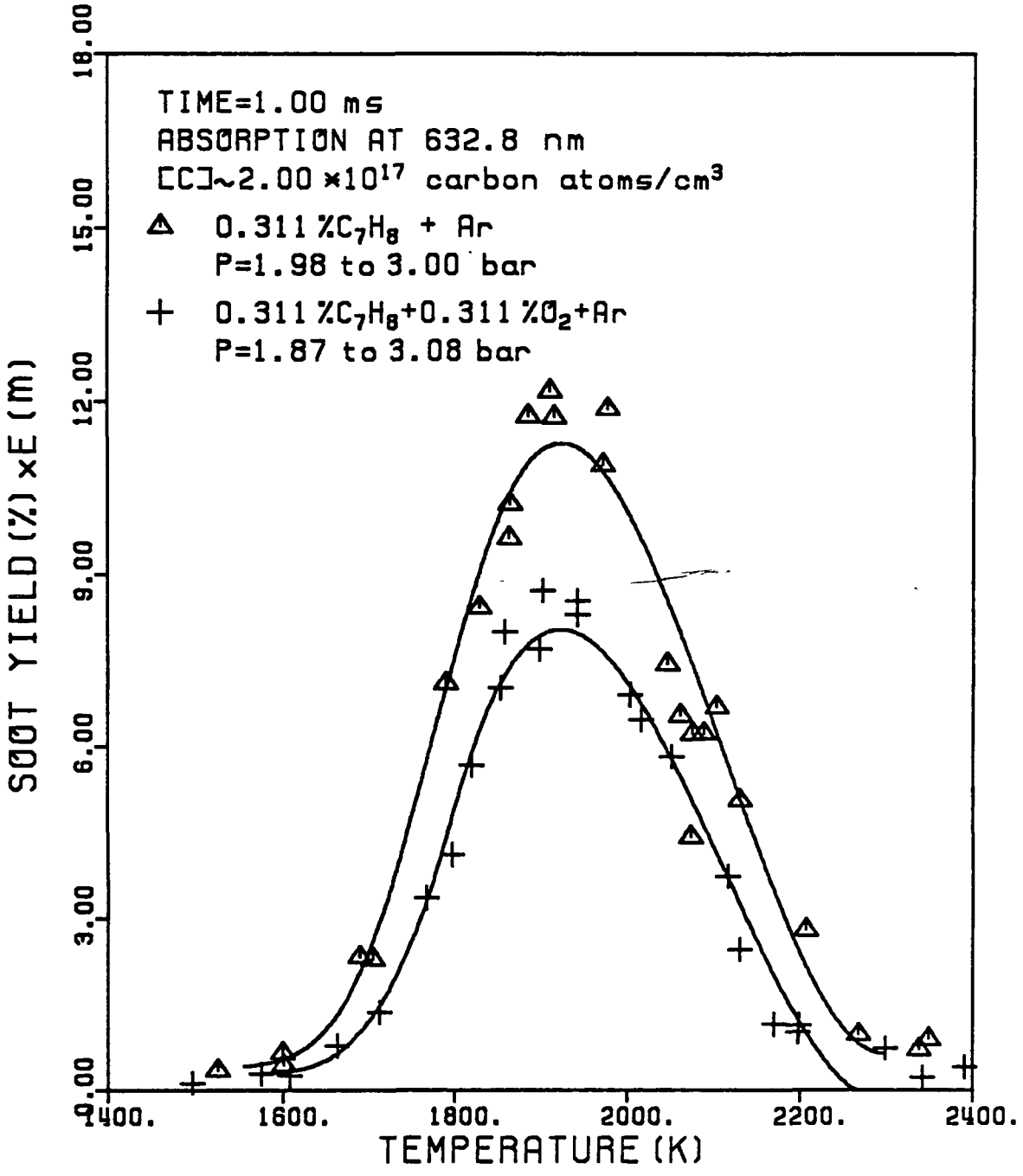

FIGURE 5. The influence of oxygen on soot yield in toluene mixtures at high pressures.

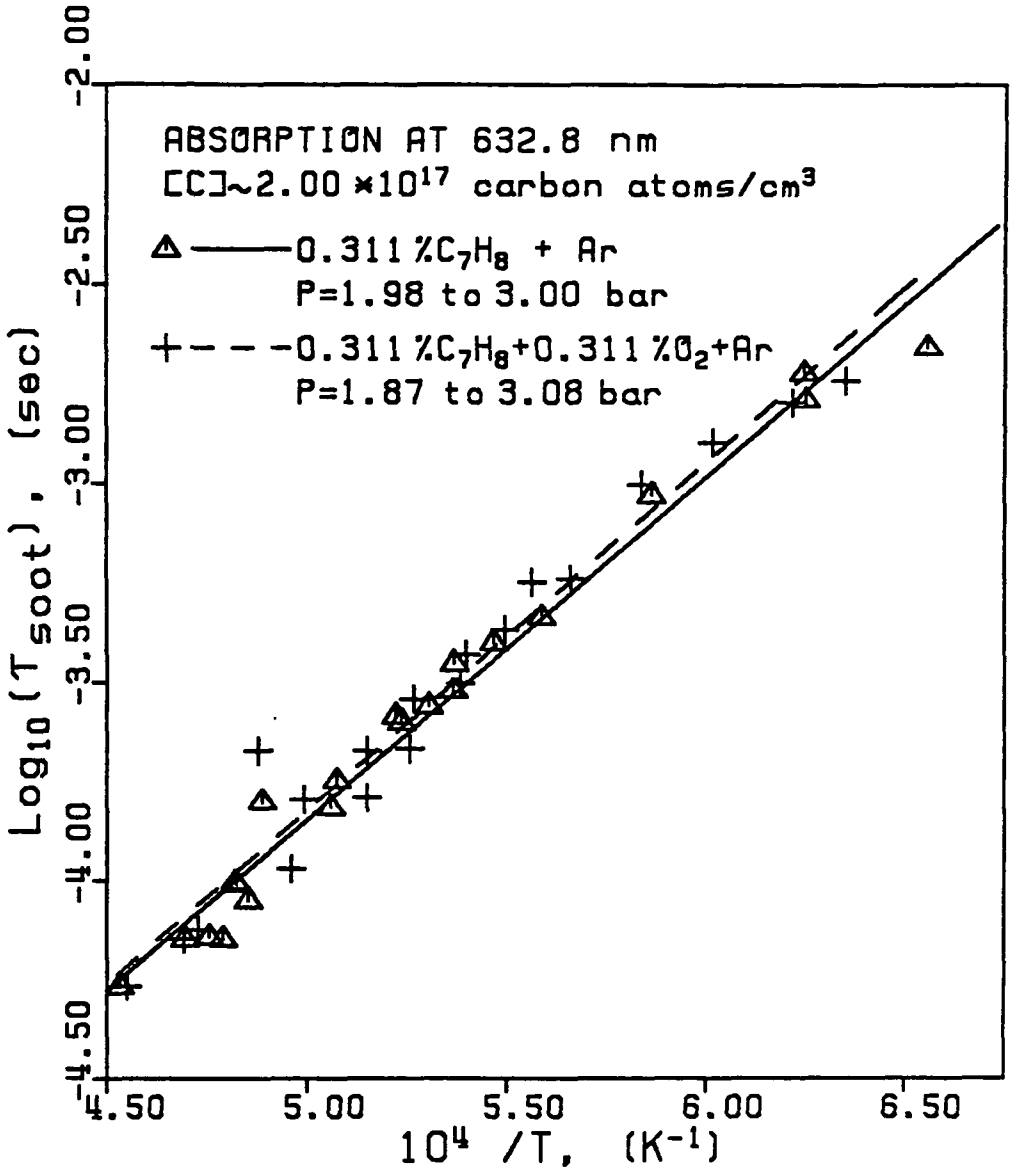

FIGURE 6. Induction times for soot appearance versus inverse temperature in toluene mixtures at high pressures.

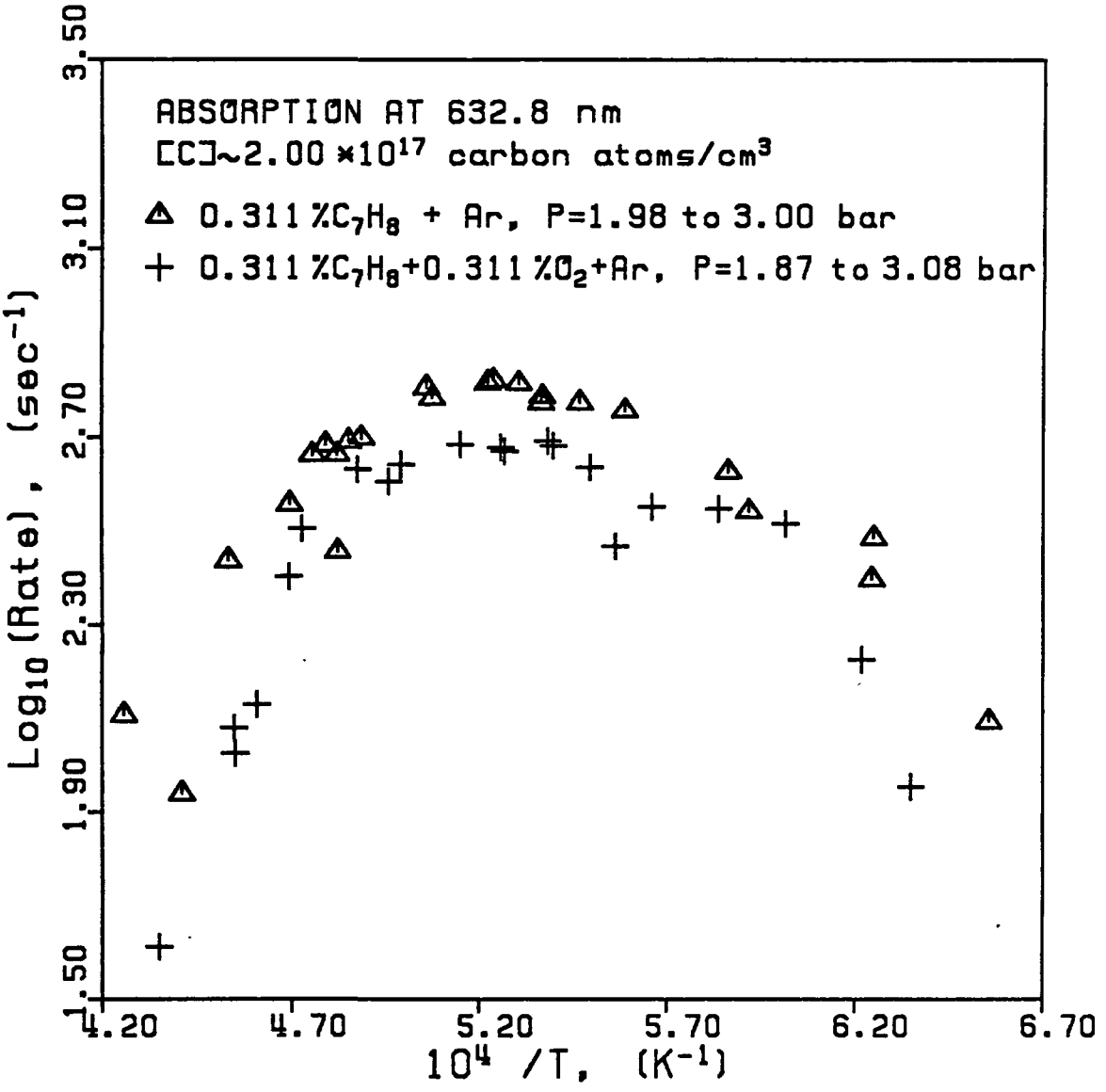

FIGURE 7. Rates of soot formation versus inverse temperature in toluene mixtures at high pressures.

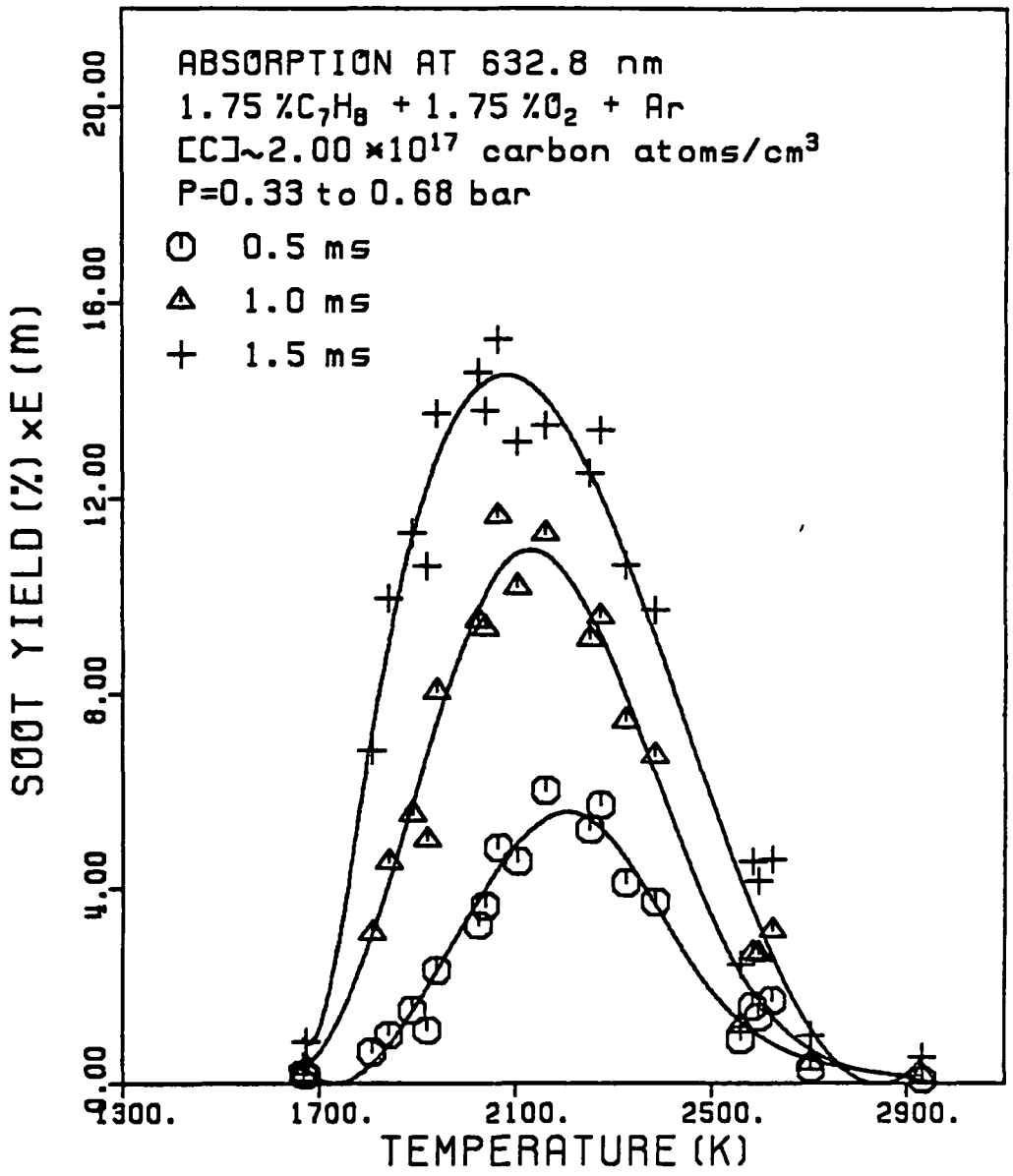

FIGURE 8. Soot yields versus temperature at different reaction times in 1.75% toluene - 1.75% oxygen-argon mixtures.

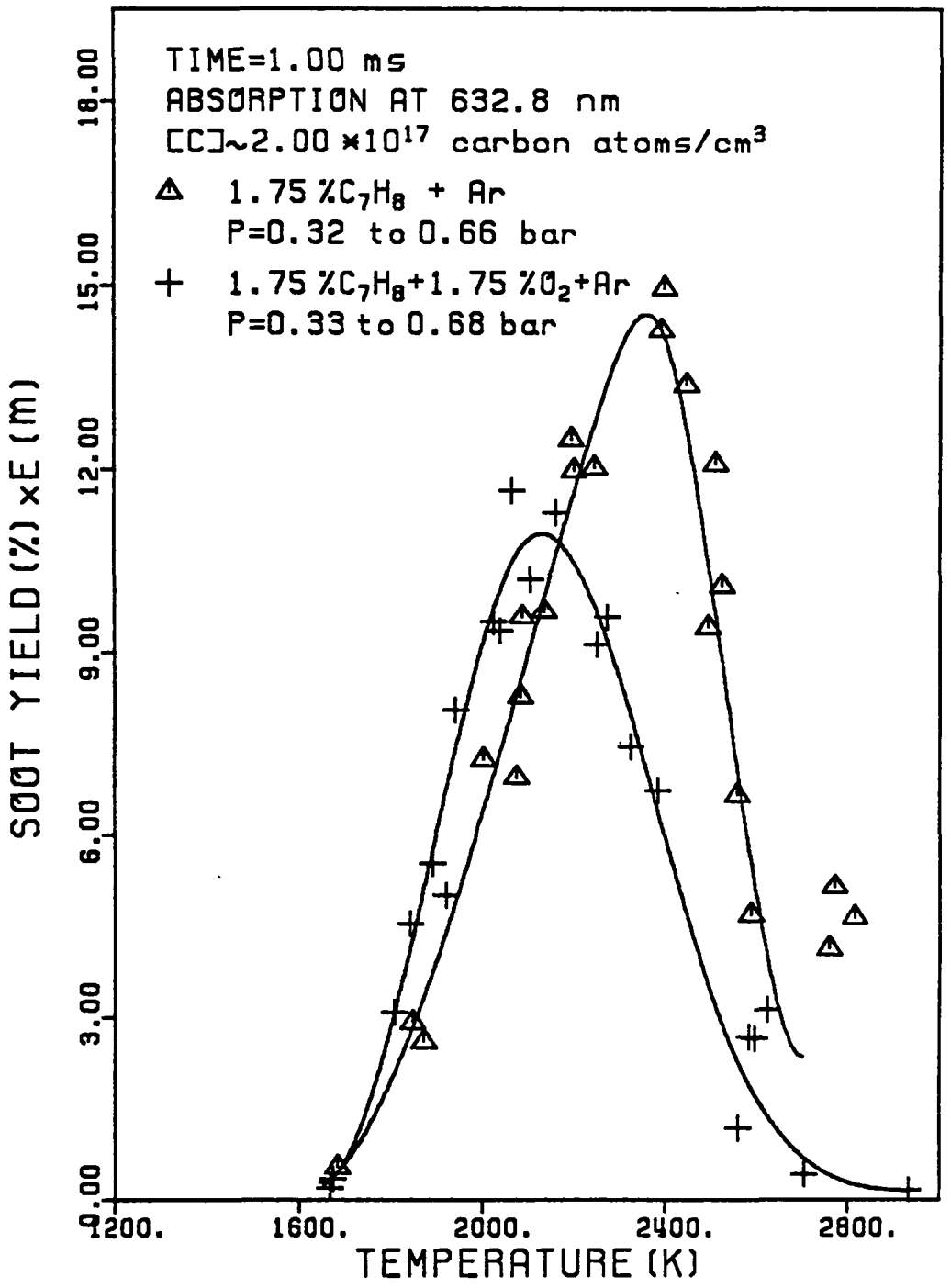

FIGURE 9. The influence of oyxgen on soot yield in toluene mixtures at low pressures.

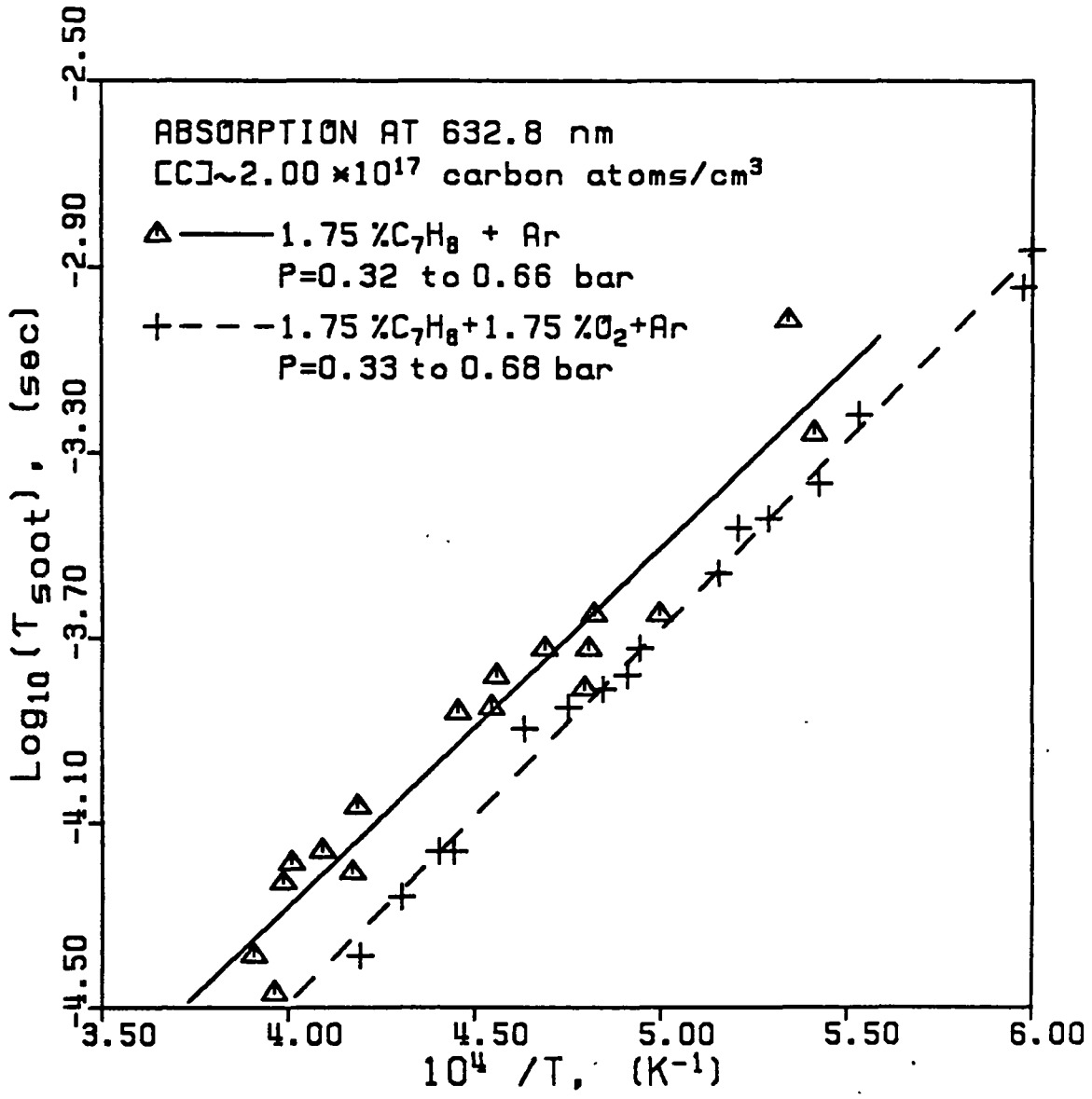

FIGURE 10. Induction times for soot appearance versus inverse temperature in toluene mixtures at low pressures.

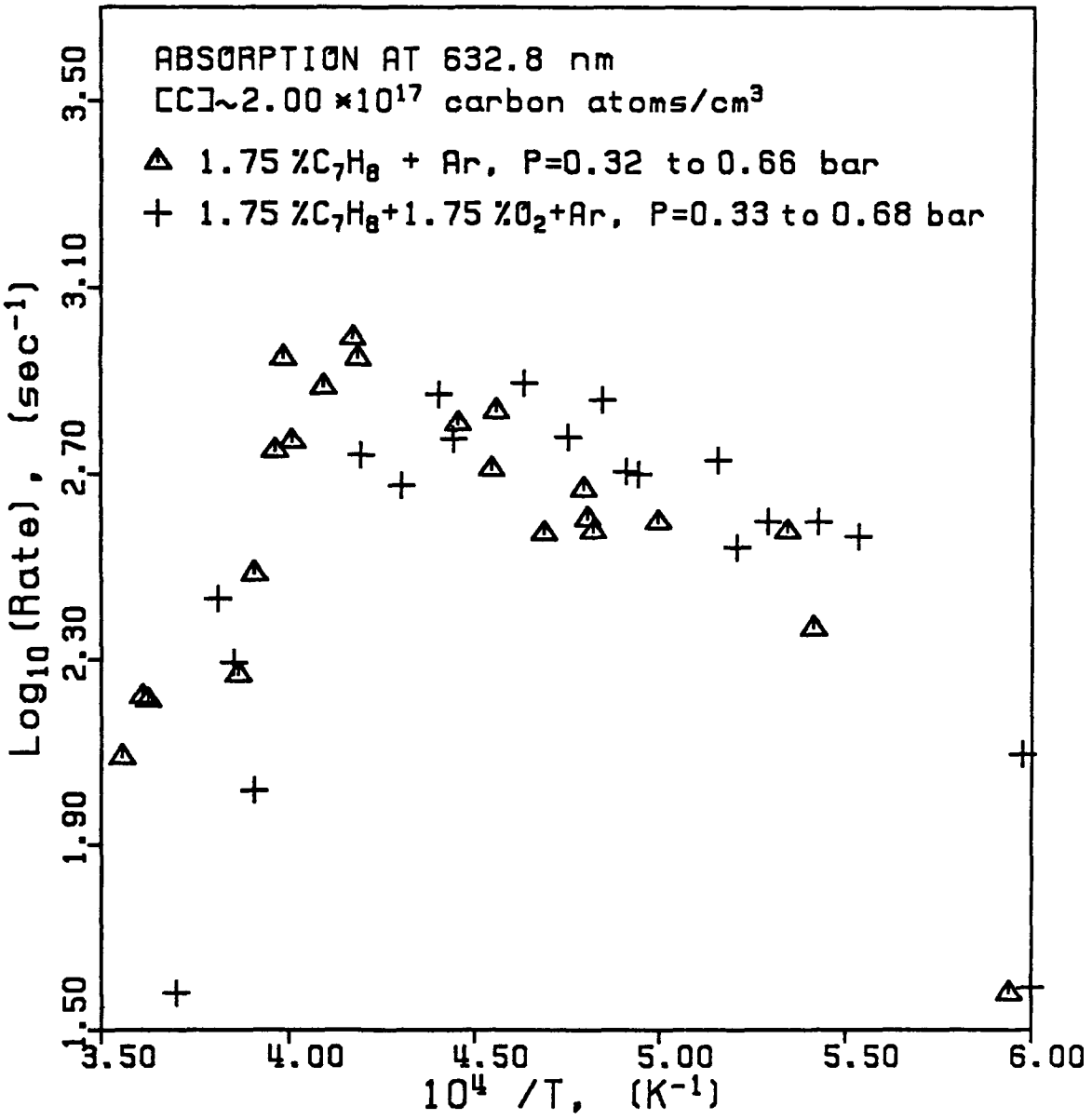

FIGURE 11. Rates of soot formation versus inverse temperature in toluene mixtures at low pressures.

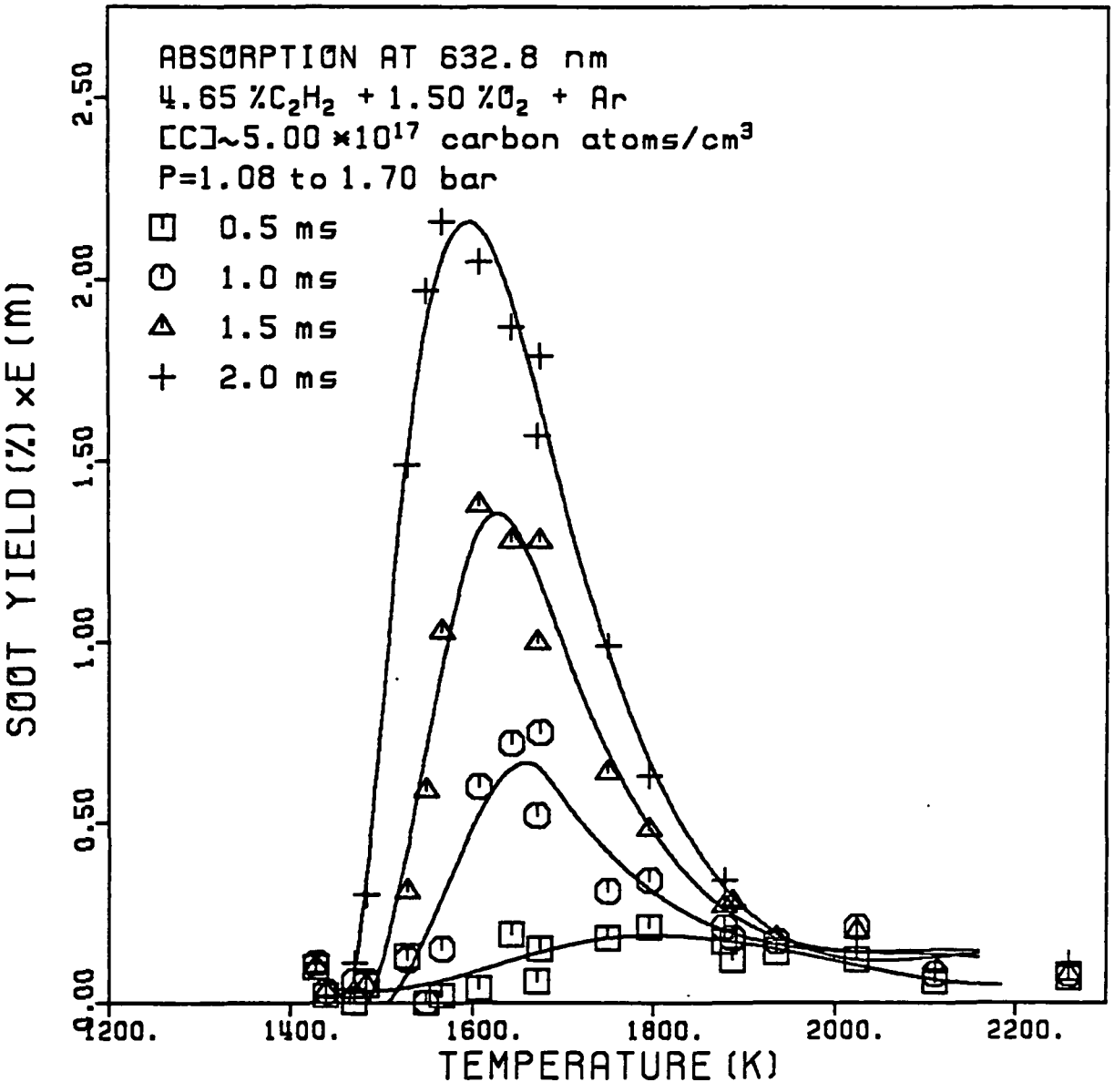

FIGURE 12. Soot yields versus temperature at different reaction times in 4.65% acetylene - 1.50% oxygen-argon mixtures.

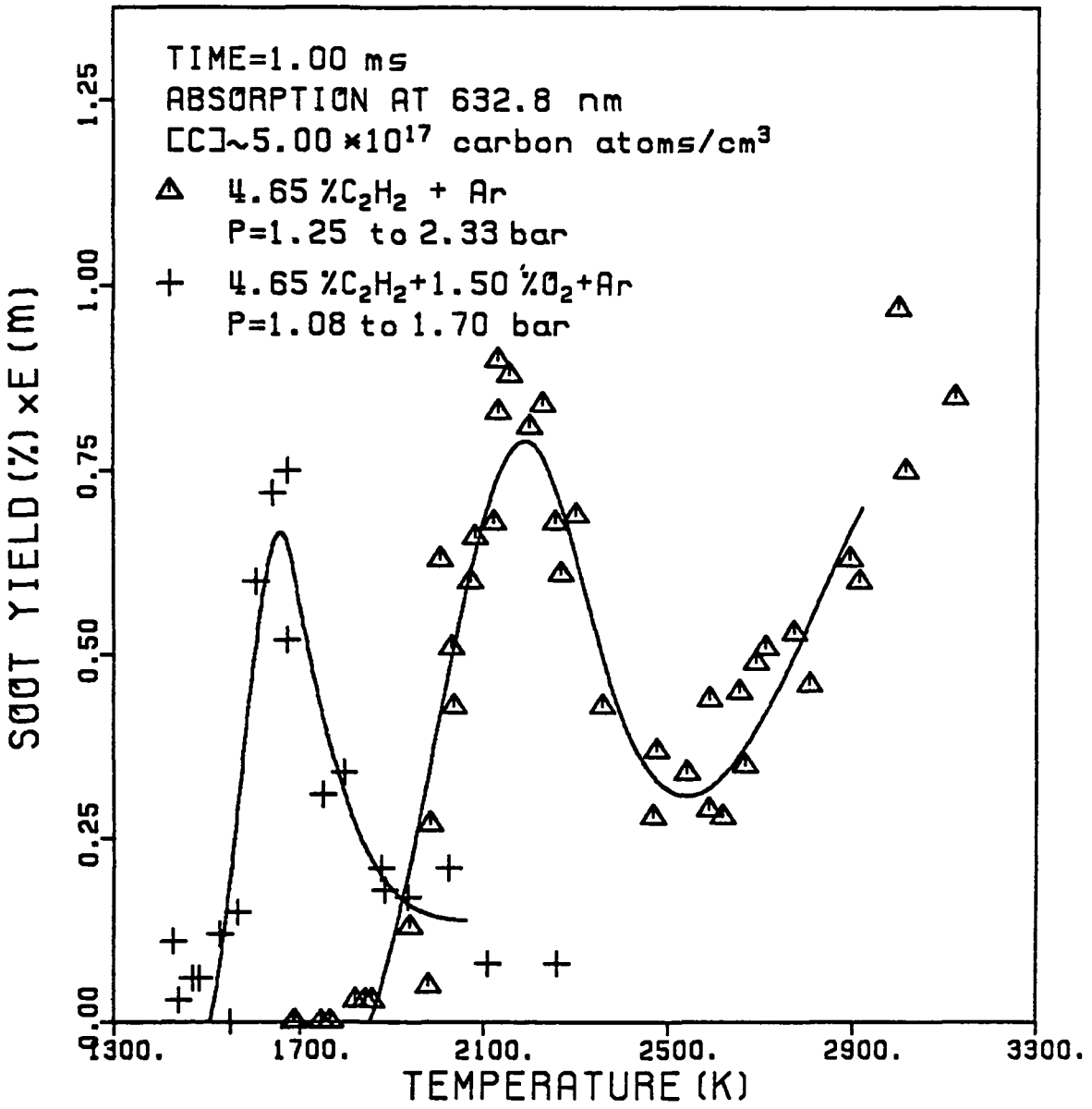

FIGURE 13. The influence of oxygen on soot yields in acetylene mixtures at high pressures.

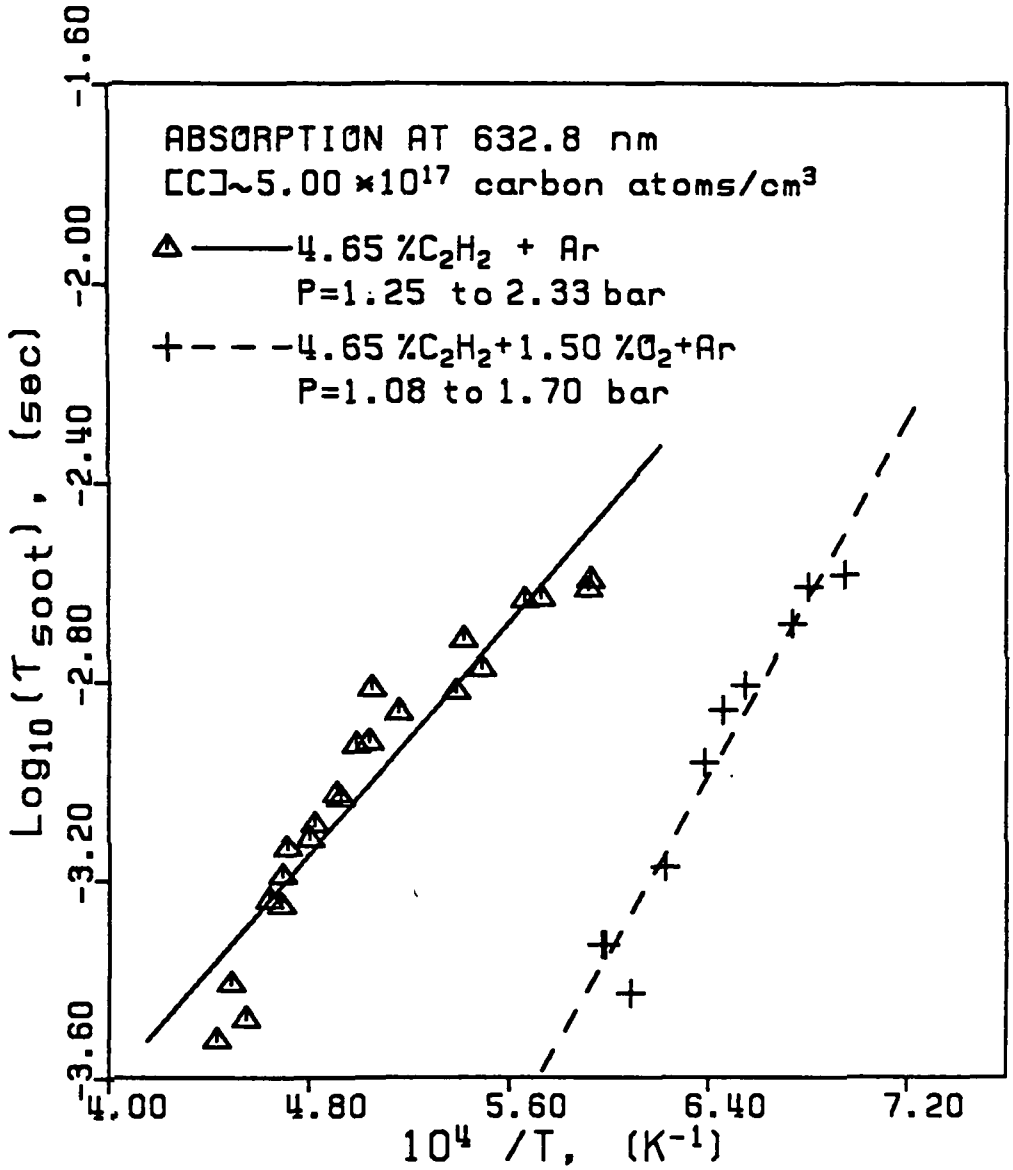

FIGURE 14. Induction times for soot appearance versus inverse temperature in acetylene mixtures at high pressures.

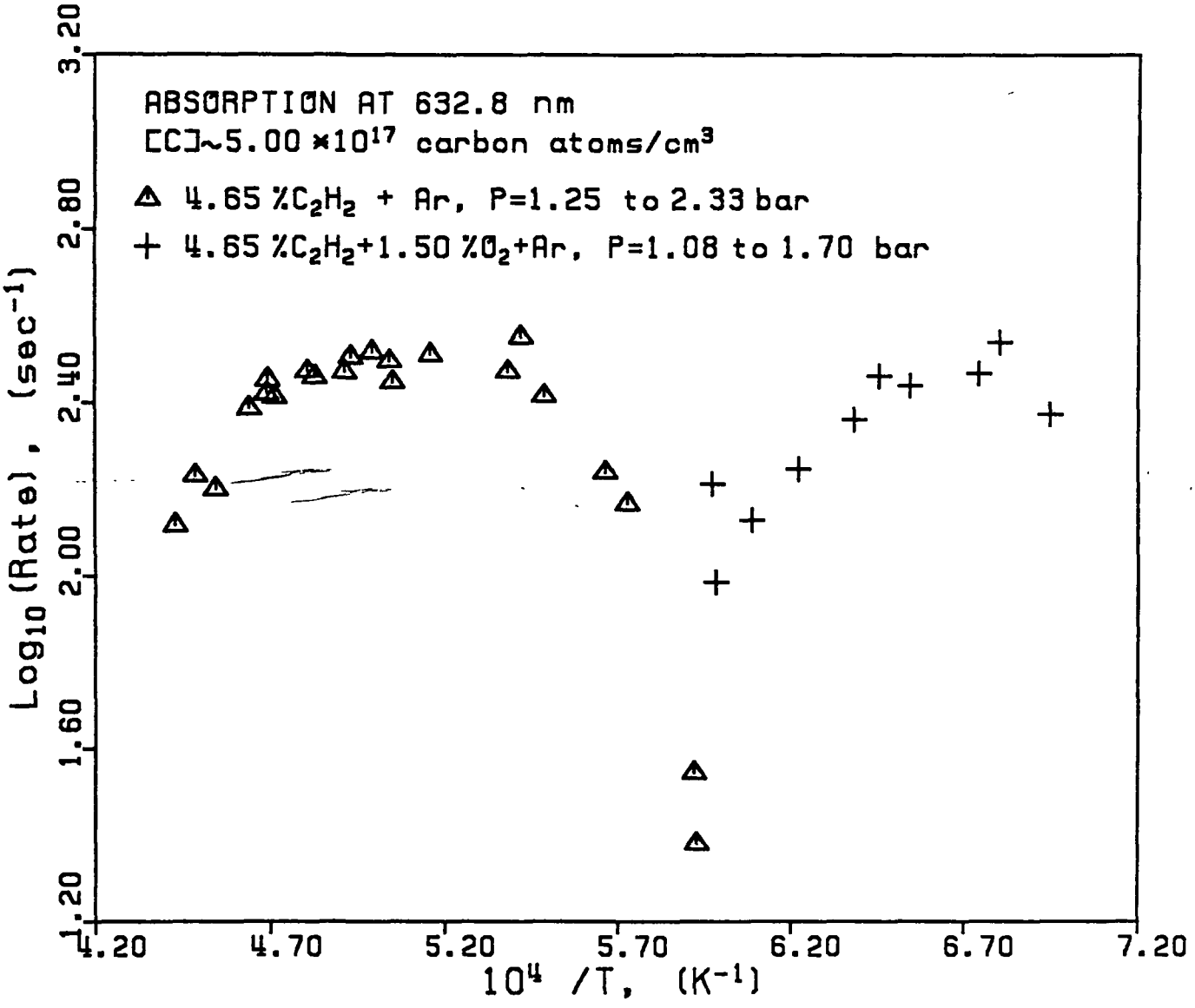

FIGURE 15. Rates of soot formation versus inverse temperature in acetylene mixtures at high pressures.

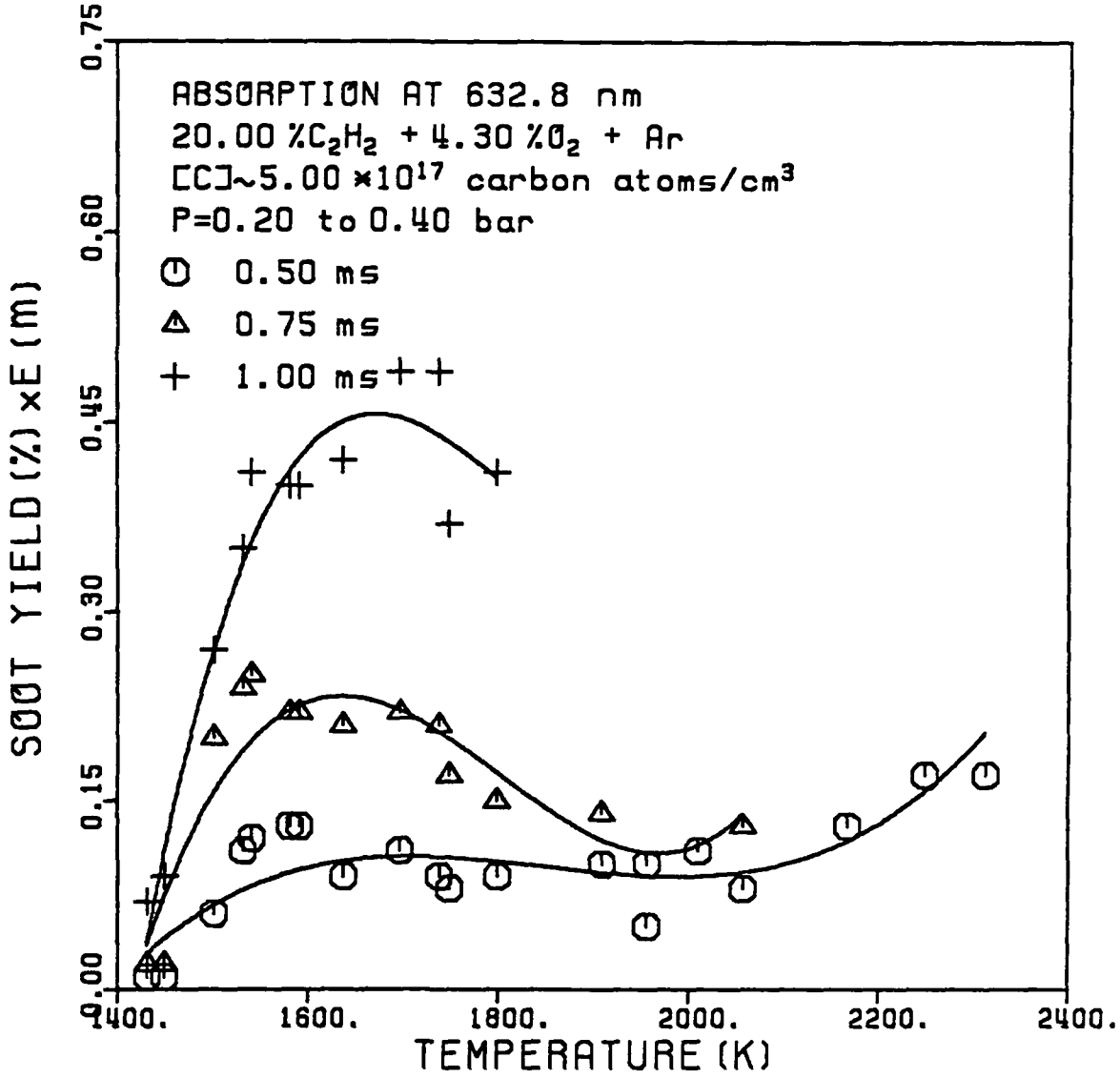

FIGURE 16. Soot yields versus temperature at different reaction times in 20.0% acetylene - 4.30% oxygen-argon mixtures.

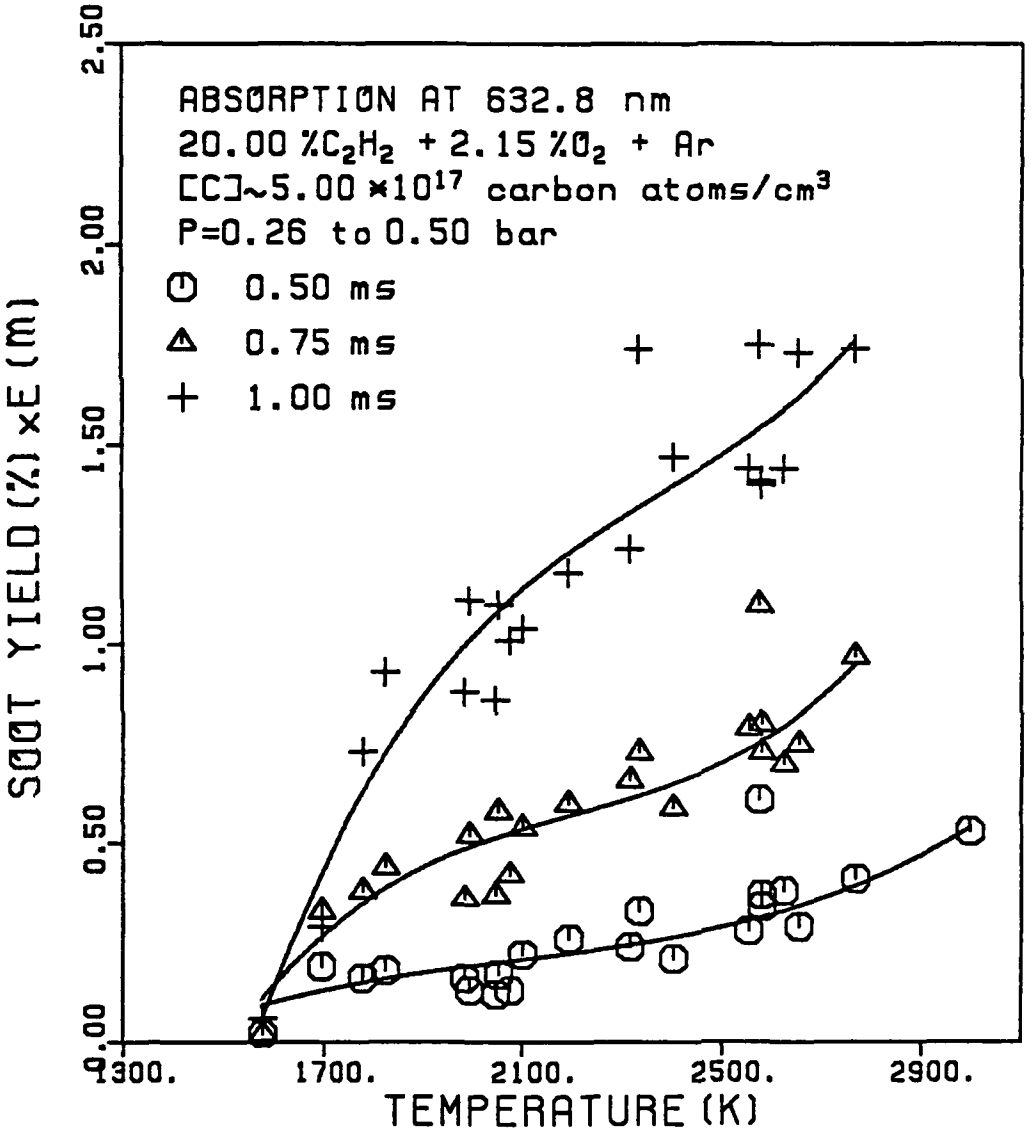

FIGURE 17. Soot yields versus temperature at different reaction times in 20.0% acetylene - 2.15% oxygen-argon mixtures.

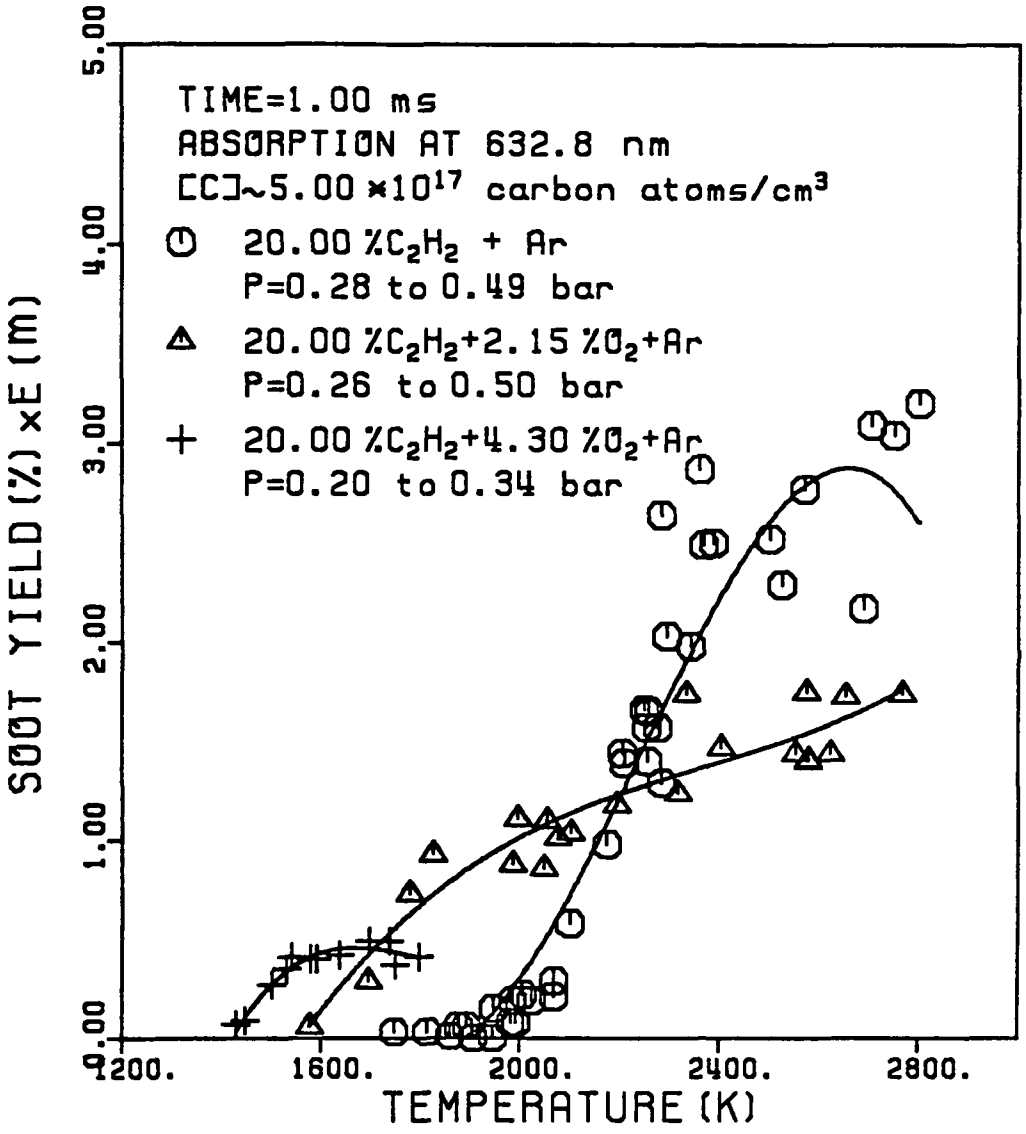

FIGURE 18. The influence of oxygen on soot yields in acetylene mixtures at low pressures.

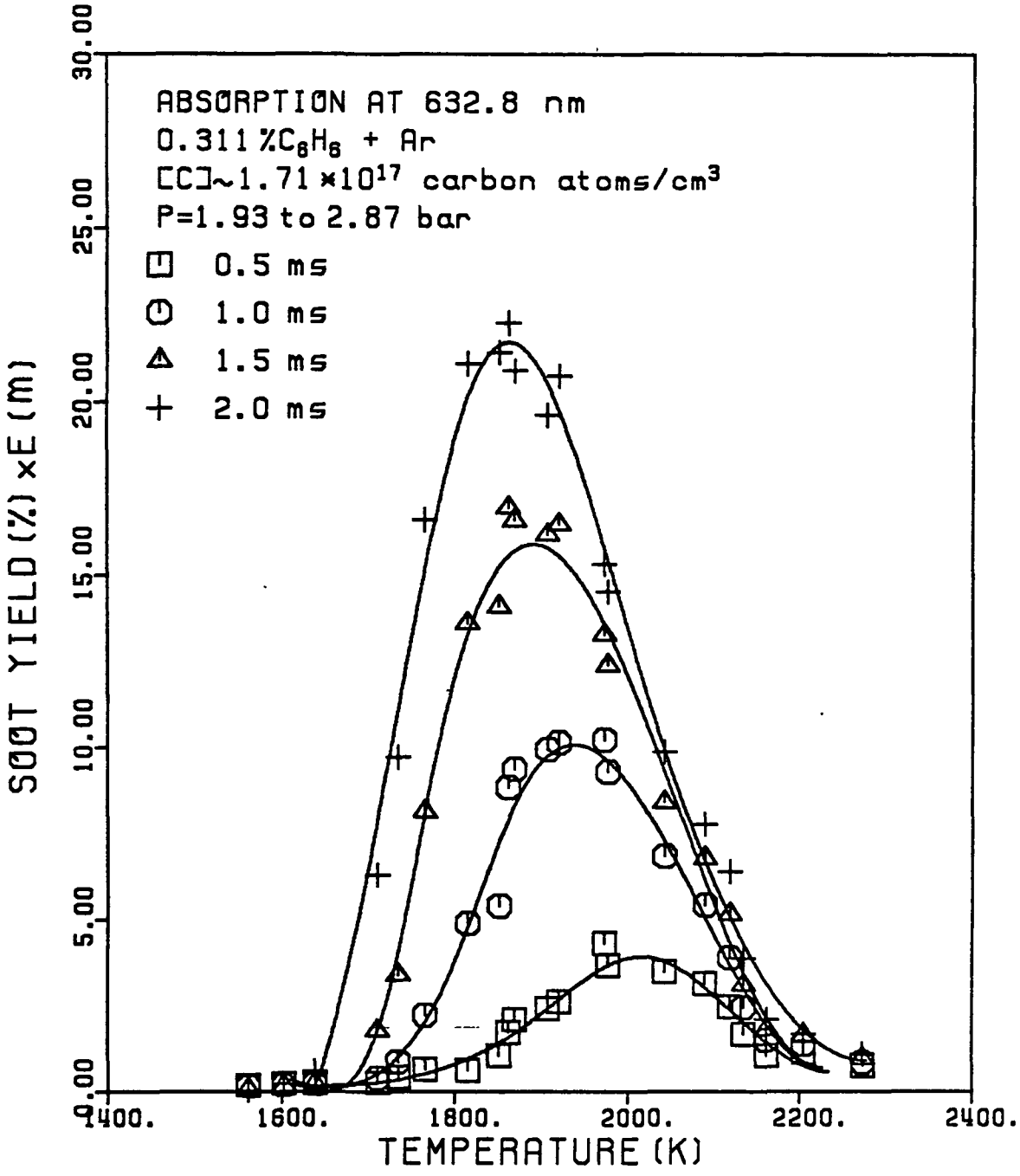

FIGURE 19. Soot yields versus temperature at different reaction times in 0.311% benzene-argon mixtures.

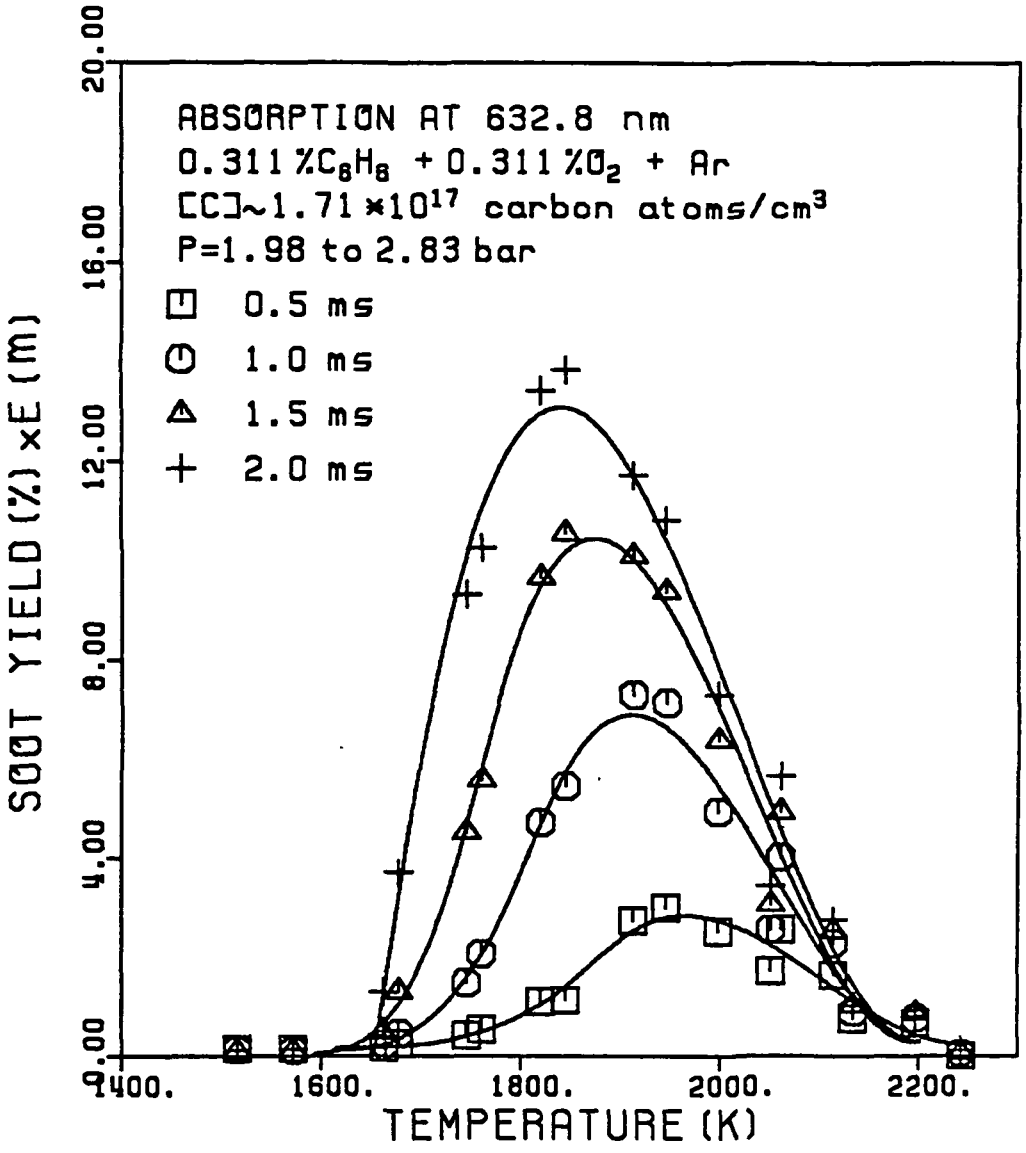

FIGURE 20. Soot yields versus temperature at different reaction times in 0.311% benzene - 0.311% oxygen-argon mixtures.

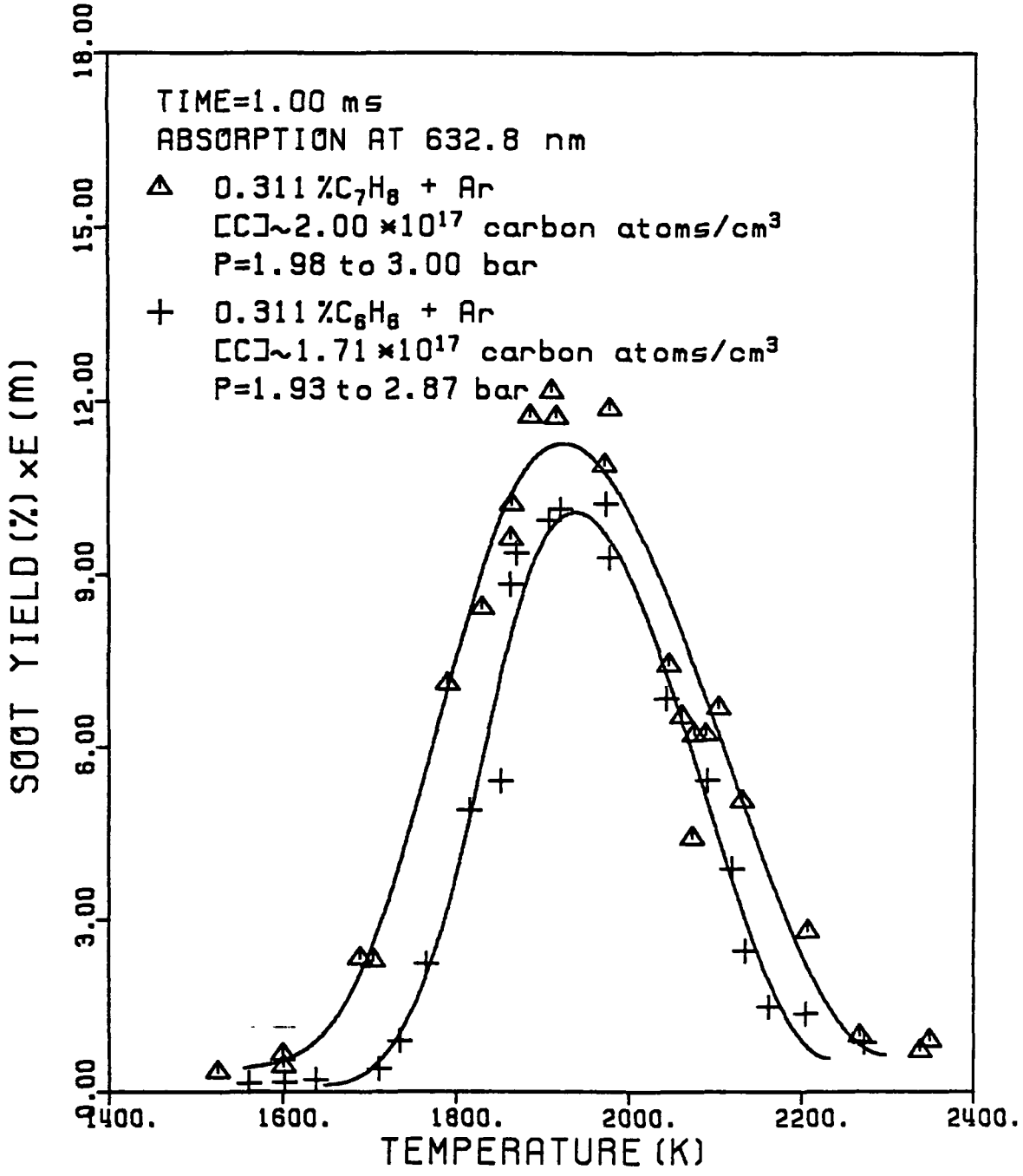

FIGURE 21. Comparsion of soot yields obtained in toluene and benzene pyrolysis.

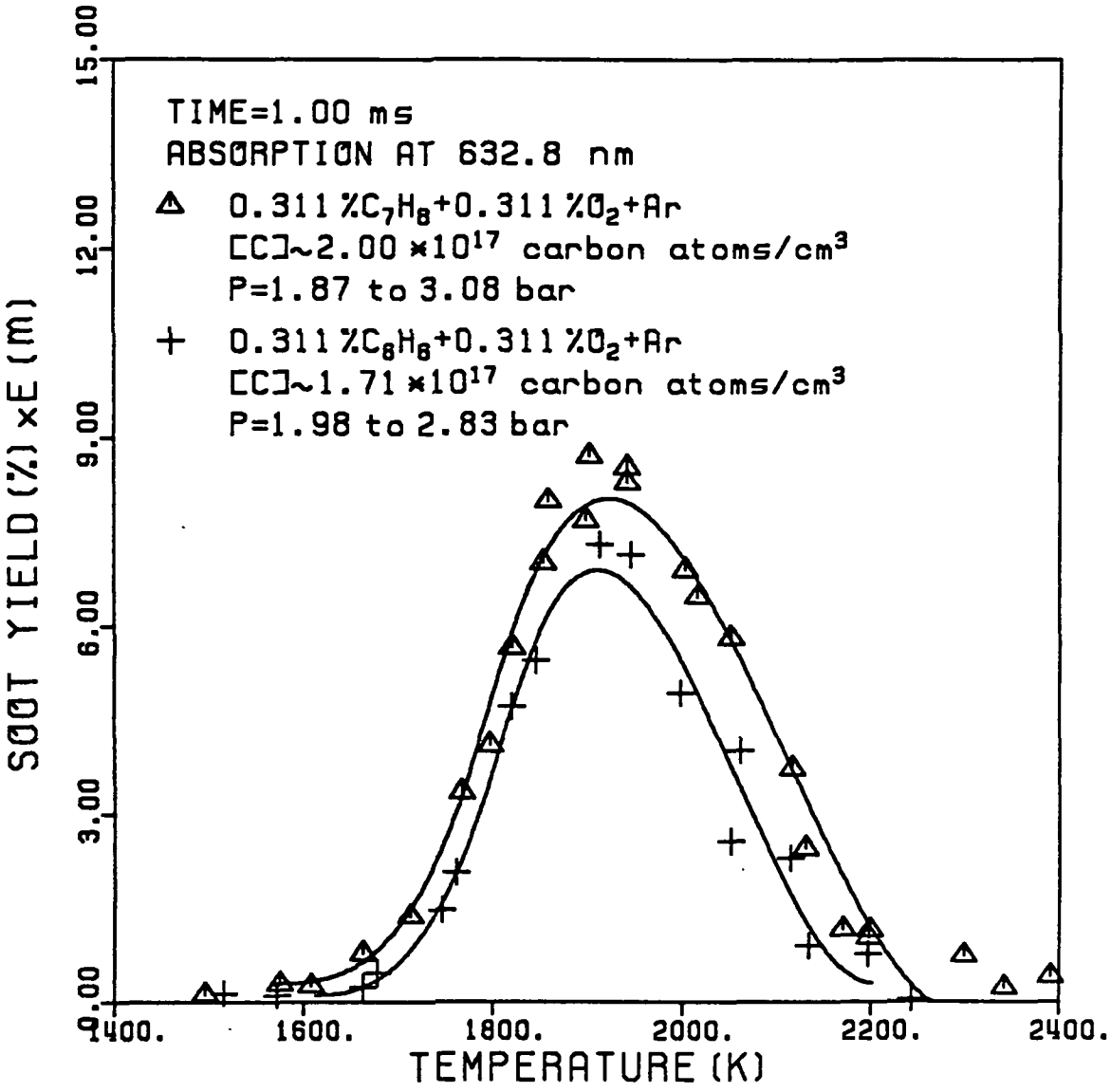

FIGURE 22. Comparison of soot yields obtained in toluene and benzene oxidation.

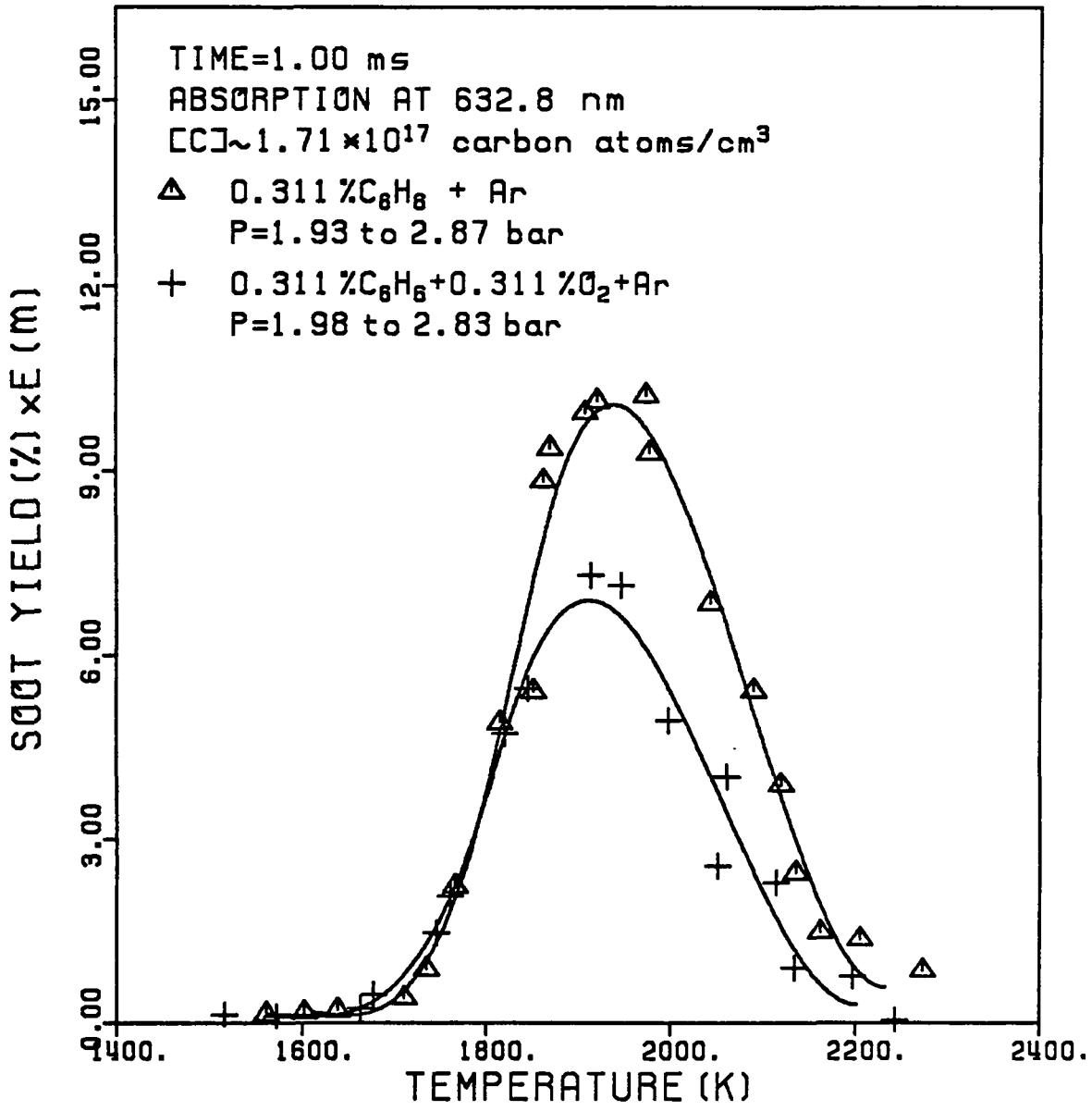

FIGURE 23. The influence of oxygen on soot yield in benzene mixtures.

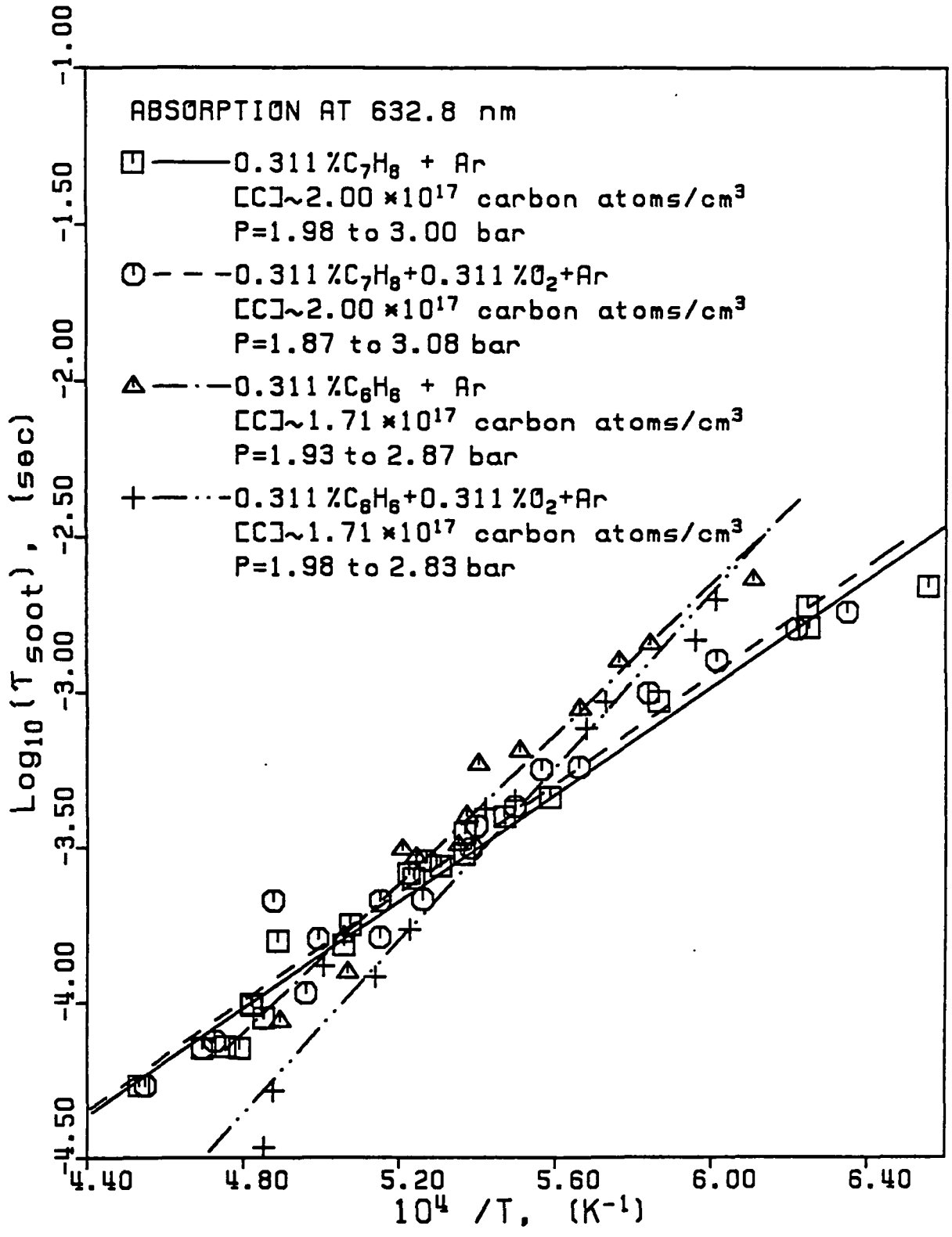

FIGURE 24. Comparison of induction times for soot appearance in toluene and benzene mixtures.

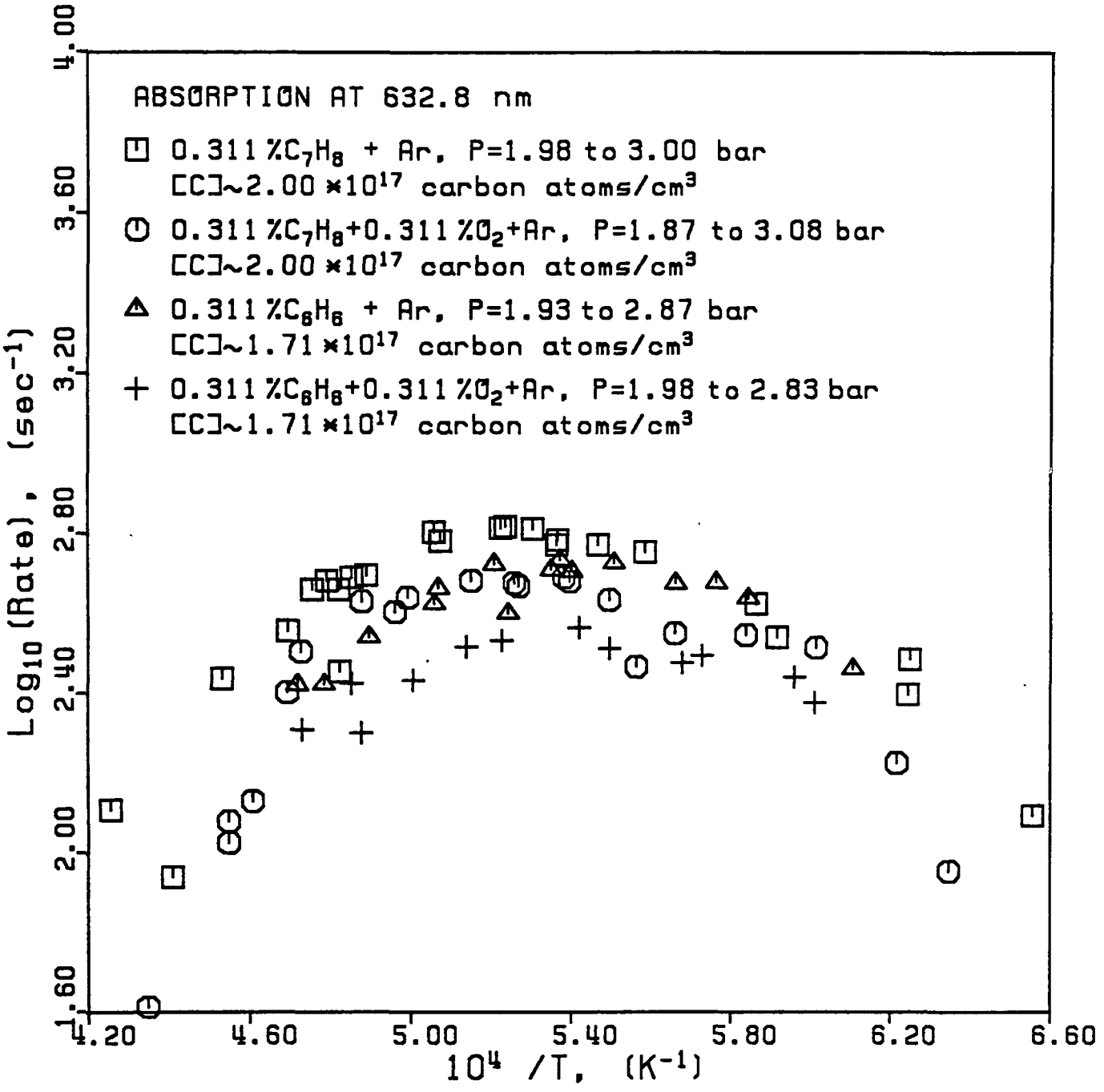

FIGURE 25. Comparison of rates of soot appearance in toluene and benzene mixtures.

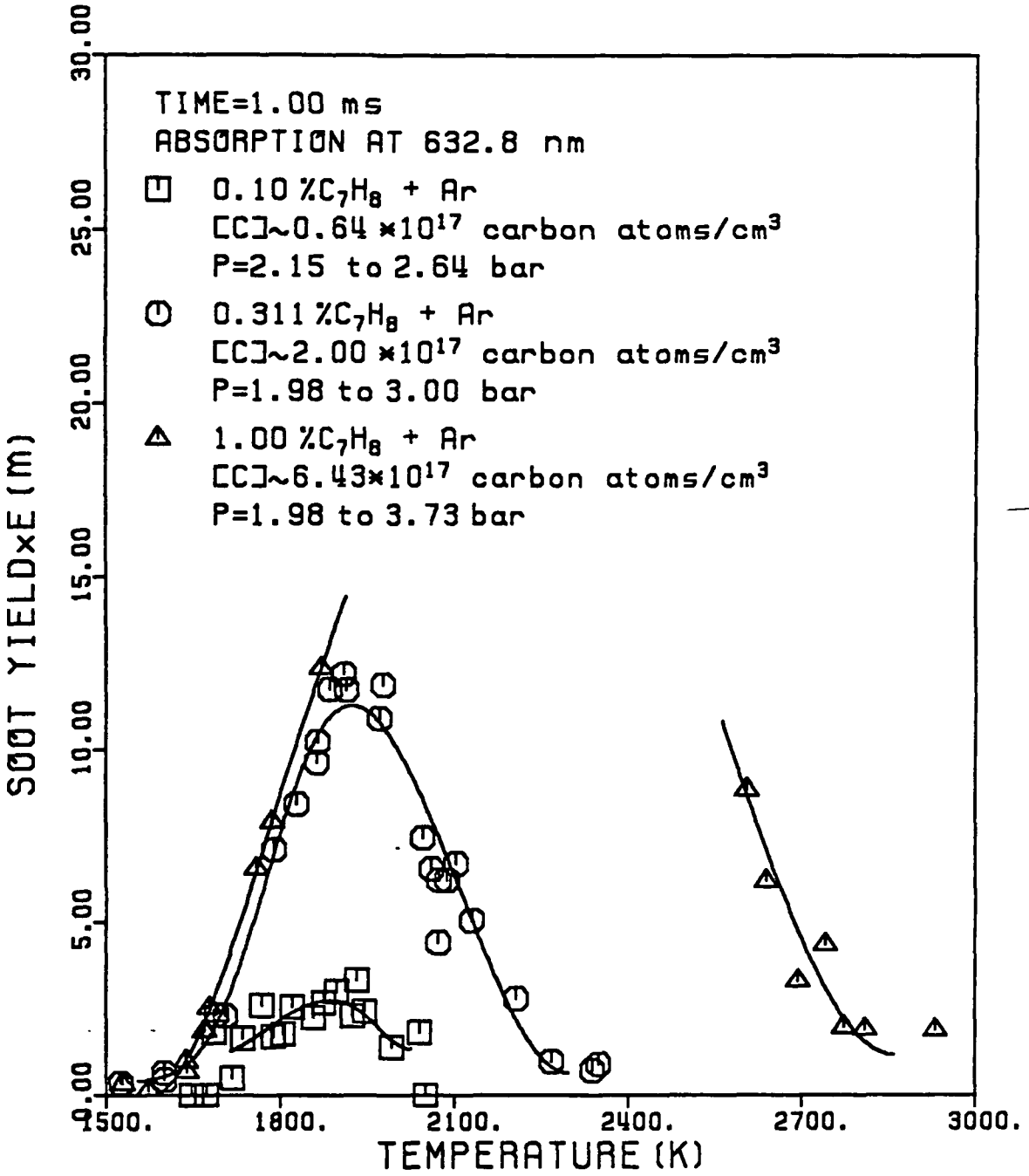

FIGURE 26. Soot yields versus temperature in toluene-argon mixtures at a reaction time of 1 ms.

addition of oxygen not only reduces the maximum soot yield but also shifts the maximum to a lower temperature. In other words, at low pressures and low temperatures oxygen actually promotes soot formation.

Figures 12 through 18 present the results obtained with acetylene mixtures. In larger amounts, oxygen completely suppresses the production of soot (Mixtures I and L). The addition of oxygen in smaller quantities shifts the soot yield "bell" to lower temperatures. This shift is much more pronounced than that in the toluene case. Furthermore, the shift in the case of acetylene is observed throughout the pressure range tested while the shift was observed in toluene mixtures only at lower pressures. It is interesting to note, however, that the sensitivity of the soot yields to oxygen concentration in acetylene mixtures is much higher at lower pressures than at higher ones.

Figures 19- 25 present soot yields observed in pyrolysis and oxidation of benzene. As can be seen in these Figures, there is no significant difference between the results obtained in benzene and toluene mixtures.

Figure 26 presents the results obtained in pyrolysis of toluene. The conditions used in these mixtures allow one to determine the dependence of soot yield on the initial concentration of toluene. The reasons for this dependance can be qualitatively understood by referring to a recently published conceptual model [54].

DISCUSSION

The most striking experimental observation is the shift of the soot-yield bell to lower temperatures when oxygen is added. However, prior to discussion of this result, one would like to estimate the temperature change during the reaction. The overall combustion mechanism is composed of many elementary

reactions, each either endothermic or exothermic; therefore, it is most probable that the temperature behind the reflected shock wave will change with time. Since we cannot measure the temperature in situ, it was decided to estimate the temperature change, which may occur in combustion of toluene and acetylene under our experimental conditions, via computer modeling.

1. Estimation of Temperature Change During Oxidation of Toluene.

To simulate the oxidation of toluene, we chose the mechanism of Jachimowski [81-83]. The mechanism involves 24 chemical species and 52 elementary reactions. The reactions and their forward rate constants are given in Table III. The reverse rate constants were calculated using the equilibrium constants, the thermochemical data for which were taken from the updated NASA polynomials of Burcat [84].

It is not suggested here that Jachimowski's mechanism represents the reaction process exactly; for example, it does not account for soot formation. However, no other mechanism is available which is clearly superior for our purposes. Although better estimates of some of the rate constants are now available, Jachimowski presented a unified mechanism which had rate constants adjusted to reproduce observed experimental data obtained in shock tubes. We believe, therefore, that the temperature changes predicted by the Jachimowski mechanism can be expected to match actual values reasonably well, allowing the estimation of possible variations in the temperature behind reflected shock waves at our conditions.

The Jachimowski mechanism was incorporated into a constant-density computer model which used the latest version (1982) of LSODE [85]. The gas mixtures used in the simulation were those of Mixture B, i.e. 0.311% toluene - 0.311% oxygen

TABLE III

Reaction Mechanism for Toluene Oxidation

Reaction Number	Reaction	Rate Constant for Forward Direction[a] $\log_{10}A$	n	θ	Reference
1	$C_7H_8+O_2 = C_7H_7+HO_2$	14.0	0	20130	[81]
2	$C_7H_8=C_7H_7+H$	15.5	0	44440	[81]
3	$C_7H_8=C_6H_5+CH_3$	17.0	0	52550	[81]
4	$H+C_7H_8=C_7H_7+H_2$	14.0	0	3420	[81]
5	$O+C_7H_8=OH+C_7H_7$	14.0	0	3625	[81]
6	$OH+C_7H_8=H_2O+C_7H_7$	13.0	0	1510	[81]
7	$O+C_7H_7=CH_2O+C_6H_5$	13.0	0	0	[81]
8	$O_2+C_7H_7=2CO+C_3H_5+C_2H_2$	12.7	0	7550	[81]
9	$C_7H_7=C_4H_3+C_3H_4$	15.0	0	51330	[81]
10	$C_3H_5=CH_3+C_2H_2$	14.0	0	27180	[81]
11	$C_3H_5=C_3H_4+H$	13.1	0	30790	[81]
12	$C_3H_4=CH_3+C_2H$	15.0	0	51330	[81]
13	$C_3H_4=C_2H_2+CH_2$	15.0	0	51330	[81]
14	$O+C_3H_4=C_2H_3+HCO$	13.0	0	0	[81]
15	$CH_4+M=CH_3+H+M$	17.3	0	44500	[81]
16	$H+CH_4=CH_3+H_2$	14.1	0	5989	[81]
17	$O+CH_4=CH_3+OH$	13.3	0	4640	[81]
18	$OH+CH_4=CH_3+H_2O$	13.5	0	3020	[81]
19	$CH_3+O_2=CH_2O+OH$	12.2	0	7045	[81]

TABLE III (continued)

Reaction Mechanism for Toluene Oxidation

Reaction Number	Reaction	Rate Constant for Forward Direction[a] $\log_{10}A$	n	θ	Reference
20	$CH_3+O=CH_2O+H$	14.1	0	1006	91
21	$CH_2O+OH=HCO+H_2O$	13.4	0	0	82
22	$HCO+OH=CO+H_2O$	14.0	0	0	83
23	$CH_2O+M=CO+H_2+M$	16.3	0	17614	82
24	$HCO+M=H+CO+M$	13.8	0	7548	83
25	$OH+CO=CO_2+H$	12.6	0	4026	83
26	$CO+O_2=CO_2+O$	13.2	0	20634	82
27	$CO+O+M=CO_2+M$	13.8	0	0	83
28	$O+H_2=OH+H$	14.3	0	6919	83
29	$H+O_2=OH+O$	17.1	-0.907	8369	83
30	$OH+H_2=H_2O+H$	13.7	0	3271	83
31	$OH+OH=H_2O+O$	13.7	0	3523	83
32	$H+H+M=H_2+M$	15.0	0	0	83
33	$H+OH+M=H_2O+M$	21.9	-2.0	0	83
34	$H_2+O_2=2OH$	13.2	0	24230	82
35	$O_2+M=2O+M$	18.4	-1.0	9410	83
36	$C_2H_2+M=C_2H+H+M$	14.0	0	57367	83
37	$C_2H_2+O_2=HCO+HCO$	14.0	0	19122	83
38	$H+C_2H_2=C_2H+H_2$	14.3	0	9561	83

TABLE III (continued)

Reaction Mechanism for Toluene Oxidation

Reaction Number	Reaction	Rate Constant for Forward Direction[a] $\log_{10}A$	n	θ	Reference
39	$OH+C_2H_2=C_2H+H_2O$	12.8	0	3523	83
40	$O+C_2H_2=C_2H+OH$	15.5	-0.6	8555	83
41	$O+C_2H_2=CH_2+CO$	13.7	0	1862	83
42	$C_2H+O_2=HCO+CO$	13.0	0	3523	83
43	$C_2H+O=CO+OH$	13.7	0	0	83
44	$CH_2+O_2=HCO+OH$	14.0	0	1862	83
45	$CH_2+O=CH+OH$	11.3	0.68	12580	83
46	$CH_2+H=CH+H_2$	11.4	0.67	12580	83
47	$CH_2+OH=CH+H_2O$	11.4	0.67	12580	83
48	$CH+O_2=CO+OH$	11.1	0.67	12580	83
49	$CH+O_2=HCO+O$	13.0	0	0	83
50	$HCO+H=CO+H_2$	14.0	0	0	83
51	$HCO+O=CO+OH$	14.1	0	0	83
52	$H+O_2+M=HO_2+M$	15.2	0	-500	91

a - The rate constants are given in the form $k=AT^n \exp(-\theta/T)$; the units are in s, mol, cm^3, K.

-argon, and Mixture D, i.e. 1.75% toluene - 1.75% oxygen-argon. Species concentrations and temperature profiles were calculated to a reaction time of 3000 microseconds for five initial temperatures: 1600K, 1800K, 2000K, 2200K, and 2400K. These temperatures were chosen as typical of the operating temperature range of interest. The temperatures at various reaction times calculated for all five cases are summarized in Tables IV and V.

Inspection of the simulation results indicates that the temperature change as the result of chemical reaction in the first three milliseconds for Mixture B is not significant, being on the order of magnitude of the uncertainty in the initial post-shock temperature, i.e. ~25K. As expected, somewhat larger temperatures changes are seen for Mixture D. However, the kinetic simulations showed that the maximum change in temperature was still moderate, being about 80°K. The typical temperature versus reaction time profile appears to be a shallow ascending s-curve. The initial temperature decrease is caused by the following endothermic reactions: the attack of O_2 on C_7H_8 to form the free radicals C_7H_7 and HO_2 (reaction 1) and the fragmentation of toluene (reaction 2). As the reaction time increases, exothermic reactions involving oxygen become important. These reactions form relatively stable products such as H_2O, CO, and CO_2. However, endothermic decompositions are occurring simultaneously, moderating the rise in temperature. At longer times, when most of the oxygen is bound in relatively stable products, the continuing pyrolytic fragmentation of the remaining toluene causes the final temperature decrease.

We also performed several adiabatic equilibrium calculations using a computer program developed at the NASA Lewis Research Center [86]. The results of these computations are given in the last column of Tables IV and V. The adiabatic equilibrium temperature is expected to provide an upper limit for

TABLE IV

Temperatures Computed for the 0.311% Toluene - 0.311% Oxygen-Argon Mixture at a carbon atom concentration of 2.0×10^{17} atoms/cm^3.

Initial Temperature (K)	Temperature Computed by Kinetic Model at Reaction Times, in μs				Equilibrium Temperature (K)
	100	500	1000	3000	
1600	1590	1588	1596	1617	1689
1800	1779	1809	1814	1798	1892
2000	1982	1989	1983	1978	2094
2200	2192	2197	2197	2197	2292
2400	2384	2385	2385	2387	2483

TABLE V

Temperatures Computed for the 1.75% Toluene - 1.75% Oxygen-Argon Mixture at a carbon atom concentration of 2.0×10^{17} atoms/cm^3.

Initial Temperature (K)	Temperature Computed by Kinetic Model at Reaction Times, in μs				Equilibrium Temperature (K)
	100	500	1000	3000	
1600	1565	1554	1576	1675	1996
1800	1717	1819	1845	1783	2195
2000	1913	1964	1934	1904	2375
2200	2157	2155	2155	2154	2532
2400	2347	2373	2382	2389	2668

temperature change since it assumes complete conversion to the stable products, whether or not production of these species is kinetically possible in the available reaction time. These equilibrium calculations, however, do not provide a precise limit, particularly in fuel-rich combustion, because many complex hydrocarbon species are not in the computer program data base. The difference between the initial post-shock temperature and the calculated adiabatic equilibrium temperature for Mixture B was moderate, ranging from 83°K for an initial temperature of 2400K to 94°K for an initial temperature of 2400K. The difference between the initial temperature and the adiabatic equilibrium temperature was, as expected, much larger for Mixture D.

In summary, the conclusion drawn from our computer modeling of toluene oxidation is that for our experimental conditions and available reaction time, the temperature change as a result of chemical reaction is not significant compared to the temperature shift of the soot bell observed experimentally. This conclusion is supported for most of the mixtures by the results of adiabatic equilibrium calculations.

2. Estimation of Temperature Change During Oxidation of Acetylene

To estimate the temperature change during oxidation of acetylene at the conditions used in this study, we chose the mechanism proposed by Gardiner and co-workers [71,87,88], the most recent mechanism known to us.

The mechanism is based in part on work done by other researchers at various experimental conditions, but it was "tuned" to match their own recent work with fuel-lean mixtures (ϕ = 0.25 to 1.0). This mechanism therefore does not exactly represent the reaction process for our fuel-rich conditions (ϕ = 7.75). However, we believe that the temperature changes predicted by Gardiner's mechanism can be

expected to predict the actual values within at least an order of magnitude, allowing the rough estimation of possible temperature variations behind reflected shock waves at our conditions.

The computer program is a constant-density model which uses the latest version (1982) of LSODE. The computer simulations were performed for the conditions of Mixture J (see Table II), i.e. 4.65% acetylene - 1.5% oxygen - argon, and Mixture M, i.e. 20.0% acetylene - 4.3% oxygen-argon. Both mixtures had a carbon atom concentration behind the reflected shock of 5.0×10^{17} atoms/cm^3. Species concentrations and temperature profiles were calculated for five initial temperatures: 1500K, 1600K, 1700K, 1800K, and 1900K for Mixture J and 1600K, 1800K, 2000K, 2200K, and 2400K for Mixture M. These temperatures were chosen as typical of the operating temperature ranges of interest (see Figs. 12 and 16). The temperatures at various reaction times calculated for all cases are summarized in Tables VI and VII.

Inspection of the computational results indicates that the temperature change as a result of chemical reaction, for our gas mixture, experimental conditions, and reaction time, is not significant, being less than 50K. The small temperature rises seen are due to the quick exothermic formation of such relatively stable species as CO, CO_2, and H_2O. Once most of the available oxygen is bound in these products, the remaining acetylene reacts very slowly, causing little temperature change.

Somewhat larger temperature changes were predicted by adiabatic equilibrium calculations, especially at low initial temperatures. This was due to the fact that the NASA computer program [86] used for the equilibrium calculations

TABLE VI.

Temperatures Computed for the 4.65% Acetylene - 1.5% Oxygen-Argon Mixture at a carbon atom concentration of 5.0×10^{17} atoms/cm^3.

Initial Temperature (K)	Temperature Computed by Kinetic Model at Reaction Times in μs				Equilibrium Temperature (K)
	50	250	500	2500	
1500	1500	1502	1501	1501	2296
1600	1600	1602	1602	1602	2363
1700	1700	1703	1702	1702	2422
1800	1803	1804	1803	1804	2472
1900	1905	1906	1905	1906	2514

TABLE VII.

Temperatures Computed for the 20% Acetylene - 4.3% Oxygen-Argon Mixture at a carbon atom concentration of 5.0×10^{17} atoms/cm^3.

Initial Temperature (K)	Temperature Computed by Kinetic Model at Reaction Times in μs				Equilibrium Temperature (K)
	50	250	500	2500	
1600	1600	1600	1601	1599	3107
1800	1800	1806	1806	1804	3167
2000	2008	2012	2012	2012	3225
2200	2215	2221	2224	2228	3282
2400	2424	2435	2441	2443	3339

includes soot-like species such as $C_{150}H_{30}$ as possible reaction products. The equilibrium calculations indicated the production of significant amounts of these large soot-like species. However, at our reaction times, the system is still in the kinetic regime for soot and is far removed from complete equilibrium.

In summary, the conclusion drawn from our computer modeling of acetylene oxidation is that for the experimental conditions tested and the available reaction times, temperature change as a result of chemical reaction is not significant compared to the experimental temperature shift of the soot bell under oxidative pyrolysis as compared to pure thermal pyrolysis.

3. Soot Formation in Hydrocarbon Oxidation

a) Toluene Mixtures

Comparing the experimental results on soot formation obtained in pyrolysis and oxidation of toluene, we conclude that while the addition of moderate amounts of oxygen can have an effect on soot levels and temperature regions where soot is formed, it seems to have little effect on the general character of soot formation observed in pyrolysis. The time development of the soot "bell" and its shift to higher temperatures when pressure is lowered are similar in both cases. Actually, addition of oxygen to toluene seems to be qualitatively equivalent to reduction of the initial concentration of toluene (cf. Figs. 5 & 26).

As in the pyrolysis case, pressure has little effect on the maximum soot yield values in oxidation. However, the observed shift of the soot yield maximum is smaller when oxygen is present (cf. Figs. 5 & 9). In other words, at relatively low pressures the addition of oxygen results in the shift of the soot yield maximum to lower temperatures while at relatively high pressures the shift

is hardly observable. This observation can be also interpreted as that at low pressures oxygen suppresses soot production at higher temperatures whereas at lower temperatures oxygen promotes the formation of soot (Fig. 9).

The observed phenomenon indicates that addition of oxygen causes reactions to occur that compete with pressure-dependent processes. In our recent analysis of soot formation during pyrolysis of aromatic hydrocarbons [54], we suggested that pressure-dependent fragmentation of an aromatic ring initiates the production of soot. Hence, oxidation reactions must compete with ring fragmentation. At low pressures, the promoting effect of oxygen on soot formation below 2100K and the suppression of soot above this temperature indicate that oxidizing agents (such as O_2, O, OH) attack the aromatic ring producing, besides oxidation products CO and CO_2 and small inefficient fragments, active intermediates for the soot-forming route. At low temperatures when thermal ring fragmentation is slow, the formation of these intermediates by oxidative reactions enhances soot production. At high temperatures, when the thermal decomposition is predominant, additional removal of aromatic rings by oxidative agents inhibits formation of soot.

b) Acetylene Mixtures

In the case of acetylene (Figs. 13 and 18), the effect of oxygen on soot yield is more pronounced and extends over the entire pressure range studied. It is interesting to note that the sensitivity of the acetylene system is much larger than that of the toluene system; that is, a smaller oxygen-to-hydrocarbon ratio is required to produce a similar effect. The sensitivity to oxygen in the acetylene case is particularly high at lower pressures (Fig. 18).

Soot formation in pyrolysis of acetylene was explained recently [78] in terms of the following conceptual model:

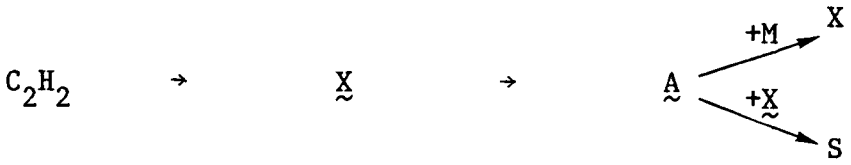

where:

M = a third body

$\underset{\sim}{X} = \{X_1, X_2, \ldots\}$ is the collection of nonaromatic intermediates;

$\underset{\sim}{A} = \{A_1, A_2, \ldots\}$ is the collection of aromatic species;

$\underset{\sim}{S} = \{S_1, S_2, \ldots\}$ is the collection of species absorbing the light at a specific wavelength.

The products of acetylene pyrolysis, $\underset{\sim}{X}$, interact among themselves, eventually forming the aromatic species $\underset{\sim}{A}$. The reactions of nascent aromatic species $\underset{\sim}{A}$ comprise two parallel routes: the pressure-dependent high-activation-energy fragmentation of an aromatic ring and a low-activation-energy radical-molecule interaction of an aromatic ring with aliphatic fragments leading to soot.

At low temperatures, the rate limiting step in acetylene pyrolysis is the production of $\underset{\sim}{X}$

$$C_2H_2 \rightarrow \underset{\sim}{X}.$$

Addition of relatively small amounts of oxygen results in formation of reactive radicals (e.g. O and OH), which promote the pyrolysis reactions. Under these conditions, the rate of formation of aromatic intermediates $\underset{\sim}{A}$ is enhanced, which, in turn, increases the rate of soot production.

At high temperatures, a partial equilibrium is quickly established and the fragmentation of aromatic rings

$$\underset{\sim}{A} \rightarrow \underset{\sim}{X}$$

becomes a dominant factor in soot formation process. As was postulated earlier, reactions of the oxidizing agents with $\underset{\sim}{A}$ results in additional removal of aromatic rings which inhibits the formation of soot.

Thus, the overall effect of oxygen on soot formation in acetylene pyrolysis should be the shift of the soot yields to lower temperature which was observed experimentally. The higher sensitivity of soot production to oxygen for acetylene compared to that for toluene can also be explained now. At low temperatures, oxygen very efficiently promotes the formation of aromatics from acetylene compared to a relatively marginal contribution to the formation of $\underset{\sim}{X}$ in toluene case. At high temperatures, oxygen promotes the ring fragmentation, which effectively retards the production of soot for both cases.

c) Benzene Mixtures

Soot formation in pyrolysis and oxidation of benzene is very similar, both qualitatively and quantitatively, to that of toluene. This fact provides further support for our conceptual model for soot formation in pyrolysis and oxidation of aromatic hydrocarbons.

d) General Conclusions

The main conclusion to be drawn from the results of this work is that the soot formation mechanism is probably the same for both pyrolysis and oxidation of hydrocarbons. That is, the addition of oxygen does not alter the soot route but rather promotes or inhibits this route by means of competitive reactions.

The above conclusion actually implies that radicals are more important than ions in the soot formation mechanism since one would expect many more ions to be present during oxidation than during pyrolysis. This is particularly obvious in the case of aromatics (toluene and benzene). If ions were the crucial intermediates for soot precursors, one would expect a very dramatic positive effect on soot yields when oxygen is added. On the contrary, the observed effect is relatively small and negative.

4. Empirical Modeling of Soot Formation

Quantitative prediction of the amount of soot formed in practical combustion systems has become one of the foremost concerns in combustion science and technology. Hitherto, no attempt has been made to develop a quantitative model, physical or empirical, that will relate the amount of soot formed with experimental conditions such as temperature, pressure, fuel concentration, et cetera. Previously, we have introduced a conceptual model for soot formation in pyrolysis of hydrocarbons which provides a starting point for empirical modeling.

An approach to empirical modeling of soot formation is presented below. The objective of the modeling is to predict soot yield for a given reaction time at various temperatures, pressures and initial reactant concentrations for various fuels. The approach is introduced by first considering the simplest case, which is soot formation in shock-tube pyrolysis of aromatic hydrocarbons.

a) Statement of the Problem

The empirical model is postulated as

$$
\begin{aligned}
&A \xrightarrow{k_f} X_0 && \text{fragmentation}\\
&A + X_0 \xrightarrow{k_p} X_1 \\
&A + X_1 \xrightarrow{k_p} X_2 \\
&\quad\cdots\cdots\cdots \\
&A + X_i \xrightarrow{k_p} X_{i+1} && \text{polymerization}
\end{aligned}
\qquad (1)
$$

which is the simplest, in a mathematical sense, kinetic scheme that has all the features of our conceptual model for soot formation in pyrolysis of aromatic

hydrocarbons [54]. Species A denotes aromatic hydrocarbon and/or their stable radicals and species X_K, X_{K+1}, ... of this system constitute what we will call soot, i.e.

$$S = \{X_K, X_{K+1}, \ldots\}. \tag{2}$$

The soot yield is then defined as

$$Y = \sum_{i=K}^{\infty} (i+1)\{[X_i]/[A]_0\} \tag{3}$$

where: Y is the soot yield;

$[X_i]$ is the concentration of species X_i;

$[A]_0$ is the initial concentration of A.

"Yield" is thus the fraction of species A originally present which has become soot. The (i+1) factor accounts for the number of A molecules "contained" in each X_i molecule.

Let us derive an expression for Y as function of experimental parameters.

b) Derivation

The differential equations for the reaction system (1) take the form of

$$\left.\begin{aligned}
\frac{d[A]}{dt} &= - k_f[A] - \sum_{j=0}^{\infty} k_p[A][X_j] \\
\frac{d[X_0]}{dt} &= k_f[A] - k_p[A][X_0] \\
\frac{d[X_1]}{dt} &= k_p[A][X_0] - k_p[A][X_0] \\
&\vdots \\
\frac{d[X_{i+1}]}{dt} &= k_p[A][X_i] - k_p[A][X_{i+1}] \\
&\vdots
\end{aligned}\right\} \tag{4}$$

with initial conditions

$$[A]_{t=0} = [A]_0$$

$$[X_i]_{t=0} = 0, \quad i = 0,1,2,\ldots .$$

Introducing the "dimensionless concentrations"

$$a \equiv [A]/[A]_0 \quad \text{and} \quad x_i \equiv [X_i]/[A]_0,$$

dividing both sides of each differential equation (4) by $k_f a$, and substituting, according to [89],

$$k_f a dt = d\tau \tag{5}$$

we obtain

$$\frac{da}{d\tau} = -1 - \sum_{j=0}^{\infty} x_j/r \tag{6a}$$

$$\left.\begin{aligned} \frac{dx_0}{d\tau} &= 1 - x_0/r \\ \frac{dx_1}{d\tau} &= x_0/r - x_1/r \\ \frac{dx_i}{d\tau} &= x_{i-1}/r - x_i/r \end{aligned}\right\} \tag{6b}$$

$$\vdots$$

with initial conditions

$$\left.\begin{aligned} a\,|_{\tau=0} &= 1 \\ x_i|_{\tau=0} &= 0, \quad i = 0,1,2,\ldots, \end{aligned}\right\} \tag{6c}$$

where:

$$r = k_f/(k_p[A]_0). \tag{7}$$

The resultant system (6b) is comprised of linear differential equations and it can be readily shown that

$$x_i \equiv [X_i]/[A]_0 = r\,P(i+1,\ \tau/r), \quad i = 0,1,2,\ldots, \tag{8}$$

where:

$$P(i+1,\ \tau/r) = \frac{1}{i!}\int_0^{\tau/r} e^{-u}u^i du \tag{9}$$

is the incomplete Gamma function [90]. It can be noted that

$$\sum_{i=0}^{\infty} x_i = \tau\ . \tag{10}$$

Indeed,

$$\sum_{i=0}^{\infty} x_i = \sum_{i=0}^{\infty} r\,P(i+1,\ \tau/r) = r\sum_{i=0}^{\infty}\frac{1}{i!}\int_0^{\tau/r} e^{-u}u^i du$$

$$= r\sum_{i=0}^{\infty}\int_0^{\tau/r}\frac{e^{-u}u^i}{i!}du = r\int_0^{\tau/r}\left(\sum_{i=0}^{\infty}\frac{e^{-u}u^i}{i!}\right)du$$

$$= r\int_0^{\tau/r} du = \tau, \tag{11}$$

since by definition of the Poisson distribution [91]

$$\sum_{i=0}^{\infty}\frac{e^{-u}u^i}{i!} = 1. \tag{12}$$

Substituting (10) into (6a), we obtain

$$\frac{da}{d\tau} = -1 - \tau/r, \tag{13}$$

the solution of which, taking into account the initial conditions (6c), is

$$a = 1 - \tau - \tau^2/2r \tag{14}$$

Substituting (14) into (5), we obtain

$$\int_0^t k_f dt = \int_0^{\tau} d\tau/(1 - \tau - \tau^2/2r)$$

or

$$k_f t = \frac{1}{q}\ln\left(\frac{\tau/\lambda_2 - r}{\tau/\lambda_1 - r}\right)$$

where:

$$\lambda_1 = -1 + q;$$

$$\lambda_2 = -1 - q;$$

$$q = \sqrt{1 + 2/r};$$

or

$$\tau = \frac{r(1-e^{qk_f t})}{\frac{1}{\lambda_2} - \frac{1}{\lambda_1} e^{qk_f t}}$$

The last expression relates the "transformed time" τ, the physical meaning of which is disclosed through equality (10), with the real time t. Hence, substitution of (7) and (15) into (8) and (14) determines the kinetic behavior of reaction system (1).

The expression for soot yield (3) can be developed in the following manner. Let us rewrite expression (3) as

$$Y = \sum_{i=K}^{\infty} (i+1)x_i = \sum_{i=0}^{\infty} (i+1)x_i - \sum_{i=0}^{K-1} (i+1)x_i \qquad (16)$$

where the first sum on the right-hand side of this expression is easily determined:

$$\sum_{i=0}^{\infty} (i+1)x_i = \sum_{i=0}^{\infty} ix_i + \sum_{i=0}^{\infty} x_i. \qquad (17)$$

However, $\sum_{i=0}^{\infty} x_i$, according to (10), equals τ and, as in derivation (11), we obtain

$$\sum_{i=0}^{\infty} ix_i = \sum_{i=1}^{\infty} i \cdot r\, P(i+1,\tau/r) = r \sum_{i=1}^{\infty} i \cdot \frac{1}{i!} \int_0^{\tau/r} e^{-u} u^i du$$

$$= r \sum_{i=1}^{\infty} \int_0^{\tau/r} \frac{e^{-u} u^i}{(i-1)!} du = r \int_0^{\tau/r} \left(\sum_{i=1}^{\infty} \frac{e^{-u} u^i}{(i-1)!} \right) du$$

$$= r \int_0^{\tau/r} u \left(\sum_{j=0}^{\infty} \frac{e^{-u} u^j}{j!} \right) du = r \int_0^{\tau/r} u\,du = \tau^2/2r \qquad (18)$$

where:

$j = i-1$ and $\sum_{j=0}^{\infty} \frac{e^{-u} u^j}{j!} = 1$ by the definition of Poisson's distribution [91].

That is

$$\sum_{i=0}^{\infty} (i+1)x_i = \tau + \tau^2/2r \qquad (19)$$

In order to determine the second sum on the right-hand side of expression (16), let us recall one of the properties of the incomplete Gamma function [90], i.e.

$$P(i+1,\tau/r) = P(i,\tau/r) - \frac{e^{-\tau/r}(\tau/r)^i}{i!} \qquad (20)$$

or

$$P(i+1, \tau/r) = 1 - \sum_{j=0}^{i} \frac{e^{-\tau/r}(\tau/r)^j}{j!} \quad . \qquad (21)$$

Therefore,

$$x_i = r \left[1 - \sum_{j=0}^{i} \frac{e^{-\tau/r}(\tau/r)^j}{j!} \right] \qquad (22)$$

and then

$$\sum_{i=0}^{\kappa-1} (i+1)x_i = \sum_{i=0}^{\kappa-1} (i+1)r \left[1 - \sum_{j=0}^{i} \frac{e^{-\tau/r}(\tau/r)^j}{j!} \right]$$

$$= r \left[\sum_{i=0}^{\kappa-1} (i+1) - \sum_{0}^{\kappa-1} (i+1) \sum_{j=0}^{i} \frac{e^{-\tau/r}(\tau/r)^j}{j!} \right]$$

$$= r \left[\frac{\kappa(\kappa+1)}{2} - \sum_{i=0}^{\kappa-1} \frac{(i+1+\kappa)(\kappa-i)}{2} \frac{e^{-\tau/r}(\tau/r)^i}{i!} \right] \qquad (23)$$

Thus, substituting (19) and (23) into (16), we obtain

$$Y = r\left[\tau/r + \tau^2/2r^2 - \frac{\kappa(\kappa+1)}{2} + \sum_{i=0}^{\kappa-1} \frac{(i+1+\kappa)(\kappa-i)}{2} \frac{e^{-\tau/r}(\tau/r)^i}{i!}\right] \qquad (24)$$

c) Model Fit

Expression (24) together with relationships (7) and (15) constitute an empirical model for soot formation, which contains 3 unknowns: κ, k_f, and k_p. Assuming Arrhenius form for the rate constants

$$k_f = A \exp(-\theta_f/T)\rho^{\alpha}$$

and $$k_p = B \exp(-\theta_p/T)\rho^{\beta}[A]_0^{\gamma}$$

where:

T is the initial reaction temperature in K;

ρ is the total density in mol/cm^3;

and $[A]_0$ is the initial concentration of toluene in mol/cm^3,

there are 8 parameters to determine, namely $A, B, \theta_f, \theta_p, \alpha, \beta, \gamma$ and κ. Although the quality of the fit was slightly better for $\kappa=3$, for physical reasons [59] we assumed $\kappa=6$.

A general approach for fitting the model would be to optimize

$$\sum_{i,t} (Y_{calc,i,t} - Y_{expt,i,t})^2, \qquad (25)$$

where $Y_{expt,i}$ and $Y_{calc,i}$ are the experimentally observed and the calculated soot yields for i-th experiment at the observation time t. The summation is taken over the entire set of experiments and the chosen number (25 in this work) of time intervals. However, the experimental determination of soot yields strongly depends on the knowledge of the complex refractive index m[54]. Since the value of m is not well-established, it was desirable that the modeling results would not depend on m. This was achieved as follows. Instead of optimizing the objective function (25), we minimized

$$\sum_{i,t} (Y_{calc,i,t}/Y^*_{calc} - Y_{expt,i,t}/Y^*_{expt})^2, \qquad (26)$$

where Y^*_{expt} is the experimental soot yield at specified, reference conditions and Y^*_{calc} is the soot yield calculated by the model at these conditions. The reference conditions in our modeling are the 0.311% C_7H_8-Ar mixture at T = 1977 K, $\rho = 1.54 \times 10^{-5}$ mol/cm^3 and time = 1.0 ms. The conditions corresponded to an actual experimental point taken at the approximate center of the ranges of the experimental variables of interest.

Actually, since the present modeling is empirical in nature and one should not expect that Eq. (24) predicts the true values of soot yields, the objective function for optimization (26) should be rewritten as

$$\sum_{i,t} [(Y/Y^*)]_{calc,i,t} - (Y/Y^*)_{expt,i,t}]^2. \qquad (27)$$

The form of expression (27) implies that $(Y/Y^*)_{calc}$ should be considered as a single entity and no physical meaning should be attached to Y_{calc} or Y^*_{calc} alone. That is, the empirical model predicts the relative values and in order to obtain the absolute value of soot yield at given conditions one must multiply the corresponding $(Y/Y^*)_{calc}$ by Y^*_{expt}.

Optimizing (27) for all 5 toluene mixtures with no oxygen present, A,C,E,F and G, the following results were obtained:

$A = 6.67 \times 10^{11}$

$\theta_f = 2.38 \times 10^4$

$\alpha = 0.858$

$B = 2.68 \times 10^{10}$

$\theta_p = 6.47 \times 10^3$

$\beta = 0.139$

$\gamma = -0.413$

$\kappa = 6$

Figures 27-29 compare the experimental and computed values of Y/Y*. Figure 27 shows the time development, Fig. 28 - pressure dependence, and Fig. 29 - concentration dependence of soot yields. Although the quality of fit is generally good, it can be improved if Mixture G is not taken into account. Thus, by optimizing (27) for only 4 mixtures, A,C,E and F, the following results were obtained:

$$A = 1.94 \times 10^{14}$$

$$\theta_f = 2.68 \times 10^{4}$$

$$\alpha = 1.27$$

$$B = 6.05 \times 10^{8}$$

$$\theta_p = -4.38 \times 10^{3}$$

$$\beta = -0.361$$

$$\gamma = 0.0114$$

$$\kappa = 6$$

Figures 30 - 32 compare the experimental and new computed values of Y/Y*. As can be seen in these figures the quality of fit is significantly improved. It is not clear, however, whether this improvement is due to some experimental problems with Mixture G or simply the result of the empirical nature of the modeling.

Although it is very tempting to assign physical meaning to the rate constants above, one should be very cautious about doing so. These constants are parameters of an <u>empirical</u> model.

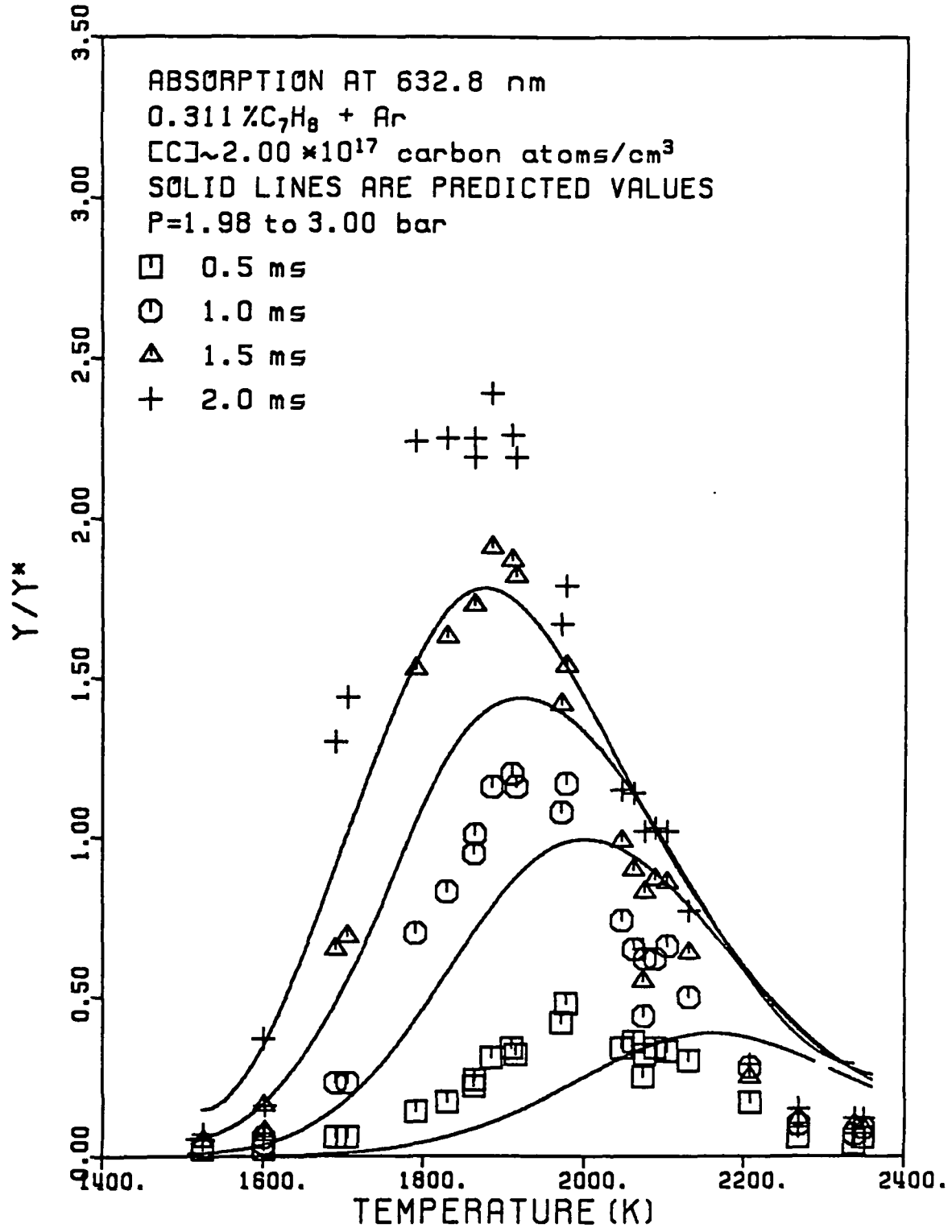

FIGURE 27. Comparison of the model prediction with experimental observations. (First parameter set). Time development.

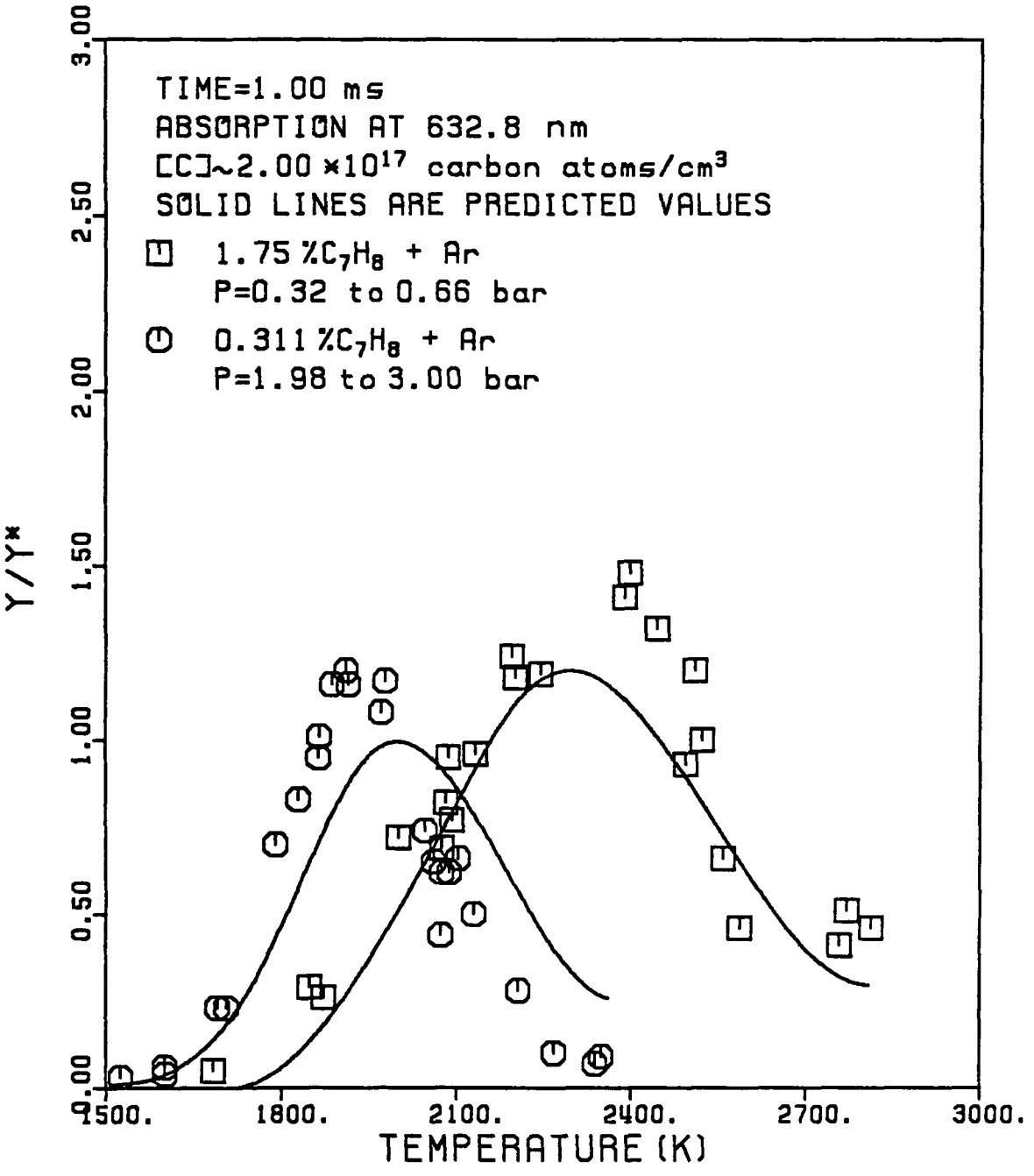

FIGURE 28. Comparison of the model prediction with experimental observations. (First parameter set). The effect of pressure.

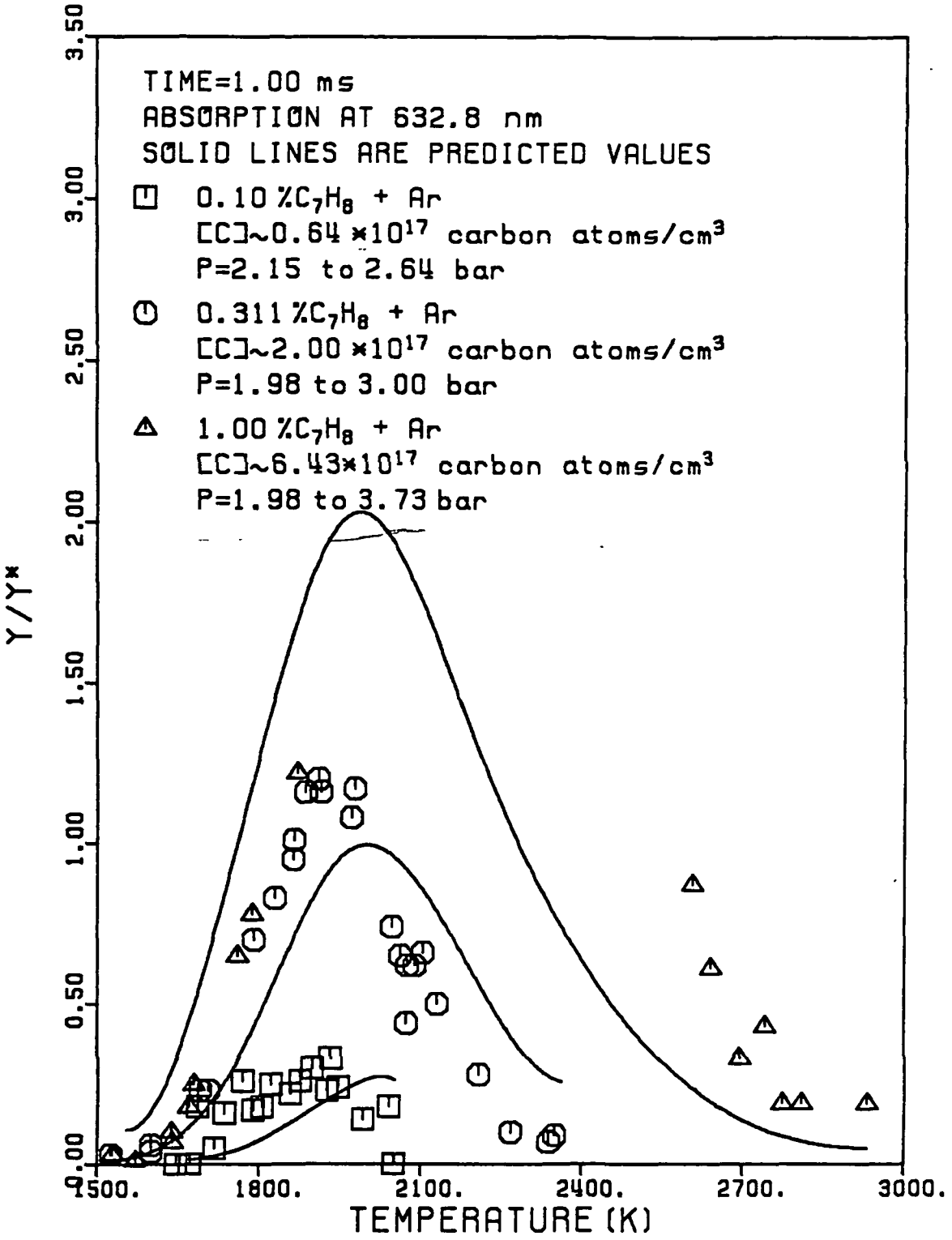

FIGURE 29. Comparison of the model prediction with experimental observations. (First parameter set). Concentration dependence.

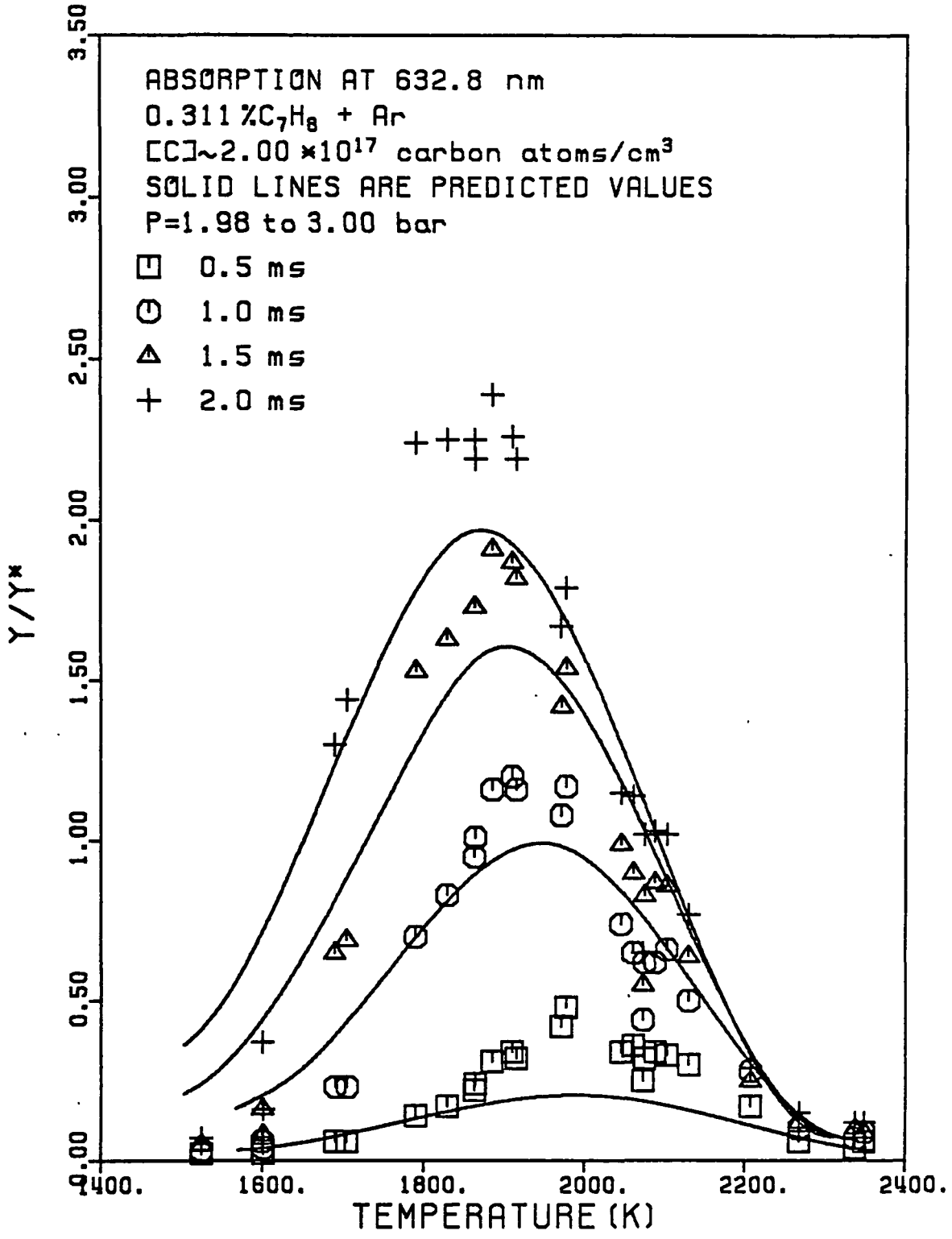

FIGURE 30. Comparison of the model prediction with experimental observations. (Second parameter set). Time development.

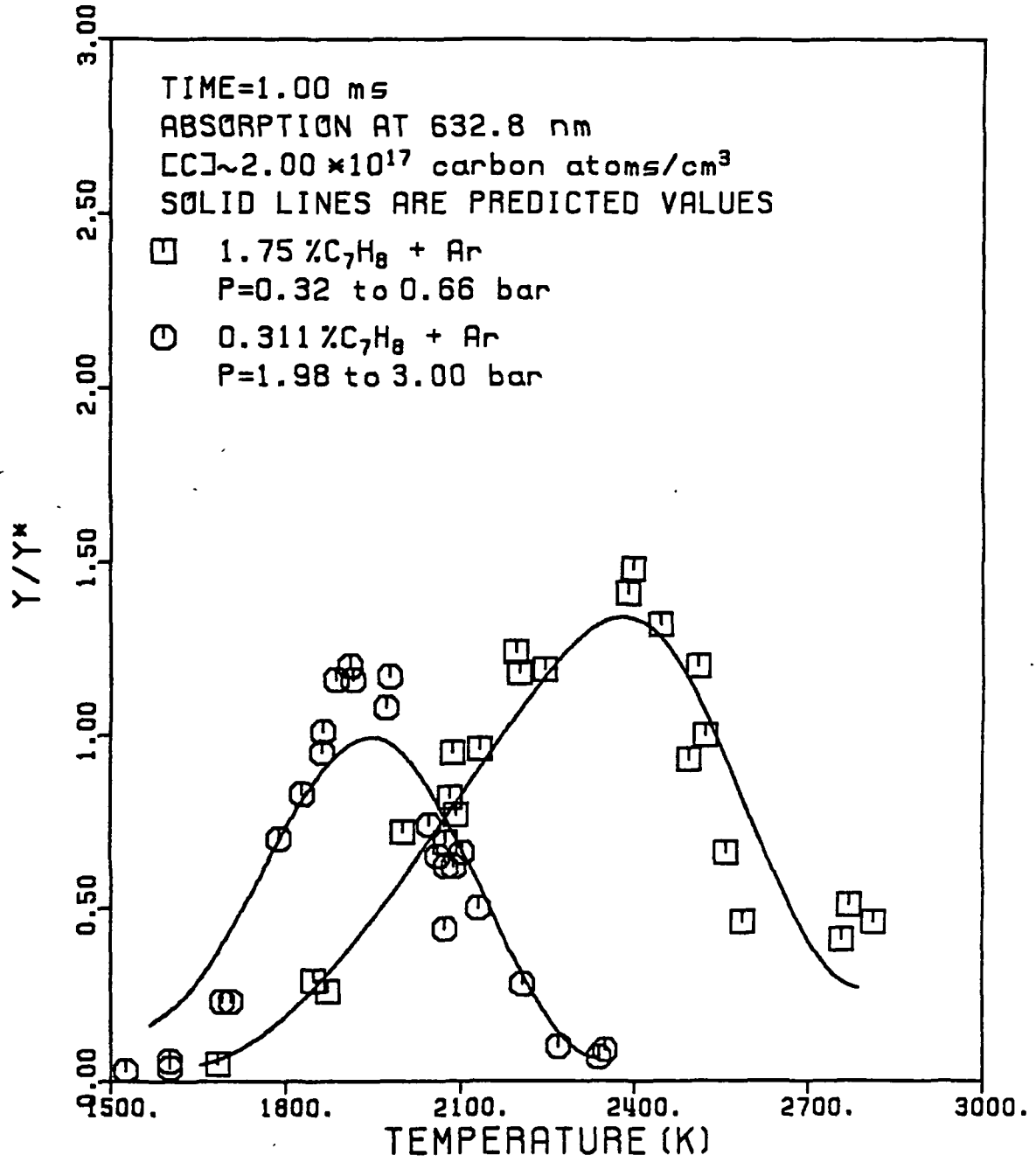

FIGURE 31. Comparison of the model prediction with experimental observations. (Second parameter set). The effect of pressure.

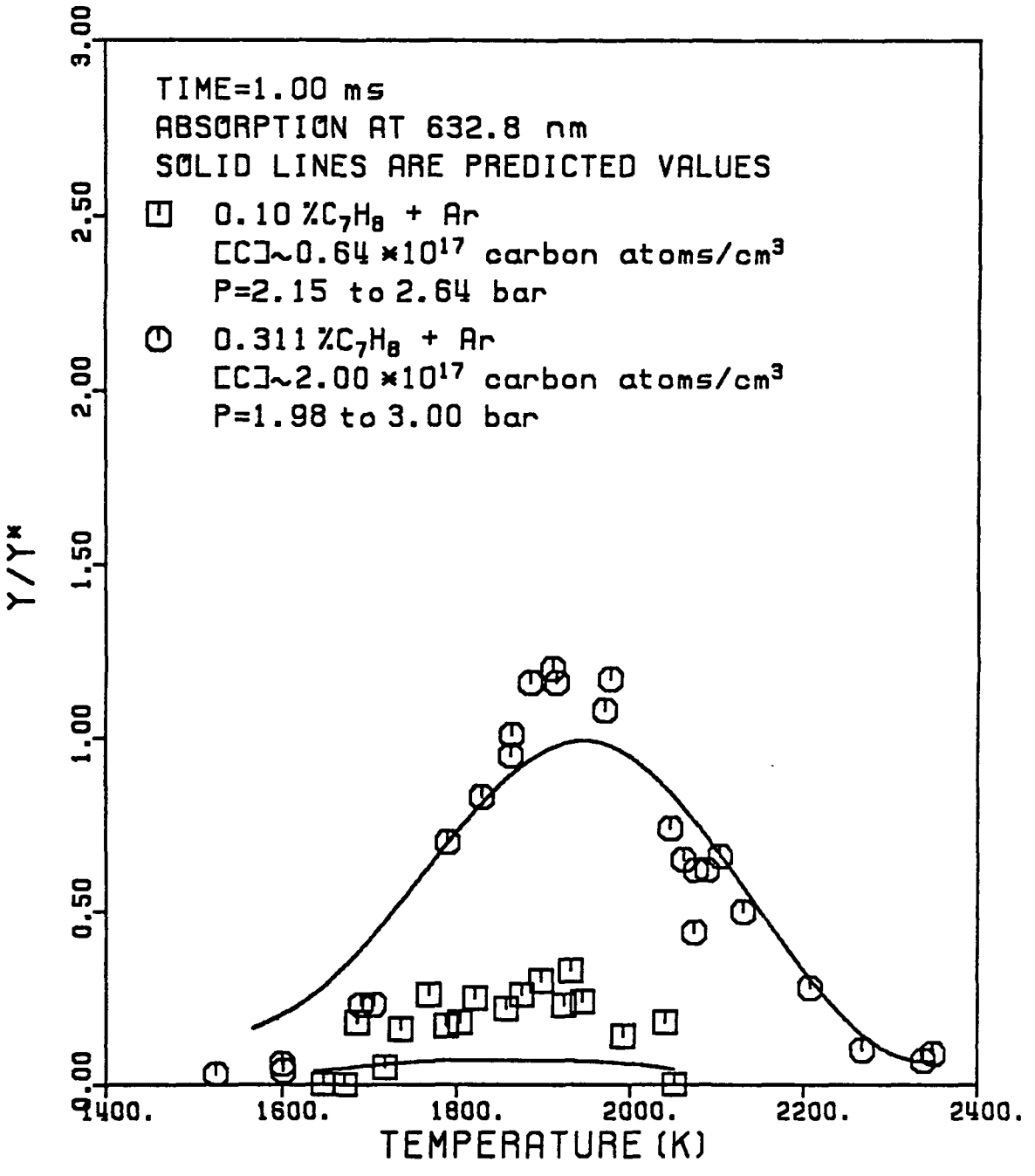

FIGURE 32. Comparison of the model prediction with experimental observations. (Second parameter set). Concentration dependence.

SUMMARY OF RESULTS

1. A conceptual model for soot formation in pyrolysis of non-aromatic hydrocarbons was developed. The most efficient "building blocks" for the formation of soot precursors in the pyrolysis of aliphatic hydrocarbons seem to be species with C-to-H ratios of approximately unity which have conjugated molecular configuration. Since aromatic form provides the ultimate delocalization of π-electron density and thus the ultimate stabilization and reactivity, the incipient soot formation from hydrocarbons should follow the route of consecutive production of the conjugated reactive structures. The difference in soot formation characteristics between various hydrocarbons is determined by the initiation process, i.e. by the reactions leading to these reactive structures.

2. Soot formation in toluene-, benzene-, and acetylene-oxygen-argon mixtures was investigated to study soot formation in a combustion environment. It was observed that high concentrations of oxygen completely suppress soot formation. The addition of oxygen at relatively low concentrations uniformly suppresses soot formation at higher pressures, while at relatively lower pressures it suppresses soot formation at higher temperatures while promoting soot production at lower temperatures. The observed behavior may indicate that oxidation reactions compete with ring fragmentation. The main conclusion to be drawn from the results of this work is that the mechanism of soot formation in shock tubes is probably the same for both pyrolysis and oxidation of hydrocarbons. That is, the addition of oxygen does not alter the soot route but rather promotes or inhibits this route by means of competitive reactions. The above conclusion actually implies a radical and not an ionic mechanism of incipient soot

formation in shock tubes (although nascent ions may play an important role in coagulation). Indeed, if ions were the crucial intermediates for soot precursors, one would expect a very strong increase in soot yields when oxygen is added. On the contrary, the observed effect is relatively small and negative.

3. An approach to empirical modeling of soot formation is suggested. An empirical model for soot formation in shock-tube pyrolysis of aromatic hydrocarbons is developed. The model predicts well the times, concentration and pressure dependecies of experimental soot yields.

FUTURE RESEARCH DIRECTIONS

The ultimate goal of our program is the development of a detailed kinetic model for soot formation in combustion of hydrocarbons. To achieve this goal, we will concentrate on the following objectives:

1. Systematic experimental investigation of sooting characteristics at carefully designed conditions. The conditions will be chosen to help in the identification of the essential steps in the mechanism of soot formation and also to provide sufficient information for empirical (part 2) and kinetic (part 3) modeling. This part of the program will be directed towards the establishment of the temperature, pressure, initial hydrocarbon concentration and molecular structure effects on soot yield for carefully selected hydrocarbons, heterocyclic compounds (for example, pyridine and chlorobenzene) and their mixtures. Both pyrolysis and oxidation will be performed. The experiments will be conducted behind reflected shock waves; soot will be monitored by the attenuation of a laser beam. Additional optical diagnostics will be employed if it will conclusively benefit the stated objectives.

2. Empirical modeling of soot formation. In this part of the program empirical relationships between soot yield and temperature, pressure and composition of the mixture will be developed based on the results obtained in part 1. The relationships will be tested for flames. The established correlations may be used, on one hand, for practical purposes such as design and optimization of combustors, and, on the other hand, will be imposed as constraints for detailed kinetic modeling in part 3 of the program.

3. Detailed kinetic modeling of soot formation. Established mechanisms for pyrolysis and oxidation of hydrocarbons will provide a basis for the modeling. The reactions leading to the formation of soot precursors and their subsequent growth will be guessed based on analysis of the results obtained in part 1 and those of other researchers. The missing thermochemical data will be estimated. The kinetic model will be subjected to constraints established in parts 1 and 2 of the program and taken from other works. Sensitivity analysis will be employed to identify the main reaction route. The model will be extended to flames.

REFERENCES

1. Wagner, H.Gg., "Soot Formation in Combustion", Seventeenth Symposium (International) on Combustion, The Combustion Institute, Pittsburgh, 1979, p. 3.
2. Haynes, B.S. and Wagner, H.Gg., "Soot Formation", Prog. Energy Combust. Sci. 7:229 (1981).
3. Wagner, H.Gg. "Soot Formation - An Overview" in Particulate Carbon: Formation During Combustion (D.C. Siegla and G.W. Smith, Eds.), Plenum, New York, 1981, p. 1.
4. Wagner, H.Gg., "Mass Growth of Soot", NATO Workshop on "Soot in Combustion Systems and its Toxic Properties", in Soot in Combustion Systems and Its Toxic Properties (J. Lahaye and G. Prado, Eds.), Plenum, New York, 1983, p. 171.
5. Calcote, H.F., "Mechanisms of Soot Nucleation in Flames - A Critical Review", Combust. Flame 42:215 (1981).
6. Santoro, R.J. and Glassman, I., "A Review of Oxidation of Aromatic Compounds", Combust. Sci. Technol. 19:161 (1979).
7. Glassman, I., "Phenomenological Models of Soot Processes in Combustion Systems", Princeton University Mechanical and Aerospace Engineering Report No. 1450, July 1979.
8. Smith, O.I., "Fundamentals of Soot Formation in Flames with Applications to Diesel Engine Particulate Emissions", Prog. Energy Combust. Sci. 7:275 (1981).
9. Golden, D.M., "Pyrolysis and Oxidation of Aromatic Compounds", Progress in Astronautics and Aeronautics 62:233 (1978).

10. Longwell, J.P., "The Formation of Polycyclic Aromatic Hydrocarbons by Combustion", Nineteenth Symposium (International) on Combustion, The Combustion Institute, Pittsburgh, 1982, p. 167.

11. Kogarko, S.M. and Borisov, A.A., Bull. Acad. Sci. USSR 8:1255 (1960).

12. Miyama, H., "Ignition of Benzene-Oxygen-Argon and Benzene-Oxygen-Nitrogen Mixtures by Shock Waves", J. Chem. Phys. 52:3850 (1970).

13. Miyama, H., "Ignition of Aromatic Hydrocarbon-Oxygen Mixtures by Shock Waves", J. Phys. Chem. 75:1501 (1971).

14. Matula, R.A. and Farmer R.C., "Combustion Kinetics of Selected Aromatic Hydrocarbons", Report AFOSR-TR-78-1294, June 1978.

15. Burcat, A., Farmer, R.C., Espinoza, R.L., and Matula, R.A., "Comparative Ignition Delay Times for Selected Ring Structured Hydrocarbons", Combust. Flame 36:313 (1979).

16. Durgaprasad, M.B., "A Shock Tube Study of the Oxidation and Pyrolysis of Some Hydrocarbon Fuels", Ph.D. Thesis, The University of Leeds, 1982.

17. Bauer, S.H. and Aten, C.F., "Absorption Spectra of Polyatomic Molecules at High Temperatures. II. Benzene and Perfluorobenzene. Kinetics of the Pyrolysis of Benzene.", J. Chem. Phys. 39:1253 (1963).

18. Orr, C.R., "Combustion of Hydrocarbons behind a Shock Wave", Ninth Symposium (International) on Combustion, Academic Press, New York, London, 1963, p. 1034.

19. Asaba, T. and Fujii, N., "Shock-Tube Study of High-Temperature Pyrolysis of Benzene", Thirteenth Symposium (International) on Combustion, The Combustion Institute, Pittsburgh, 1971, p. 155.

20. Fujii, N. and Asaba, T., "Shock-Tube Study of the Reaction of Rich Mixtures of Benzene and Oxygen", Fourteenth Symposium (International) on Combustion, The Combustion Institute, Pittsburgh, 1973, p. 433.

21. Fujii, N., Asaba, T., and Miyama, H., "Ignition of Lean Benzene Mixtures with Oxygen in Shock Waves.", Acta Astronautica 1:417 (1974).

22. McLain, A.G., Jachimowski, C.J., and Wilson, C.H., "Chemical Kinetic Modeling of Benzene and Toluene Oxidation Behind Shock Waves", NASA Technical Paper 1472, August 1979.

23. Astholz, D.C., Durant, J., and Troe, J., "Thermal Decomposition of Toluene and of Benzyl Radicals in Shock Waves," Eighteenth Symposium (International) on Combustion, The Combustion Institute, Pittsburgh, 1981, p. 885.

24. Dzarnoski, J., Ring, M.A., and O'Neal, H.E., "Shock-Initiated Decomposition of Tetramethylgermane and the Reaction of Methyl Radicals with Toluene", Int. J. Chem. Kinet. 14: 279 (1982).

25. Kenley, R.A., Davenprort, J.E., and Hendry, D.G., "Gas-Phase Hydroxyl Radical Reactions. Products and Pathways for the Reaction of OH with Aromatic Hydrocarbons", J. Phys. Chem. 85:2740 (1981).

26. Lin, M.C. and Texault, D.E., "A Possible Role of Triplet-State Species as Chain-Initiators in High-Temperature Oxidations of Aromatic Hydrocarbons", Combust. Flame 42:139 (1981).

27. Tully, F.P., Ravishankara, A.R., Thompson, R.L., Nicovich, J.M., Shah, R.C., Kreutter, N.M., and Wine, P.H., "Kinetics of the Reactions of Hydroxyl Radical with Benzene and Toluene", J. Phys. Chem. 85:2262 (1981).

28. Nicovich, J.M., Thompson, R.L., and Ravishankara, A.R., "Kinetics of the Reactions of the Hydroxyl Radicals with Xylenes", J. Phys. Chem. 85:2913 (1981).

29. Nicovish, J.M., Gump, C.A., and Ravishankara, A.R., "Rates of Reactions of $O(^3P)$ with Benzene and Toluene", J. Phys. Chem. 86:1684 (1982).

30. Nicovich, J.M., Gump, C.A., and Ravishankara, A.R., "Rates of Reactions of O (^{3}P) with Xylenes", J. Phys. Chem. 86:1690 (1982).

31. Nelson, H.H. and McDonald, J.R., "Reaction of the Benzyl Radical with O_2 and $C\ell_2$", J. Phys. Chem. 86:1242 (1982).

32. Kern, R.D., Singh, H.J., Esslinger, M.A., and Winkeler, P.W., "Product Profiles Observed During the Pyrolyses of Toluene, Benzene, Butadiene, and Acetylene", Nineteenth Symposium (International) on Combustion, The Combustion Institute, Pittsburgh, 1982, p. 1351.

33. Smith, R.D., "A Direct Mass Spectrometric Study of the Mechanism of Toluene Pyrolysis at High Temperatures", J. Phys. Chem. 83:1553 (1979).

34. Smith, R.D., "Formation of Radicals and Complex Organic Compounds by High-Temperature Pyrolysis: The Pyrolysis of Toluene", Combust. Flame 35:179 (1979).

35. McMillen, D.F., Trevor, P.L., and Golden, D.M., "Highly Stabilized Radicals: Benzylic Radicals in Polycyclic Aromatic Systems", J. Am. Chem. Soc. 102: 7401 (1980).

36. Barton, B.D. and Stein, S.E., "Pyrolysis of Alkyl Benzenes. Relative Stabilities of Methyl-Substituted Benzyl Radicals", J. Phys. Chem. 84:2141 (1980).

37. Robaugh, D.A. and Stein, S.E., "Very-Low-Pressure Pyrolysis of Ethylbenzene, Isopropylbenzene, and tert-Butylbenzene", Int. J. Chem. Kinet. 13:445 (1981).

38. Venkat, C., Brezinsky, K., and Glassman, I., "High Temperature Oxidation of Aromatic Hydrocarbons", Nineteenth Symposium (International) on Combustion, The Combustion Institute, Pittsburgh, 1982, p. 143.

39. Mar'yasin, L. and Nabutovskii, Z.A., "An Investigation of the Kinetics of the Pyrolysis of Benzene in Shock Waves. I"., Kinetics and Catalysis 10:800 (1969).

40. Mar'yasin, L. and Nabutovskii, Z.A., "Investigation of the Kinetics of Carbon Black Formation During the Thermal Pyrolysis of Benzene and Acetylene in a Shock Wave. III.", Kinetics and Catalysis 14:139 (1973).

41. Park, C. and Appleton, J.P., "Shock-Tube Measurements of Soot Oxidation Rates", Combust. Flame 20:369 (1973).

42. Graham, S.C., Homer, J.B., and Rosenfeld, J.L.J., "The Formation and Coagulation of Soot Aerosoles Generated by the Pyrolysis of Aromatic Hydrocarbons", Proc. R. Soc. Lond. A344:259 (1975).

43. Graham, S.C., Homer, J.B., and Rosenfeld, J.L.J., "The Formation and Coagulation of Soot Aerosols", Proceedings of the Tenth International Shock Tube Symposium, Kyoto, 1975, p. 621.

44. Graham, S.C., "The Collisional Growth of Soot Particles at High Temperatures", Sixteenth Symposium (International) on Combustion, The Combustion Institute, Pittsburgh, 1977, p. 663.

45. Graham, S.C., "The Modelling of the Growth of Soot Particles During the Pyrolysis and Partial Oxidation of Aromatic Hydrocarbons", Proc. R. Soc. Lond. A377:119 (1981).

46. Wang, T.S., Matula, R.A., and Farmer, R.C., "Combustion Kinetics of Soot Formation from Toluene", Eighteenth Symposium (International) on Combustion, The Combustion Institute, Pittsburgh, 1981, p. 1149.

47. Wang, T.S., "Soot Formation from Toluene", Ph.D. Thesis, LSU, 1980.

48. Vaughn, S.N., Lester, T.W., and Merklin, J.F., "A Single Pulse Shock Tube Study of Soot Formation from Benzene Pyrolysis", Proceedings of the 13th International Symposium on Shock Tubes and Waves, State University of New York Press, 1982.

49. Vaughn, S.N., Merklin, J.F., and Lester, T.W., "Isotopic Studies of the Chemical Mechanisms of Soot Nucleation", Engineering Experimental Station Kansas State University Report 149, January 1982.

50. Nelson, G., Merklin, J.F., and Lester, T.W., "Isotopic Studies of the Chemical Mechanisms of Soot Nucleation", Engineering Experimental Station Kansas State University Report 150, January 1982.

51. Evans, M. and Williams, A., "Shock Tube Studies on the Formation of Soot from the Combustion and Pyrolysis of Some Hydrocarbons", Fuel 60:1047 (1981).

52. Farmer, R.C., Edelman, R., and Wong, E., "Modeling Soot Emissions in Combustion Systems" in Particulate Carbon: Formation During Combustion (D.C. Siegla and G.W. Smith, Eds.), Plenum, New York, 1981, p. 299.

53. Edelman, R.B., Farmer, R.C., and Wang, T.S., "Analysis and Modeling of the Combustion and Emissions Characteristics of Typical Synthetic Fuel Components", 183 National ACS Meeting, Las Vegas, March 28 - April 2, 1982.

54. Frenklach, M., Taki, S., and Matula, R.A., "A Conceptual Model for Soot Formation in Pyrolysis of Aromatic Hydrocarbons", Combust. Flame, 49:275 (1983).

55. Frenklach, M., Taki, S., Li Kwok Cheong, C.K., and Matula, R.A., "Soot Particle Size and Soot Yield in Shock Tube Studies", Combust.Flame, 51:37 (1983).

56. Rawlins, W.T., Schertzer, S.P., and Tanzawa, T., "Shock Tube Combustion of Aromatic Compounds", 183 National ACS Meeting, Las Vegas, March 28 - April 2, 1982.

57. Rawlins, W.T., Schertzer, S.P., and Tanzawa, T., "Observations of Soot Initiation in the Pyrolysis and Combustion of Toluene", Fall Technical Meeting of The Combustion Institute (Eastern Section), December 14-16, 1982.

58. Colket, M.B., III, and Seery, D.J., "Pyrolysis of Toluene in a Single-Pulse Shock Tube", Fall Technical Meeting of The Combustion Institute (Eastern Section), December 14-16, 1982.

59. Bauer, S.H. and Zhang, L.M., "Shock Tube Pyrolysis of Polycyclic Aromatics - Detection of Soot Precursors", 14th International Symposium on Shock Tubes and Waves, Sydney, Australia, August 1983.

60. Khandelwal, S.C. and Skinner, G.B., "Shock Tube Studies of Hydrocarbon Oxidation", in Shock Waves in Chemistry (A. Lifshitz, Ed.), Dekker, New York, 1981, p. 1.

61. Frank. P. and Just, Th., "High Temperature Thermal Decomposition of Acetylene ad Diacetylene at Low Relative Concentrations", Combust. Flame 38:231 (1980).

62. Bar-Nun, A. and Dove, J.E., "Acetylene Pyrolysis and Its Oxidation by Water Vapor Behind High Temperature Shock Waves", Proceedings of the 12th International Symposium on Shock Tubes and Waves, Magness, Jerusalem, Israel, 1980, p. 457.

63. Koike, T. and Morinaga, K., "Shock Tube Studies of the Acetylene and Ethylene Pyrolysis by UV Absorption", Bull. Chem. Soc. Jpn. 54:530 (1981).

64. Kiefer, J.H., Al-Alami, M.Z. and Budach, K.A., "A Shock Tube, Laser-Schlieren Study of Propene Pyrolysis at High Temperatures", J. Phys. Chem. 86:808 (1982).

65. Al-Alami, M.Z. and Kiefer, J.H., "Shock-Tube Study of Propane Pyrolysis. Rate of Initial Dissociation from 1400 to 2300 K", J. Phys. Chem. 87:499 (1983).

66. Kiefer, J.H., Kapsalis, S.A., Al-Alami, M.Z. and Budach, K.A., "The Very High Temperature Pyrolysis of Ethylene and the Subsequent Reactions of Product Acetylene", Combust. Flame 51:79 (1983).

67. Colket, M.B., III, "Pyrolysis of 1,3-Butadiene in a Single Pulse Shock Tube", Fall Technical Meeting of the Combustion Institute (Eastern Section), November 8-10, 1983.

68. Tanzawa, T. and Gardiner, W.C., Jr., "Thermal Decomposition of Acetylene", Seventeenth Symposium (International) on Combustion, The Combustion Institute, Pittsburgh, 1979, p. 563.

69. Tanzawa, T. and Gardiner, W.C., Jr., "Rate Mechanism of the Homogeneous Thermal Decomposition of Acetylene", J. Phys. Chem. 84:236 (1980).

70. Gay, I.D., Kistiakowsky, G.B., Michael, J.V. and Niki, H., "Thermal Decomposition of Acetylene in Shock Waves", J. Chem. Phys. 43:1720 (1965).

71. Gardiner, W.C., Jr., Hwang, S.M. and Warnatz, J., "Combustion Mechanism of Acetylene Flames and Ignition Using a Truncated Reaction Mechanism", 9th International Colloquium on Dynamics of Explosions and Reactive Systems, Universite de Poitiers, France, July 3-8, 1983.

72. Levy, J.M., "Higher Hydrocarbon Combustion. 1. Primary Process in Fuel-Rich Acetylene Combustion", Combust. Flame 46:7 (1982).

73. Miller, J.A., Mitchell, R.E., Smooke, M.D. and Kee, R.J., "Towards a Comprehensive Chemical Kinetic Mechanism for the Oxidation of Acetylene: Comparison of Model Predictions with Results from Flame and Shock Tube Experiments", Nineteenth Symposium (International) on Combustion, The Combustion Institute, Pittsburgh, 1982, p. 181.

74. Fussey, D.E., Gosling, A.J. and Lampard, D., "A Shock Tube Study of Induction Times in the Formation of Carbon Particles by Pyrolysis of the C_2 Hydrocarbons", Combust. Flame 32:181 (1978).

75. Cundall, R.B., Fussey, D.E., Harrison, A.J. and Lampard, D., "Shock Tubes Studies of the High Temperature Pyrolysis of Acetylene and Ethylene", J. Chem. Soc. Faraday I 74:1403 (1978).

76. Cundall, R.B., Fussey, D.E., Harrison, A.J. and Lampard, D., "High Temperature Pyrolysis of Ethane and Propylene", J. Chem. Soc. Faraday I 75:1390 (1979).

77. Yoshizawa, Y., Kawada, H. and Kurokawa, M., "A Shock-Tube Study on the Process of Soot Formation from Acetylene Pyrolysis", Seventeenth Symposium (International) on Combustion, The Combustion Institute, Pittsburgh, 1979, p. 1375.

78. Frenklach, M., Taki, S., Durgaprasad, M.B. and Matula, R.A., "Soot Formation in Shock-Tube Pyrolysis of Acetylene, Allene and 1,3-Butadiene", Combust. Flame, 54:81 (1983).

79. Gardiner, W.C., Jr., Walker, B.F. and Wakefield, C.B., "Mathematical Methods for Modeling Chemical Reactions in Shock Waves" in Shock Waves in Chemistry (A. Lifshitz, Ed.), Dekker, New York, 1981, Ch. 7.

80. Rawlins, W.T., Tanzawa, T., Schertzer, S.P. and Krech, R.H., "Synthetic Fuel Combustion: Pollutant Formation. Soot Initiation Mechanisms in Burning Aromatics", Report TR-361, Physical Sciences, 1982.

81. McLain, A.G.; Jachimowski, C.J., and Wilson, C.H. "Chemical kinetics modeling of benzene and toluene oxidation behind shock waves", NASA Technical Paper 1472 (1979).

82. Jachimowski, C.J. "Kinetics of oxygen atom formation during the oxidation of methane behind shock waves", Combust. Flame 23:233 (1974).

83. Jachimowski, C.J. "An experimental and analytical study of acetylene and ethylene oxidation behind shock waves", Combust. Flame 29:55 (1977).

84. Burcat, A., "Thermochemical Data for Combustion Calculations" in Chemistry of Combustion Reactions (W.C. Gardiner, Jr., Ed.), Springer-Verlag, New York, 1984, to appear.

85. Hindmarsh, A.C., "Towards a Systematized Collection of ODE Solvers", 10th IMACS World Congress on Systems Simulation and Scientific Computation, Montreal, Candada, August 8-13, 1982.

86. Gordon, S. and McBride, B., "Computer program for calculation of complex chemical equilibrium compositions, rocket performance, incident and reflected shocks, and Chapman-Jouget detonations", NASA-Lewis Research Center, 1976.

87. Gardiner, W.C., Jr., "Reaction Mechanism of the High Temperature Oxidation of Acetylene", 185 ACS National Meeting, Seattle, Washington, March 20-25, 1983.

88. Hidaka, Y., Eubank, C.S., Gardiner, W.C., Jr. and Hwang, S.M., "Shock Tube Modeling Study of Acetylene Oxidation", to appear.

89. Holland, C.D. and Anthony, R.G., Fundamentals of Chemical Reaction Engineering, Prentice-Hall, New Jersey, 1979, Ch. 10.

90. Davis, Philip J., "Gamma Function and Related Functions" in Handbook of Mathematical Functions, (M. Abramowitz and I.A. Stegun, Eds.), Dover, New York 1972, Ch. 6.

91. Zelen, M. and Severo, N.C., "Probability Functions" in Handbook of Mathematical Functions, (M. Abramowitz and I.A. Stegun, Eds.), Dover, New York 1972, Ch. 26.

92. Jackimowski, C.J. Erratum for reference 83. Combust. Flame 31:102 (1978).

APPENDIX A - PUBLICATIONS AND PRESENTATIONS

The following list of publications has resulted from this program:

1. Frenklach, M. and Clary, D., "Aspects of Autocatalytic Reaction Kinetics", Ind. Eng. Chem. Fundam., 1983, 22:433 (1983).
2. Frenklach, M., Taki, S., Durgaprasad, M. and Matula, R.A., "Soot Formation in Shock-Tube Pyrolysis of Acetylene, Allene and 1,3-Butadiene", Combust. Flame, 54:81 (1983).
3. Frenklach, M., Clary, D., and Matula, R.A., "Empirical Modeling of Soot Formation in Pyrolysis of Aromatic Hydrocarbons", in preparation for submission to Combust. Sci. Techol.
4. Frenklach, M., Clary, D.W., Gardiner, W.C., Jr., and Stein, S., "Detailed Kinetics Modeling of Soot Formation in High-Temperature Pyrolysis of Hydrocarbons", Submitted to the Twentieth Symposium (International) on Combustion.
5. Frenklach, M., Ramachandra, M.K. and Matula, R.A., "Soot Formation in Shock-Tube Oxidation of Hydrocarbons", Submitted to the Twentieth Symposium (International) on Combustion.

Based on the work done under this program, the following presentations have been made:

1. "Effects of Fuel Structure on Soot Formation - A Shock Tube Study", Seminar at MIT, Department of Chemical Engineering Combustion Research Group, December 17, 1982.

2. "Soot Formation in Pyrolysis of Acetylene, Allene and 1,3-Butadiene", M. Frenklach, S. Taki, M.B. Durgaprasad and R.A. Matula, the Spring Technical Meeting of the Combustion Institute, Western States Section, Pasadena, California, April 11-12, 1983.
3. "Shock Tube Study of the Fuel Structure Effects on the Chemical Kinetic Mechanisms Responsible for Soot Formation", M. Frenklach, research review on "Oxidation Kinetics and Soot Formation", NASA-Lewis Research Center, Cleveland, Ohio, October 6, 1983.
4. "Soot Formation in Shock-Tube Oxidation of Acetylene and Toluene", M. Frenklach, M.K. Ramachandra and R.A. Matula, Sixteenth Fall Technical Meeting of the Eastern Section of the Combustion Institute, Providence, Rhode Island, November 8-10, 1983.
5. "Empirical Modeling of Soot Formation in Pyrolysis of Aromatic Hydrocarbons", M. Frenklach, D. Clary and R.A. Matula, Sixteenth Fall Technical Meeting of the Eastern Section of the Combustion Institute, Providence, Rhode Island, November 8-10, 1983.
6. "Shock Tube Study of Soot Formation from Hydrocarbons", Department of Physical Chemistry, University of Heidelberg, West Germany, December 14, 1983.

APPENDIX B - PROFESSIONAL PERSONNEL

Dr. M. Frenklach	-	Principal Investigator
Dr. R.A. Matula	-	Participating Faculty
Dr. M.K. Ramachandra	-	Research Associate
D. Clary	-	Graduate Student
D. Thigpen	-	Undergraduate Student
J. Wust	-	Undergraduate Student
P. Laughlin	-	Undergraduate Student